UC Berkeley
UC Berkeley Electronic Theses and Dissertations

Title

Impacts of Native and Introduced Species on Native Vertebrates in a Salmon-Bearing River Under Contrasting Thermal and Hydrologic Regimes

Permalink

https://escholarship.org/uc/item/0wf2q0pk

Author

Georgakakos, Philip Blythe

Publication Date

2020

Peer reviewed|Thesis/dissertation

Impacts of Native and Introduced Species on Native Vertebrates in a Salmon-Bearing River
Under Contrasting Thermal and Hydrologic Regimes

By

Philip Blythe Georgakakos

A dissertation submitted in partial satisfaction of the

requirements for the degree of

Doctor of Philosophy

in

Integrative Biology

in the

Graduate Division

of the

University of California, Berkeley

Committee in charge:

Professor Mary E. Power, Chair
Professor Stephanie M. Carlson
Professor Wayne P. Sousa

Fall 2020

Impacts of Native and Introduced Species on Native Vertebrates in a Salmon-Bearing River
Under Contrasting Thermal and Hydrologic Regimes

Copyright 2020

by

Philip Blythe Georgakakos

Abstract

Impacts of Native and Introduced Species on Native Vertebrates in a Salmon-Bearing River
Under Contrasting Thermal and Hydrologic Regimes

by

Philip Blythe Georgakakos

Doctor of Philosophy in Ecology

University of California, Berkeley

Professor Mary E. Power, Chair

As organisms undergo life history transitions, track resources, avoid stress, and evade death, they distribute themselves across landscapes. Organismal co-occurrence sets the stage for biotic interactions, which can feed back to control the distribution and abundance of interacting species in ecological communities. Classically, competition and bottom-up forces have been thought to be the most important drivers of community structure, however, examples of predation, parasitism, mutualism, and facilitation highlight the ubiquity and importance of these other interactions. In freshwaters, anthropogenic impacts, especially species introductions and climate warming, have resulted in novel species assemblages, with altered webs of interactions compared to historic conditions. Human management often seeks to provide conditions that favor native species and inhibit non-natives. Success requires an understanding species interactions and their roles in community dynamics. In my first chapter, I describe the distributional dynamics of the assemblage of aquatic fishes, reptiles and amphibians in the South Fork Eel River. In Chapter 2, I describe the seasonal migration of an introduced predatory fish, Sacramento Pikeminnow (*Ptychocheilus grandis),* and how climate warming and water withdrawals could increase their negative impact on rearing native salmonids and other fauna. In Chapter 3, my colleagues and I explore the positive interactions between Pacific Lamprey (*Entosphenus tridentatus*), juvenile Steelhead trout (*Oncorhynchus mykiss),* and Foothill Yellow-legged Frogs (*Rana boylii)*. These case studies emphasize the need to consider ecological interactions, and in general, community ecology thinking, as we try to restore and manage ecosystems.

Acknowledgements

So many people helped me complete my dissertation and all the work involved. At the onset, I didn't realize that completing a PhD takes a community, and the contributions of my friends, collaborators, mentors, and family made myself and my work better in every respect. For her involvement at every step, I extend my dearest thanks to Julie Gonzalez. Whether helping with fieldwork, providing much needed advice on design and aesthetics, turning hastily written sentences into coherent ones, or lifting me up from emotional troughs while writing, Julie provided unwavering support. You've helped make graduate school the best time of my life, and I'm so grateful to go through life by your side. To my parents, Aris Georgakakos and Leslie Blythe, thank you for fostering my curiosity from my earliest years. I could not have asked for better models for the importance of hard work, independent thought, and self-education. Thank you for your unconditional love and support. To my sister Christine, thank you for optimism and insight while always listening to my speculations about ecology, personal relationships, and my most recent animal encounter. I wish you the best finishing your degree and look forward to our next adventure.

It has been my great fortune to work with truly amazing academic advisors. At Georgia Tech I thank for Gerald Pullman for exposing me to how exciting research can be. Thanks to Joseph Montoya for demonstrating the importance of attention to detail and good planning in field efforts. During my undergraduate studies at Georgia Tech, I had the pleasure of taking Mark Hay's ecology classes. Mark's lectures on the complexity of natural systems, organismal chemical warfare, importance of species interactions, and the power of predators to shape communities were formative for me. Mark recommended getting in touch with Mary Power, as a potential graduate school advisor, and better advice could not have been given. Mary has been the best graduate advisor I could have imagined. Just to name a few of the areas Mary been a role model for me: good scholarship, strong ethics, deep ecological knowledge, natural history insight, and graceful clear writing. In addition, Mary is kindhearted, generous with her time, and humble. Thank you for taking me as a graduate student, it has been an honor, and you have shaped my skills, thought processes, and priorities as a mentor and friend. I'm grateful to Wayne Sousa for his guidance and feedback on all aspects of this dissertation. In addition, during our discussions Wayne provided the historical context to understand the state of ecology today and helped me understand sound study design. I thank Stephanie Carlson for being an outstanding mentor. I benefited from Stephanie's dedicated teaching first, as a student, my first semester at Berkeley, when I enrolled in her fish ecology class. Later, as co-instructor for a field ecology course In Moorea, French Polynesia. Stephanie's enthusiasm for aquatic systems and dedication to equitable learning and research, continues to inspire me. Thanks to Sarah Kupferberg for always lending her ear and giving feedback, Sarah can always be counted on for keen insight, especially when thinking about what motivates organisms as they make decisions. I'm also grateful to Caroline Williams and Justin Brashares for spending so much of their time in discussions with me as I prepared for my qualifying exam, our conversations continue to shape my thinking. I've benefited hugely from the generosity of all my mentors, and I hope to pay it forward, doing my best to help my mentees in the future.

In addition to my mentors, a I had the pleasure of interacting with a great group of graduate students and post-doctoral researchers. No one thinks like a juvenile salmonid better than Gabe Rossi. Gabe's enthusiasm is infectious, and he's always willing to help think through a tricky

Introduction

Organisms distribute themselves in relation to resources (Power 1984), avoid stressful conditions (Sinervo et al. 2010), undergo life history transitions (Kupferberg 1996), and interact with other organisms (Power et al. 1985). In addition, humans are reshuffling the global distribution of organisms through species introductions (Zaret and Paine 1973), climate induced range shifts (Rubidge et al. 2011), and local removal (Burkepile and Hay 2008, Sinervo et al. 2010). These processes rearrange species into novel assemblages, often with diminished economic returns from recreation, harvest, and other ecosystem services (Moyle 2013). Human induced climate change may also affect species within assemblages. Predicted warming and extended periods of drought (Pierce et al. 2018) can stress organisms physiologically (Sunday et al. 2011) and modify the strength and directions of biotic interactions between and within species (Reese and Harvey 2002, Harley 2011). My dissertation research examined conditions that drive organismal distributions and highlights the role species interactions play in community dynamics, in the context of a changing climate. My study system was the community of aquatic organisms of the South Fork Eel River in Mendocino Co, northern California.

In Chapter 1, I report observations from extensive snorkel surveys documenting the seasonal, interannual, longitudinal, and habitat type variation in through densities, abundances, and size distributions of aquatic vertebrates over five consecutive years.

In Chapter 2, I investigate how the negative impacts of an invasive predator might be exacerbated under warmer future conditions. I document the first observation of migration by this invasive piscine predator, the Sacramento pikeminnow (*Ptychocheilus grandis),* within its introduced range, the South Fork Eel River. We developed a statistical temperature model to forecast the timing and extent of upstream migration by pikeminnow under combinations of discharge and air temperature that were not observed. This model was calibrated with our field observations that showed that river temperature decreased with river flow and increased downstream, and with air temperature.

In Chapter 3, I investigate a number of positive interactions. In Northwestern California great numbers of Pacific Lamprey (*Entosphenus tridentatus*) swim into coastal rivers annually to spawn. While engineering their redds, lamprey mobilize and rearrange large amounts of sediment and disturb the macroinvertebrates living in and on the benthos. In California's Eel River we investigated how bioturbation during lamprey redd construction influenced invertebrate drift, whether juvenile Steelhead (*Oncorhynchus mykiss*) foraged more behind active redds, how redd building influenced foraging profitability (as estimated from bioenergetic models), and the effects of built lamprey redds on local water velocity.

These studies highlight the need to consider whole stream communities as we seek to manage species. Organisms do not exist in isolation, and their management, conservation and restoration of natural systems can be improved if context dependent interactions of species are taken into account.

Literature cited

Burkepile, D. E., and M. E. Hay. 2008. Herbivore Species Richness and Feeding Complementarity Affect Community Structure and Function on a Coral Reef. Proceedings of the National Academy of Sciences of the United States of America 105:16201–16206.

Harley, C. D. G. 2011. Climate Change, Keystone Predation, and Biodiversity Loss. Science 334:1124–1127.

Kupferberg, S. J. 1996. Hydrologic and Geomorphic Factors Affecting Conservation of a River-Breeding Frog (Rana Boylii). Ecological Applications 6:1332–1344.

Moyle, P. B. 2013. Novel Aquatic ecosystems: the new reality for streams in California and other Mediterranean climate regions. River Research and Applications 30:1335–1344.

Power, M. E. 1984. Habitat quality and the distribution of algae-grazing catfish in a Panamanian stream. The Journal of animal ecology 53:357–374.

Power, M. E., W. J. Matthews, and A. J. Stewart. 1985. Grazing minnows, piscivorous bass, and stream algae: dynamics of a strong interaction. Ecology 66:1448–1456.

Reese, C. D., and B. C. Harvey. 2002. Temperature-dependent interactions between juvenile steelhead and Sacramento pikeminnow in laboratory streams. Transactions of the American Fisheries Society 131:599–606.

Rubidge, E. M., W. B. Monahan, J. L. Parra, S. E. Cameron, and J. S. Brashares. 2011. The role of climate, habitat, and species co-occurrence as drivers of change in small mammal distributions over the past century. Global Change Biology 17:696–708.

Sinervo, B., F. Mendez-de-la-Cruz, D. B. Miles, B. Heulin, E. Bastiaans, M. Villagran-Santa Cruz, R. Lara-Resendiz, N. Martinez-Mendez, M. L. Calderon-Espinosa, R. N. Meza-Lazaro, H. Gadsden, L. J. Avila, M. Morando, I. J. De la Riva, P. V. Sepulveda, C. F. D. Rocha, N. Ibarguengoytia, C. A. Puntriano, M. Massot, V. Lepetz, T. A. Oksanen, D. G. Chapple, A. M. Bauer, W. R. Branch, J. Clobert, and J. W. Sites. 2010. Erosion of Lizard Diversity by Climate Change and Altered Thermal Niches. Science 328:894–899.

Sunday, J. M., A. E. Bates, and N. K. Dulvy. 2011. Global analysis of thermal tolerance and latitude in ectotherms. Proceedings of the Royal Society B: Biological Sciences 278:1823–1830.

Yoshiyama, R. M., and P. B. Moyle. 2010. Historical review of Eel River anadromous salmonids, with emphasis on Chinook salmon, coho salmon and steelhead. Report for California Trout. Center for Watershed Science.

Chapter 1. Longitudinal, Seasonal, and Inter-Annual Variation in the Fishes, Aquatic Amphibians, and Reptiles of the South Fork Eel River

Abstract

Organisms distribute themselves across landscapes in response to environmental conditions, resource abundance, and interactions with other species. Riverscapes, as branched hierarchical networks, restrict the long-distance movements of some organisms to one dimension, upstream or downstream. Species assemblages change longitudinally from headwaters to estuaries, but this spatial variation can itself be dynamic. We describe the seasonal, yearly, longitudinal, and habitat type variation in densities of each aquatic vertebrate censused during repeated snorkel surveys over five years. Almost all species varied longitudinally, and their longitudinal densities changed over time (either between seasons or years). Generally, invasive animals were more abundant in downstream reaches and in slower water habitats. Populations of native species tended to be denser upstream, especially in late summer, when invasive numbers were high downstream. Identifying the drivers that favor native species could help guide restoration efforts to shift assemblages towards more desirable historical states

Introduction

The composition of assemblages within habitats shift as organisms distribute themselves in relation to resources (Power 1984a), avoid stressful conditions (Sinervo et al. 2010), undergo life history transitions (Kupferberg 1996), and interact with other organisms (Power et al. 1985). Rivers are dynamic branched hierarchical networks (Leopold et al. 1965), and at reach scales (100s of m to kilometers), organisms move in one dimension, upstream or downstream. At smaller scales, organisms exploit local heterogeneity in many conditions such as: food abundance, temperature, water velocity and turbulence, and predation pressure (Fausch et al. 1991, Wang et al. 2020, Power 1984b). Longitudinally, distributions of organisms are somewhat predictable. Changes in physical conditions associated with transitioning from lotic headwaters to more lentic meanders in floodplains and eventually estuaries are accompanied with changes in species assemblages and functional guilds (Vannote and Minshall 1980). However, the boundaries between assemblages are often fuzzy as assemblages shift in space and time (Baxter 2002). To assess organismal distributions and population sizes, and avoid inaccurate inference, sampling must occur on organismally-relevant spatial and temporal scales (Power et al. 1988).

In northwestern California, the Eel River's fish assemblage historically consisted of 12-14 species (Brown and Moyle 1997) and was dominated by large populations of Pacific lamprey (*Entosphenus tridentatus*), the river's namesake, and Pacific salmon (Steelhead, *Oncorhynchus mykiss;* Coho, *Oncorhynchus kisutch;* and Chinook, *Oncorhynchus tshawytscha*) (Yoshiyama and Moyle 2010). Annual salmon runs of up to one million and the fisheries they supported collapsed due to overfishing and habitat destruction via deforestation, with the most severe effects resulting from massive sedimentation of stream channels during the great floods of 1955 and 1964 (Yoshiyama and Moyle 2010). Lamprey numbers also declined during this period, but

their decline is not as well quantified (Goodman and Reid 2012). Currently, other native species including Green sturgeon (*Acipenser medirostris*), Sacramento sucker (*Catostomus occidentalis*), Three-spined stickleback (*Gasterosteus aculeatus)*, and three sculpin species (*Cottus spp.)* are present, but most have likely experienced populations reductions and are currently more limited in spatial extent. A number of reptiles and amphibians also occupy mainstems, Western Pond Turtles (*Actinemys marmorata)*, Foothill Yellow-legged Frogs (*Rana boylii),* and Rough-skinned newts (*Taricha granulosa)*, but little is known about their changes in abundance over time. A number of non-native species introductions have also occurred (Brown and Moyle 1997). At least 16 species have been introduced to the Eel (Brown and Moyle 1997), including the two that are currently numerically dominant: Sacramento Pikeminnow (*Ptychocheilus grandis,* Brown and Mole 1991) and North Coast Range Roach (*Hesperoleucus venustus*, Baumsteiger et al. 2017). As some of these species established, novel assemblages of aquatic vertebrates were created as non-native organisms spread throughout the drainage (Moyle and Marchetti 2006) and many native organisms shifted their habitat use (Brown and Moyle 1991).

Many factors may shift organismal distribution and abundance in space and time. Most native vertebrates in the Eel River have somewhat migratory life histories (Moyle 2002, Kelson et al. 2020, Whitehorn 2010), resulting in the seasonal absence of one or more life history stages in many reaches. For example, Chinook eggs hatch in winter, and smolts migrate downstream to the ocean in spring. In most reaches, Chinook are absent during summer. Other species like Foothill yellow-legged frogs migrate from adult habitat in tributaries to river mainstems in spring, where they deposit egg clutches in historic lek sites, and their larva hatch and inhabit these mainstems for the summer (Kupferberg 1996). In addition to this intra-annual variation there is also inter-annual variation in numbers because of different strengths of certain year-classes. In other organisms, like American Bullfrogs (*Rana catesbeiana*), episodic conditions within a year like flow greatly influence survival (Kupferberg 1997). Peak winter flows can be an important source of disturbance in Mediterranean climate rivers (Wootton et al. 1996) displacing and killing organisms, freeing up habitat space for other organisms (Sousa 1984). These variations in time can interact with variation in space. Some reaches might be favorable in certain years or seasons but stressful in others, and thus organisms may distribute differently longitudinally between years or seasons (Wang et al. 2020). Finally, organisms interact with each other: competitors, predators, and facilitators influence each other's distributions and alter assemblage composition (Connell 1961, Brown and Moyle 1991, Power 1984b, Bertness 1991, Paine 1974). All these factors contribute to a dynamic aquatic vertebrate assemblage. By understanding each organism's life histories and environmental preferences, we can start to make predictions about where and when organisms will occur and what conditions might favor native species whose conservation and restoration we prioritize (Moyle 2013).

Here, our objectives were to (1), describe the current assemblage of aquatic vertebrates in our 10.5 km study reach of the South Fork Eel River headwaters and (2) investigate how each species varied in time between years and seasons, and in (3) space: longitudinally and by habitat. To accomplish these goals, we counted organisms along a 10.5 km study reach, surveying pools, riffles and runs by snorkeling twice a year from 2016-2020, once in the late spring and again in late summer.

Methods

Study site

We studied a 10.5 - km reach of the Upper South Fork Eel River, in and around the Angelo Coast Range Reserve, a UC Natural Reserve System reserve managed by the University of California, Berkeley in Mendocino Co., Northern California. Our study reach extended from the Angelo Reserve's Environmental Science Center (39.7189°N, 123.6529°W) downstream to Hunter's Pool (39.7579°N, 123.6368°W)(Figure 1).
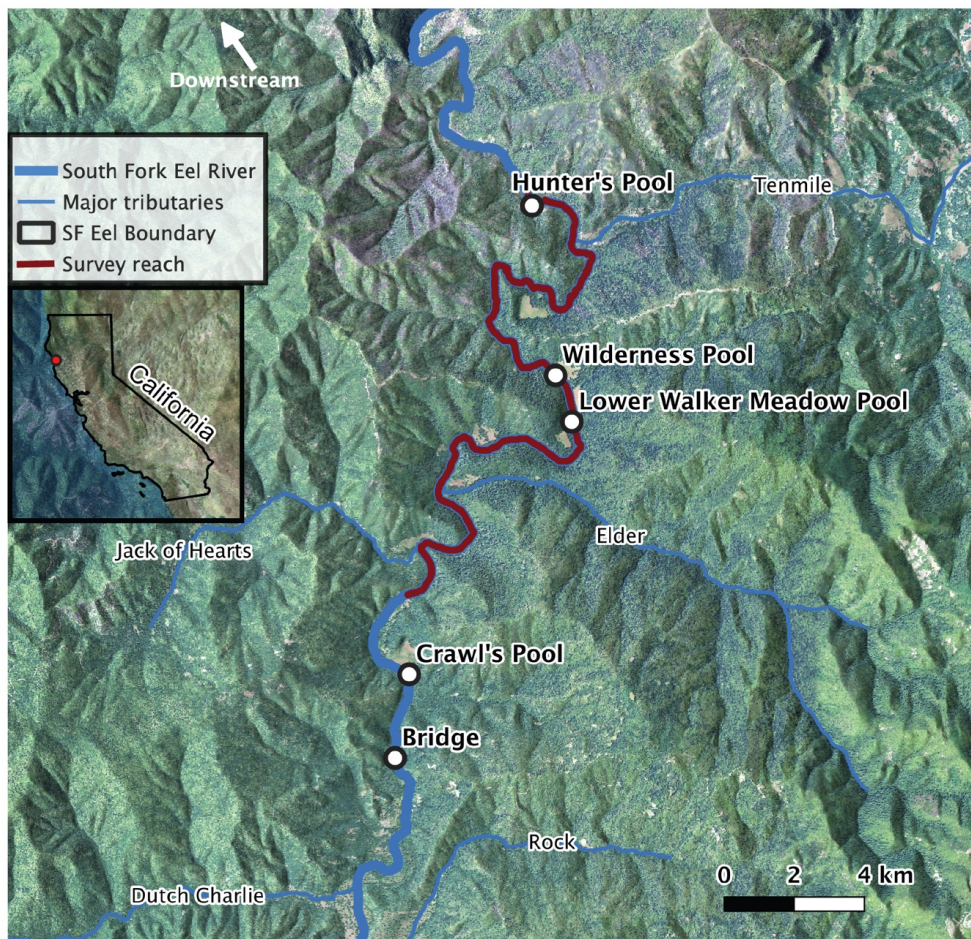
Color imagery from the National Agriculture Imagery Program, United States Department of Agriculture, Farm Service Agency

Figure 1: Map of the study reach and surrounding tributaries, Study reach is highlighted in maroon. River km zero was set at the Wilderness Lodge Road Bridge "Bridge".

Physical attributes of units

We measured several physical characteristics of each hydrologic unit surveyed. At the time of the survey, units were visually categorized as pools, riffle or run. Width and lengths of units were measured with a laser range finder (Nikon Forestry Pro Laser Range Finder), unit lengths were used to calculate linear densities (# / km). We recorded maximum depth of shallower units with a ruled wading rod, and of deeper units with a weighted measuring tape. Average flow was estimated and binned in the following categories: 0 – 5, 5 – 10, 10 – 20, 20 – 30, 30 – 50, 50 – 100 and greater than 100 cm/second. We recorded dominant and sub-dominant substrates using the Wentworth scale. We also recorded the dominant and sub-dominant primary producers present. Visibility was estimated and recorded with a Secchi disk. GPS points were taken at both the top and the bottom of each unit. River km zero was set at the Wilderness Lodge Road Bridge

that crosses the South Fork Eel at (39.70293°N, 123.6540°W). River km was set for each unit by snapping (moving its coordinates to the nearest point on the line) its upstream GPS point to a river channel derived from LiDAR (2014 ERCZO) and measuring the distance along the channel to the Wilderness Lodge Road Bridge, thus River km increased from upstream to downstream. Temperature sensors were placed in the river during the summer months 2015-2020 (see Chapter 2 Supplemental Material Table 1, for locality specifics).

Snorkel Surveys

From 2016-2018, each hydraulic unit (pools, riffles, and runs) in our entire 10.5-km study reach study reach was surveyed by two divers. Units were surveyed once at the end of May and once in the beginning of August. In 2019, we surveyed 5.47 km of units, 52% of the total units surveyed; as in 2016-2018, we surveyed these units once in late May and once in early August. In 2020 we did a smaller subset of units, surveying 2.57 km, approximately 23% of the total units, and only surveyed these units in early August. During surveys, two divers swam upstream along the edges of the unit, counting animals and communicating to avoid double counting. If the unit was too wide or the visibility was too poor for divers to see the middle, one of the divers swam downstream, surveying the middle, after reaching the upstream limit of the unit. During these surveys, all fishes, aquatic amphibians and reptiles sighted were counted, with their body lengths estimated in categories (Table 1). Both live and dead Pacific Lamprey were counted but are displayed and analyzed separately.

Table 1. All vertebrates encountered during snorkel surveys. Species-specific size classes used to categorize organisms during snorkel surveys and grouped size classes used in analyses.

Species	Size classes recorded (cm)	Measurement type	Size classes used in analysis(cm)
Hesperoleucus venustus, North Coast Range Roach	(0-2), (2-5), (5-10), (10-15)	Total length	Fry 0-2 Juveniles 2-5 Adults 5-15
Ptychocheilus grandis, Sacramento pikeminnow	(0-5), (5-10), (10-15), (15-20), (20-25), (25-30), (30-40), (40-60)	Total length	Sub-adult 5-20 Adult 20-60
Catostomus occidentalis, Sacramento sucker	(0-5), (5-10), (10-15), (15-20), (20-25), (25-30), (30-40), (40-60)	Total length	Fry and Juvenile 0 -10 Sub-adult 10-20
Oncorhynchus tshawytscha, chinook salmon	(5-10), (10-15), (15-20)	Total length	Parr 5-15
Oncorhynchus kisutch, coho salmon	(0-5), (5-10) (10-15), (15-20)	Total length	Parr 0-15
Oncorhynchus mykiss, steelhead	(0-5), (5-10) (10-15), (15-20), (20-25), (25-30), (30-40), (40-60)	Total length	Fry 0-5 Small Parr 5-10 Large Parr 10-20 Small Adult/ Large Smolt 20-30 Adult 30-40 Large Adult 40-60
Gasterosteus aculeatus, three-spined stickleback	(0-2), (2-4), (4-10)	Total length	Fry and Juvenile 0-4 Adult 4-10

Entosphenus tridentatus, Pacific lamprey	(0-10), (10-40), (40-100)	Total length	Adult Alive Adult Dead
Lepomis cyanellus, green sunfish	(0-5), (5-10), (10-15), (15-20), (20-30)	Total length	Juvenile & adult 5-20
Amerius sp., bullhead catfish	(0-5), (5-10), (10-15), (15-20), (20-30)	Total length	
Thamnophis atratus, aquatic garter snake	(0-20), (20-40), (40-60), (60-80)	Total length	All sizes
Actinemys marmorata, western pond turtle	(0-5), (5-10), (10-20), (20-30)	Carapace length	All sizes
Rana boylii, foothill yellow-legged frog	Not surveyed	Larva: Total length Frog: snout-vent length	Not surveyed
Rana catesbeiana, bullfrog	Larvae (0-2), (2-5), (5-10), (10-15) Frog (0-3), (3-15)	Larva (with tail): Total length Frog (no-tail): snout-vent length	Larva 0-15
Taricha granulosa, rough-skinned newt	Larvae: (0-4) Adult: (0-5), (5-10)	Larva : Total length Adult: snout-vent length	Adult 0-10

Analysis of counts and interpretation of distributional changes in time and space

We investigated the distributions of all organisms encountered during surveys in time and space using a generalized linear mixed – effect modeling (GLMM) framework. Separate models were created for species-size class combinations that reflected distinct life history stages (Table 1), and for species with enough observations. All models used Poisson distributions and log link functions, appropriate for count data, and where possible, included a random – effect of year. Mixed – effect models were not used for species encountered in fewer than 3 years. In these cases (Chinook), we used a generalized linear model and analyzed only the year when the organism was most abundant. The response variables in all models were counts of individuals within a unit. However, counts were normalized by unit length, effectively making the response variable linear density, while not transforming the data from integer counts, and allowing use of a Poisson distribution. This allowed us to compare units of varying length. Potential explanatory variables included Season (May vs. August), Year, River km, Habitat type (pool, riffle, or run), and 5 interaction terms: Season x Habitat type, Season x Year, Season x River km, Year x River km, and Season x Year x River km. The model syntax in the lme4 package of the R statistical program is shown below (1) Model depicting all possible explanatory variables, notation used is for Generalized Linear Mixed-effect models implemented in lme4 package. colons denote interaction terms. "Offset()" term normalizes counts by unit length, which is included as a log because of the log-link function.

glmer(Count$_{\text{speciesx, size class}}$ ~ Season + Year + River km + Habitat type + Season:Habitat type +
Season:Year + Season:River km + Year:River km + Season:Year:River km +
(1|Year) + offset(log(length)))

(1)

Model selection and reporting on significant predictors

In models where counts of a level of categorical explanatory variable (Year, River km, Season, and Habitat type) were all zero counts, none of the interaction terms including that variable were included. If 50% or more of levels in a categorical predictor were all zero counts, then that predictor was dropped. Once a full model, which included all potential explanatory variables for a species – size class combination, was selected, each predictor was dropped from the full model to create a reduced model. The Akaike information criterion (AIC) was used to compare full and reduced models. The reduced model with the lowest AIC was selected and the new reduced models were created and compared to this model as the new full model. This process stopped when ΔAIC was less than 2, and this model was determined to be the best model for this species – size class combination (Richards et al. 2010). The parameter estimates for the best models are reported in tables for each species (Supplemental Material Tables 1-11).

For all data analysis, manipulation, statistics and visualization, we used the statistical program R (R Development Core Team, 2018, version 3.14), with the CRAN packages lme4, tidyverse, and lmeTest.

Results

Physical Attributes of units

On average, pools comprised 4.23 km, riffles 2.66 km and runs 3.74 km in each season's survey. Riffles had the highest water velocities, runs intermediate, and pools the lowest (Figure 2). Pools were deepest, followed by runs and riffles (Figure 3). Greatest peak flows occurred in water year 2017 and lowest in 2020 (892.0 and 197.6 cubic meters per second, respectively (Figure 4). Mean flows were also greatest in water year 2017 and lowest in 2020 (41.5 and 6.5 cubic meters per second (Figure 4). Water temperatures increased downstream (Figure 5). Elder Creek, a cool water tributary entered the South Fork between River km 4.313 and 4.499, and its influence on temperature can be seen later in the season (Figure 5). On average, 2016 was the warmest year and 2019 the coolest (For a comparison of temperatures between years at one location see Chapter 2 Figure 2a).
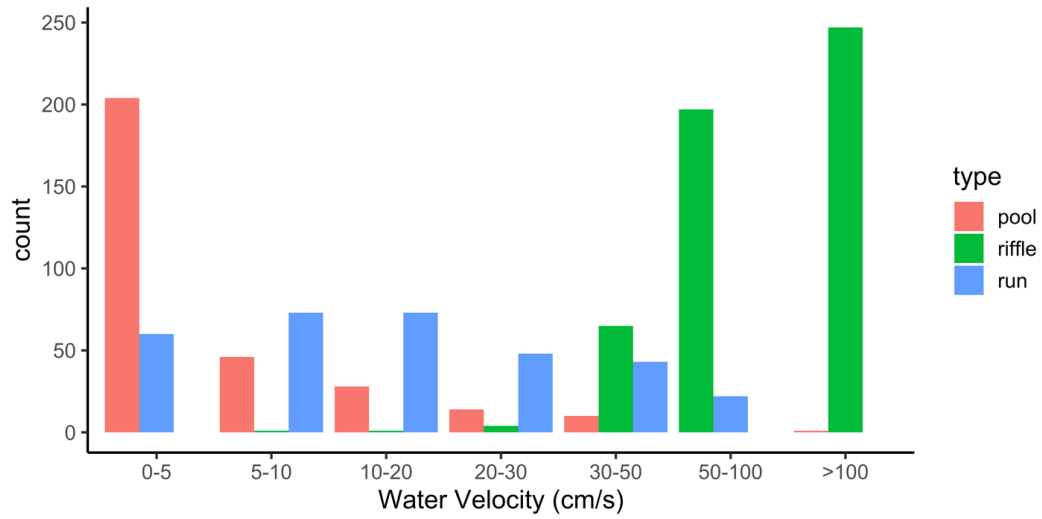
Figure 2. Histogram of water velocity colored by habitat type. Counts represent each unit surveyed in all years (2016-2020) and all seasons. Water velocity was binned and visually estimated at each unit at the time of the survey.
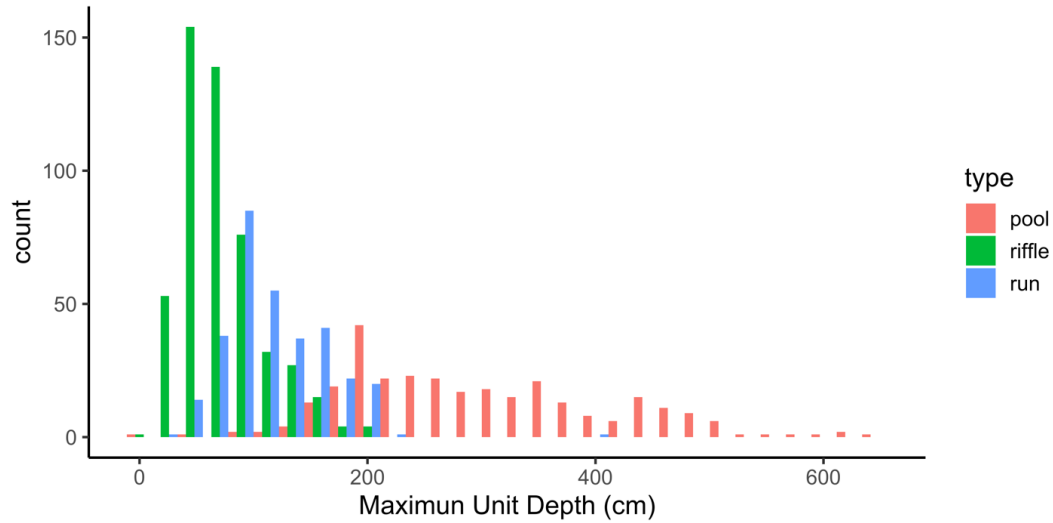
Figure 3. Histogram of maximum depth in units. Counts represent each unit surveyed in all years (2016-2020) and all seasons.
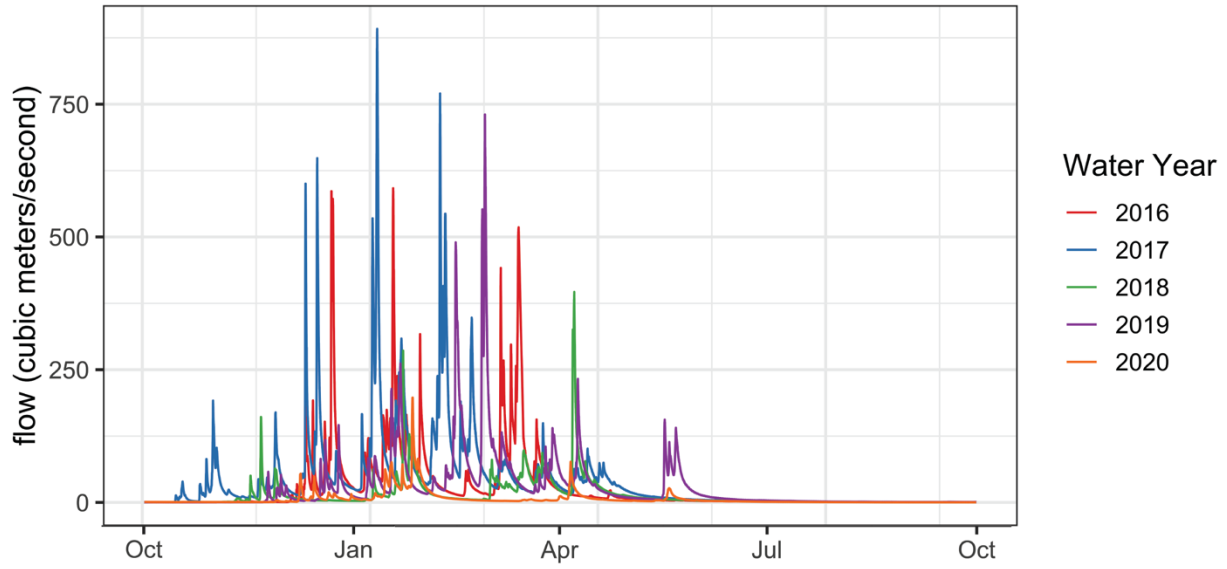
Figure 4. Discharge by water year data from the USGS Legget Gauge #11475800
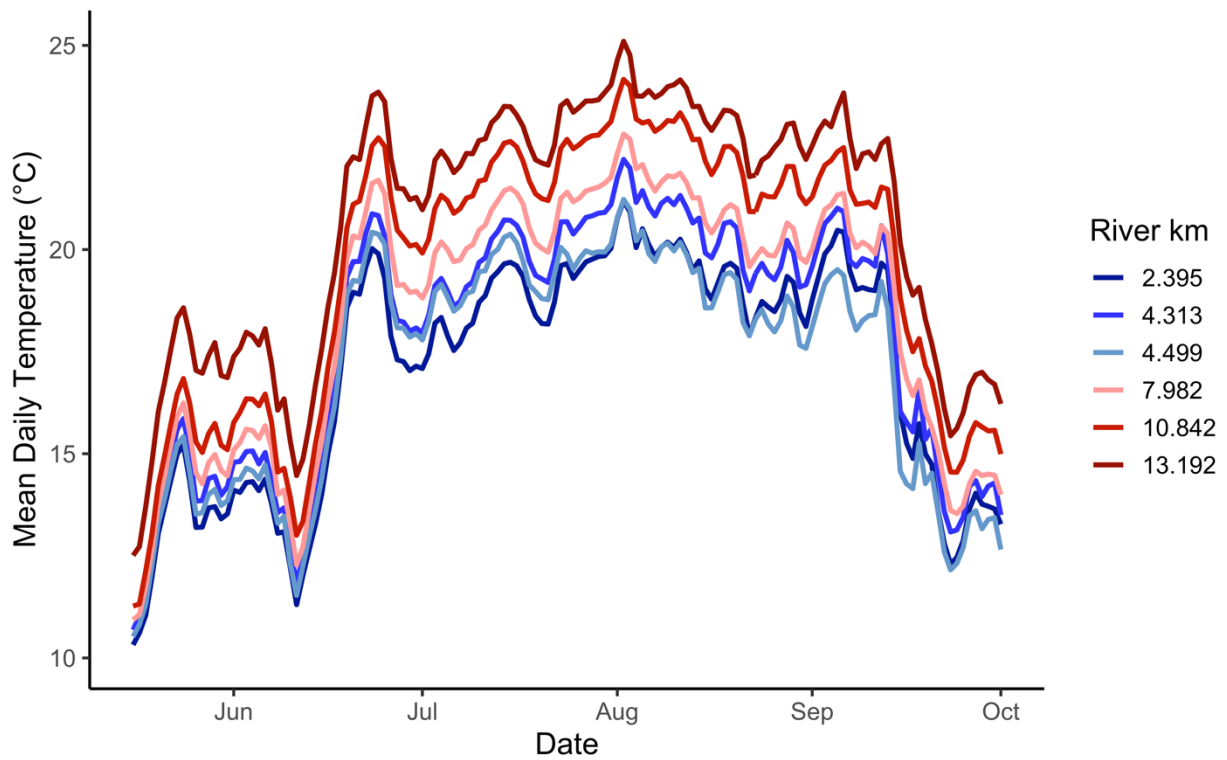
Figure 5. Mean daily temperatures (degrees Celsius) in 2017 from May 15 – October 2. Colors show sensor location. Greater river kilometers are further downstream

Vertebrate distribution and abundance

North Coast Range Roach, Hesperoleucus venustus

Roach were the most abundant vertebrate in all 5 years of survey. Over this period, a total of 372,251 roach were counted along 34.5 km for an average annual density of 10,789 individuals/km.
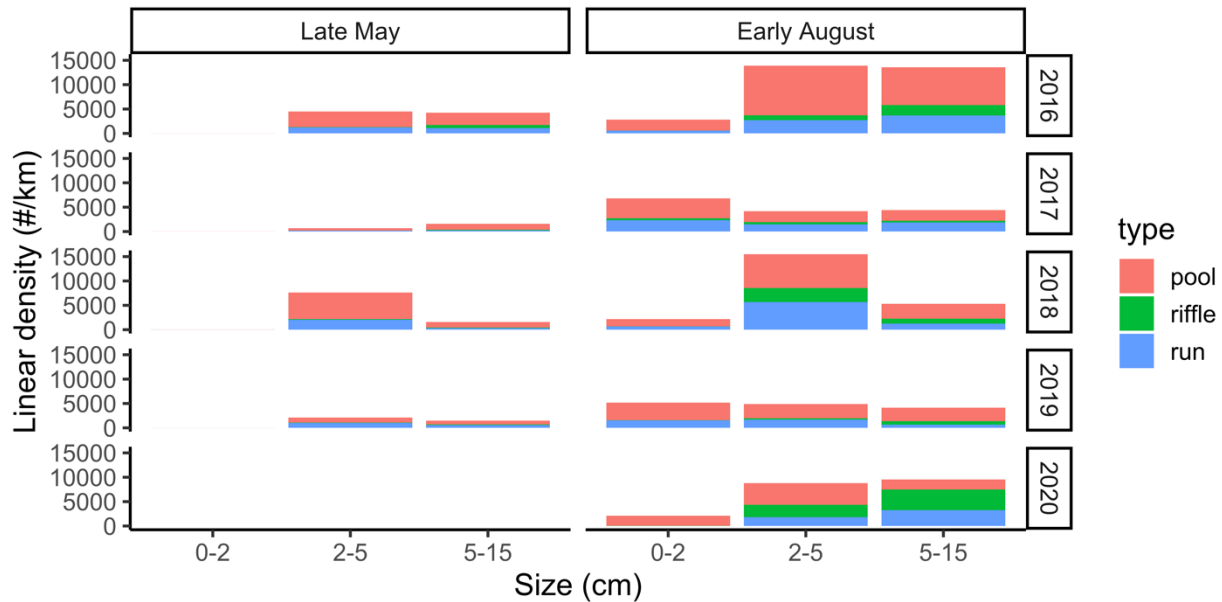
Figure 6. Stacked histograms of linear densities of Coast Range Roach (*Hesperoleucus venustus*) calculated by summing the total counts within each season of each year and dividing by the total distance surveyed. Size classes are on the x-axis, the left columns of plots depict late May surveys and right columns show early August surveys, rows of plots correspond to years. Colors depict habitat types. No surveys occurred in Late May of 2020.
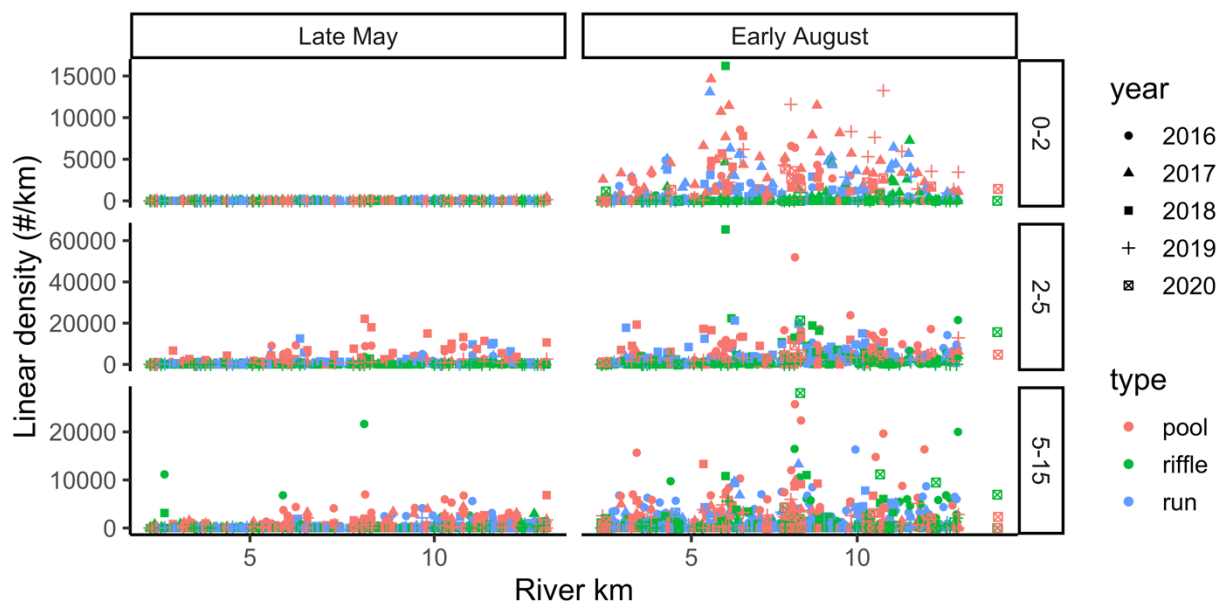
Figure 7. Linear densities of Coast Range Roach (*Hesperoleucus venustus*) calculated by summing the total counts within each unit and dividing by its length. Densities are plotted against River km which increases downstream. Each point represents one

survey. Left column of plots show surveys in late May and the right Surveys in early August. Rows of plots correspond to size classes. Years are shown as shapes and habitat types as colors.

Roach Fry, 0-2cm: Counts of the smallest size class of roach varied by Season, Year, Habitat type, River km and Year x River km (generalized linear mixed-effect model, supplemental table 1). Very few roach fry were seen in the early season surveys in any year (Figures 6 & 7). The highest density occurred in 2017 (2588 individuals/ km), which was 298% greater than and the lowest density 2018 (869 individuals/km). Roach fry (0-2 cm) were most numerous in pools, then runs, then riffles (mean densities 2838, 1250, 147 individuals/km respectively), and slightly more abundant upstream (GLMM, p <0.001). However, River km interacted significantly with year. Proportionately, roach were most numerous upstream in 2018 and most numerous downstream in 2019.

Juvenile Roach, 2-5cm: Counts varied by Season, Year, Habitat type, River km, and significant interactions occurred between Year x River km, Season x River km, and Season x Year x River km (Figures 6 & 7, supplemental table 1). 2-5cm roach were 238% more abundant in Early August compared to late May (3678 and 1541 individuals/ km respectively). The highest densities occurred in 2018 (4034 individuals/ km), which were 298% greater than the lowest densities in 2017 (943 individuals/km, Figure 6). Like roach fry, 2-5cm roach were found most frequently in pools, followed by runs, and were least common in riffles (mean densities 4088, 2076, and 624 individuals/ km respectively), however, their habitat use changed by season. From late May to Early August densities increased in riffles by 1503%, 201% in pools, and 252% in runs (Figure 7). Counts were higher downstream, and varied with year (Figure 7, River km x year, supplemental table 1); 2-5 cm roach were proportionally most abundant upstream in 2017 and most at highest densities downstream in 2018 and 2019. The effect of River km also varied with season (River km x Season, Figure 7), 2-5cm roach were proportionally more abundant downstream in Late May than in Early August. Finally, this seasonal change in proportional densities downstream also varied across years (three-way interaction: River km x Season x Year), downstream densities changed least in 2017 and most in 2019.

Adult Roach, 5-15 cm: Counts varied by Season, Year, Habitat type, River km and significant interactions occurred between Year x River km, Season x River km, and Season x Year x River km (Figures 6 & 7, Supplemental table 1). For this largest size class of roach, adults, counts were on average 322% higher in Early August than in late May (2688 and 835 individuals/ km respectively, Figure 6). The highest counts of adults occurred in 2016 (3213 individuals / km) which were 278% higher than the lowest counts in 2018 (1150 individuals / km, Figure 6). Like the other size classes of roach, adult roach were found at highest densities in pools, then runs, and least dense in riffles (mean densities 2622, 1323, 757 individuals/ km respectively), and like the 2-5 cm roach, their habitat use changed by Season. In Early August Roach were 490% more abundant in riffles, 377% more abundant in runs, and 273% more abundant in pools (Figure 7). Adult roach were more abundant downstream, and like 2-5 cm roach there were significant interactions between River km x Year and River km x Season. Adult Roach cm roach were proportionally most abundant upstream in 2017 and most abundant downstream in 2018. Adult roach were proportionally more abundant downstream in late May. The seasonal change in densities downstream also varies by year, though this effect was much smaller than either the effect of season, year, or either of their interactions with River km (Supplemental Material Table 1.)

Sacramento Pikeminnow, Ptychocheilus grandis

In our 5 years of surveys 736 pikeminnow were counted, along 34.5 km for a density of 21.3 individuals/km.

Figure 8. Linear densities of Sacramento Pikeminnow, (*Ptychocheilus grandis*) calculated by summing the total counts within each season of each year and dividing by the total distance surveyed. Size classes are on the x-axis, the left columns of plots depict Late May surveys and right columns show early August surveys, rows of plots correspond to years. Colors depict habitat types. No surveys occurred in Late May of 2020.

Figure 9. Stacked histograms of linear densities of Sacramento Pikeminnow, (*Ptychocheilus grandis*) calculated by summing the total counts within each unit and dividing by its length. Each point represents one survey. Densities are plotted against River km which increases downstream. Left column of plots show surveys in late May and the right Surveys in early August. Rows of plots correspond to size classes. Years are shown as shapes and habitat types as colors.

Counts of juvenile/ sub-adult pikeminnow, 5 – 20 cm: varied by Season, Year, Habitat type, and River km, and a significant interaction occurred between River km x Year (Figures 8 &9, generalized linear mixed-effect model, Supplemental Material Table 2). None of this smallest

size class of pikeminnow were counted in any of the late May surveys. Also, none were counted in any units during 2016. Densities were highest in 2020 (83 individuals / km) which were 103% higher than in the least dense year, 2017 (0.8 individuals / km, Figure 8). Juvenile pikeminnow were most dense in pools, less dense in runs and least dense in riffles (6.3, 0.9, and 0.2 individuals/km respectively). Smaller pikeminnow were more likely to be found in downstream units (Figure 9), but their distribution varied dramatically between years. The Year x River km interaction had a larger effect than river km alone (River km x year, Table 2).

Adult Pikeminnow, 20 – 60 cm: Adult pikeminnow counts varied by Season, Year, Habitat type, River km, and a significant interaction occurred between River km and Year (Figures 8 & 9, generalized linear mixed-effect model, Supplemental Material Table 2). Few adult pikeminnow were counted in the Late May surveys, counts were much higher in Early August (0.5, and 14.0 individuals/ km respectively, Figure 9). The greatest densities occurred in 2020 (53.1 individuals / km) and the lowest in 2018, when none were seen during these surveys (Figure 8). All adult pikeminnow were counted across years (403 total) in pools. Like Juvenile/ sub-adult pikeminnow, adults were more likely to occur downstream (Figure 9), but the Year x River km interaction had a larger effect than River km.

Sacramento Sucker, Catostomus occidentalis

In our 5 years of surveys 2254 Sacramento Suckers were counted, along 34.5 km for an average density of 65.3 individuals/km.
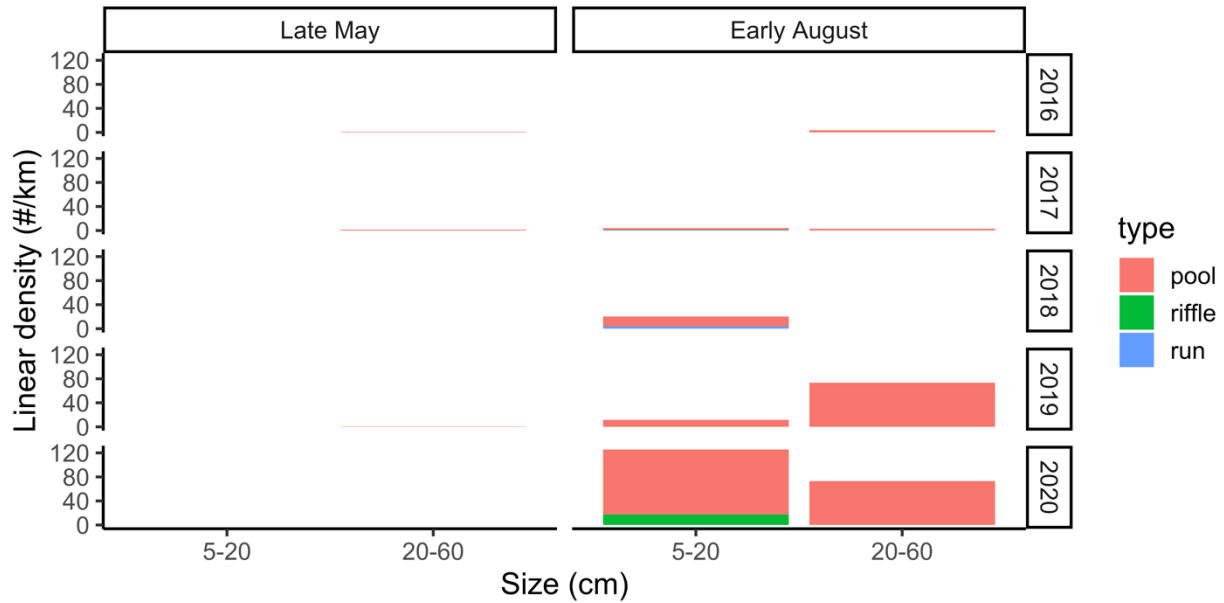

Figure 10. Linear densities of Sacramento Sucker, (*Catostomus occidentalis*) calculated by summing the total counts within each season of each year and dividing by the total distance surveyed. Size classes are on the x-axis, the left columns of plots depict Late May surveys and right columns show early August surveys, rows of plots correspond to years. Colors depict habitat types. No surveys occurred in Late May of 2020.
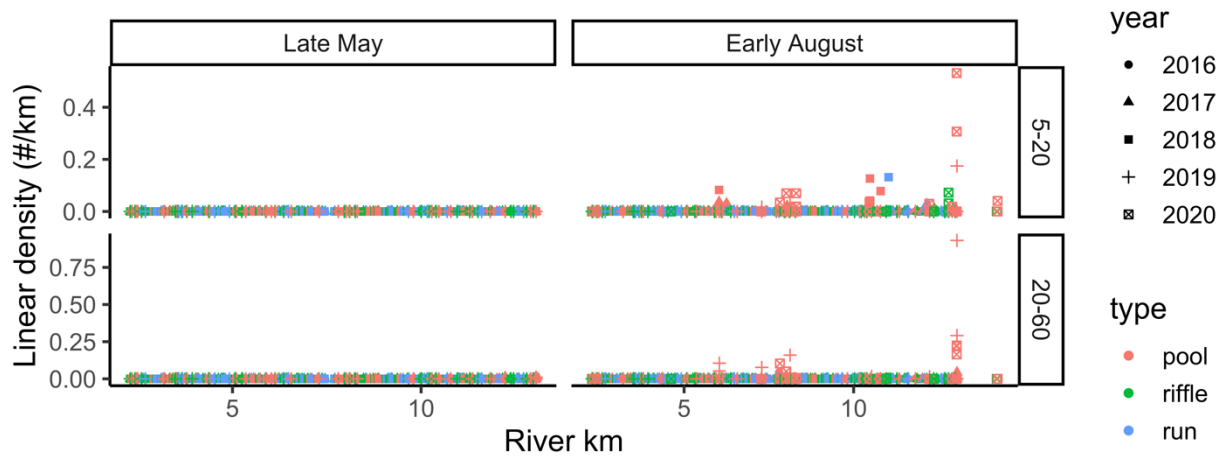
14

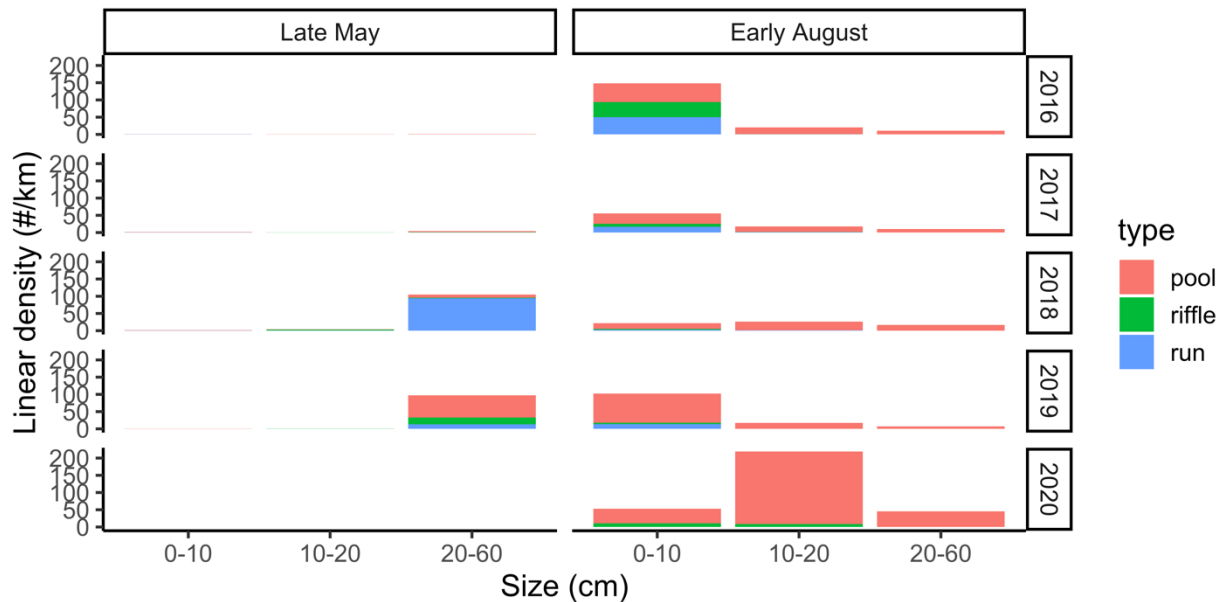*Figure 11.* Stacked histograms of linear densities of Sacramento Sucker, (*Catostomus occidentalis)* calculated by summing the total counts within each unit and dividing by its length. Each point represents one survey. Densities are plotted against River km which increases downstream. Left column of plots show surveys in late May and the right Surveys in early August. Rows of plots correspond to size classes. Years are shown as shapes and habitat types as colors.

Fry and Juvenile suckers, 0 – 10: Juvenile sucker counts varied by Season, Year, Habitat type, and River km, and there was a significant interaction between River km x year. Densities were highest in 2020 and lowest in 2018 (39.7 and 5 individuals / km respectively, Figure 10). Very few juvenile suckers were counted in Late May (20 across all years). Juvenile suckers showed the least habitat preference of all the sucker size classes, but still strongly favored pools, then runs and lastly riffles (24, 12, 9 individuals/ km respectively). Juvenile suckers were denser in downstream units, but their longitudinal densities varied by year (River km x Year, Figure 11)

Sub-adult suckers, 10 – 20 cm: Sub-adult sucker counts varied by Season, Year, Habitat type, and River km, and interactions between River km x year and River Km x Season were significant. Few sub-adult suckers were counted in late May across all years (16 total). The highest densities occurred in 2018 and the lowest in 2016 (6.6 and 2.3 individuals/ km, Figure 10) Sub-adult suckers showed a strong preference for pools over riffles and runs (9.1, 0.9, and 0.5 individuals / km respectively, Figure 11). Sub- adult suckers were more numerous downstream overall but were denser upstream in early August (River km x Season, Table 3). Longitudinally, densities varied by Year (River km x year, Supplemental Material Table 3, Figure 11).

Adult suckers, 20 – 60 cm: Adult suckers counts varied by Season, Year, Habitat type, and River km, and interactions between River km x year and River Km x Season were significant. More adult suckers were counted in Early August than Late May (3.4 and 2.7 individuals/ km) but counts varied less by season than in the smaller size classes. The lowest densities occurred in 2020 and the highest in 2019 (1.0 and 6.7 individuals/ km, Figure 10). Adult suckers were more abundant in pools compared to riffles and runs (6.0, 0.8 and 0.5 individuals/ km respectively), and all observations in riffles and runs occurred during Late May surveys (Figure 11). Linear densities were higher downstream, however, higher counts of adult suckers occurred upstream in early August compared to late May (River km x Season, Supplemental Material Table 3, Figure 11). Like the smaller size classes longitudinal distribution of linear densities interacted with year.

15

Chinook Salmon, Oncorhynchus tshawytscha

In our 5 years of surveys 834 Chinook Parr were counted along 34.5 km for an average density of 24.2 individuals/km, however almost all these counts occurred in one year, 2018.
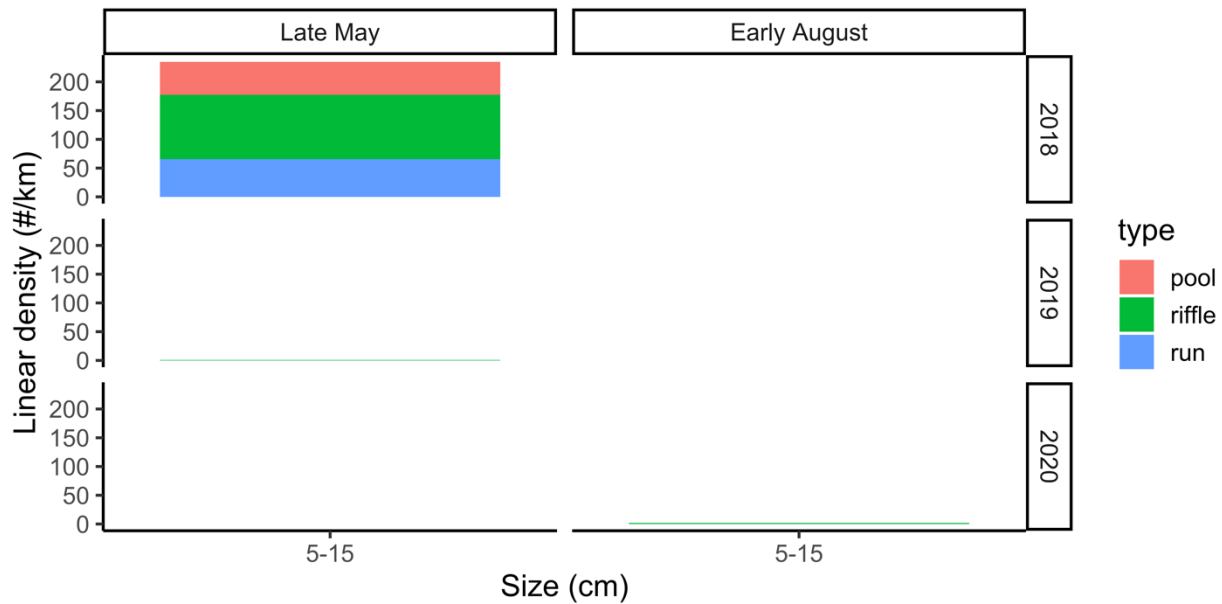
Figure 12. Stacked histograms of linear densities of Chinook Salmon, (*Oncorhynchus tshawytscha*) calculated by summing the total counts within each season of each year and dividing by the total distance surveyed. Size classes are on the x-axis, the left columns of plots depict Late May surveys and right columns show early August surveys, rows of plots correspond to years. Colors depict habitat types. No surveys occurred in Late May of 2020.
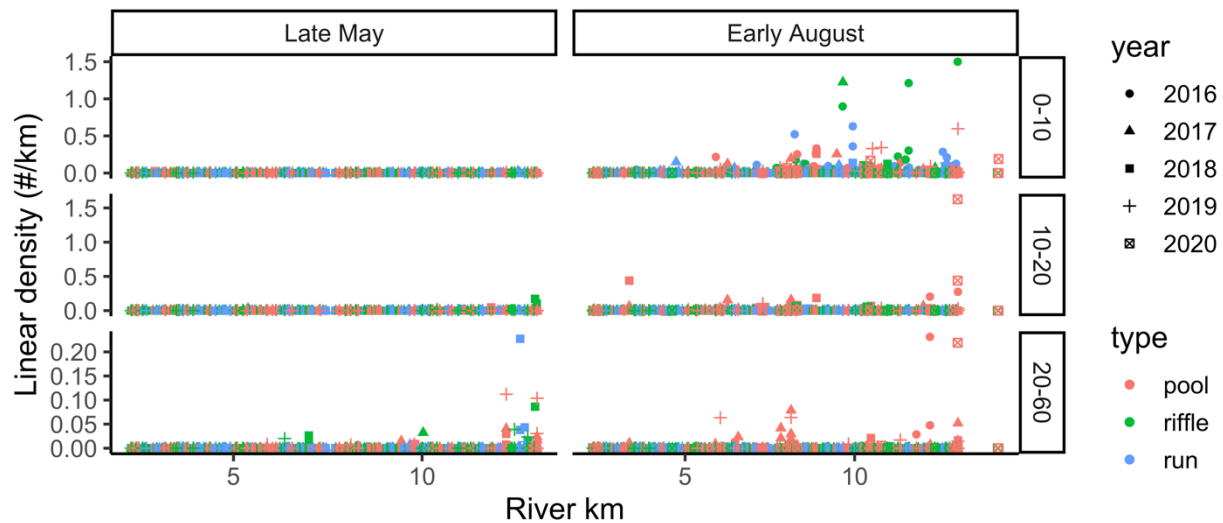

Figure 13. Linear densities of Chinook Salmon, (*Oncorhynchus tshawytscha* calculated by summing the total counts within each unit and dividing by its length. Each point represents one survey. Densities are plotted against River km which increases downstream. Left column of plots show surveys in late May and the right Surveys in early August. Rows of plots correspond to size classes. Years are shown as shapes and habitat types as colors.

Chinook parr, 5 – 15 cm: Seen in large numbers only during 2018 (Figure 12), when 832 (41.7 individuals/ km) were counted. One individual was seen in both 2019 and 2020. In 2018 counts varied by Habitat type and River km (generalized linear model, Figure 13, Supplemental Material Table 5). They were most common in riffles, then runs, and least common in pools (linear densities 42.3, 26.3, and 16.0 individuals / km respectively), and were denser in downstream units (Figure 13).

Coho Salmon, Oncorhynchus kisutch

In our 5 years of surveys 2161 Coho Parr were counted, along 34.5 km for an average density of 62.6 individuals/km.
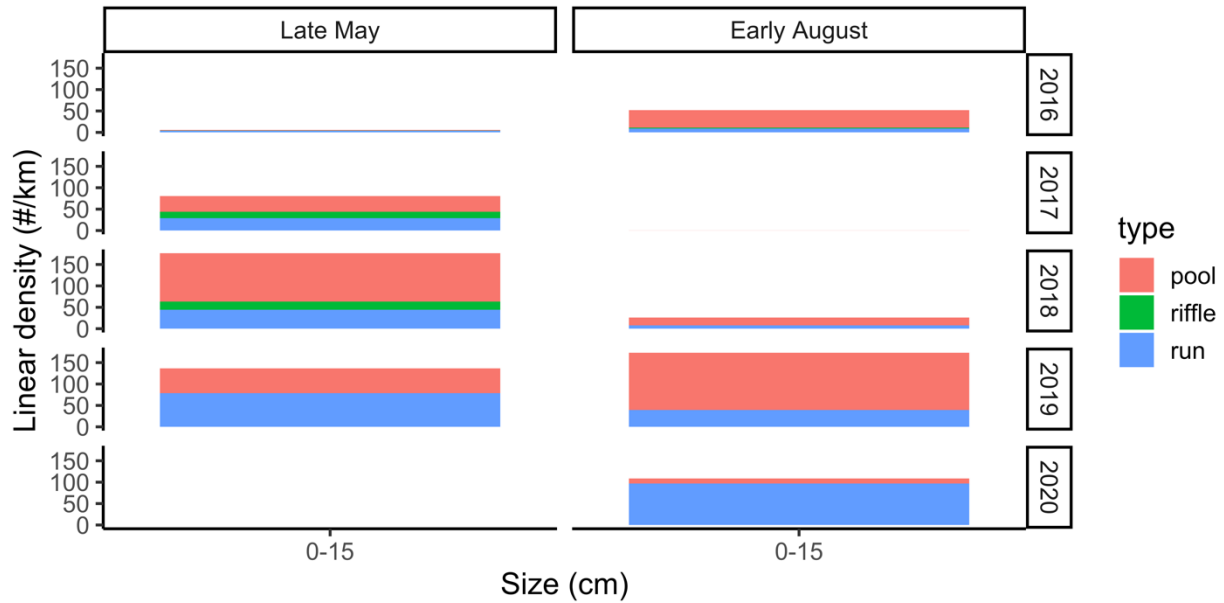
Figure 14. Stacked histograms of linear densities of Coho Salmon, (*Oncorhynchus kisutch*) calculated by summing the total counts within each season of each year and dividing by the total distance surveyed. Size classes are on the x-axis, the left columns of plots depict Late May surveys and right columns show early August surveys, rows of plots correspond to years. Colors depict habitat types. No surveys occurred in Late May of 2020.

Figure 15. Linear densities of Coho Salmon, (*Oncorhynchus kisutch* calculated by summing the total counts within each unit and dividing by its length. Each point represents one survey. Densities are plotted against River km which increases downstream. Left column of plots show surveys in late May and the right Surveys in early August. Rows of plots correspond to size classes. Years are shown as shapes and habitat types as colors.

Coho parr, 0 – 15 cm: Counts of coho parr varied by Season, Year, Habitat type, and River km. The best model also included the Year x River km, Year x Season, Habitat type x Season, River

17

Figure 18.18 The author (middle) and his lab mates Gabriel Rossi (left) and Keith Bouma-Gregson (right) congratulating each other and their advisor (Mary Power, the photographer) on original pieces of research. Photo taken before an Eyes on the Eel sampling event near Jordan Creek on the Mainstem Eel River June, 2017.

km x Season, and Season x Year x River km interactions (Figures 14 & 15, generalized linear mixed-effect model, Supplemental Material Table 6). Linear densities of Coho parr were 70% greater in Late May than Early August (37.1 and 21.3 individuals/ km). The highest densities occurred in 2019 and the lowest in 2016 (67.2 and 12.0 individuals/ km, Figure 14). Coho were densest in pools, followed by runs and were least dense in riffles (47.7, 21.4, 5.7 individuals / km), and this preference became more pronounced as summer progressed; Coho proportionally increased in pools (52% in late May and 77% in Early August, Figure 15) and decreased in riffles and runs (Season x Habitat Type). Coho were slightly denser downstream, on average, but were more abundant upstream in early August than in late May (Figure 15). Also, longitudinal distribution (River km) of Coho parr interacted with Year (River km x Year) and with Season within year (Season x River km x Year).

Steelhead, Oncorhynchus mykiss

Steelhead were the most abundant salmonid, and second most abundant fish in our study reach. In our 5 years of surveys 39,052 Steelhead were counted, along 34.5 km for an average density of 1131.9 individuals/km.
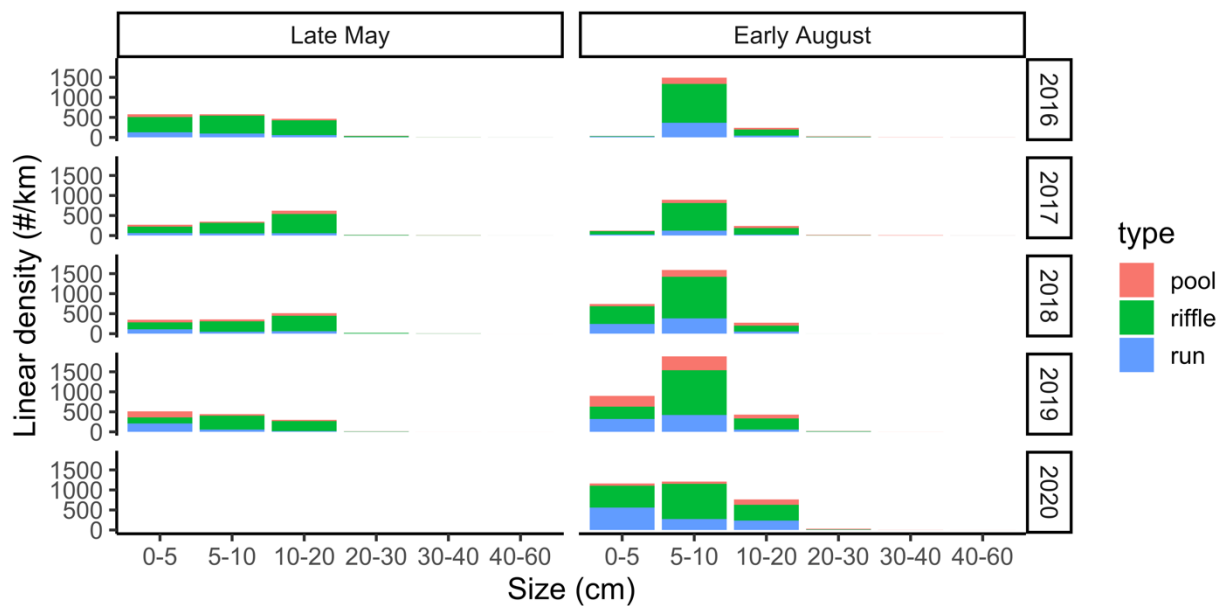
Figure 16: Linear densities of Steelhead, (*Oncorhynchus mykiss*) calculated by summing the total counts within each season of each year and dividing by the total distance surveyed. Size classes are on the x-axis, the left columns of plots depict Late May surveys and right columns show early August surveys, rows of plots correspond to years. Colors depict habitat types. No surveys occurred in Late May of 2020.
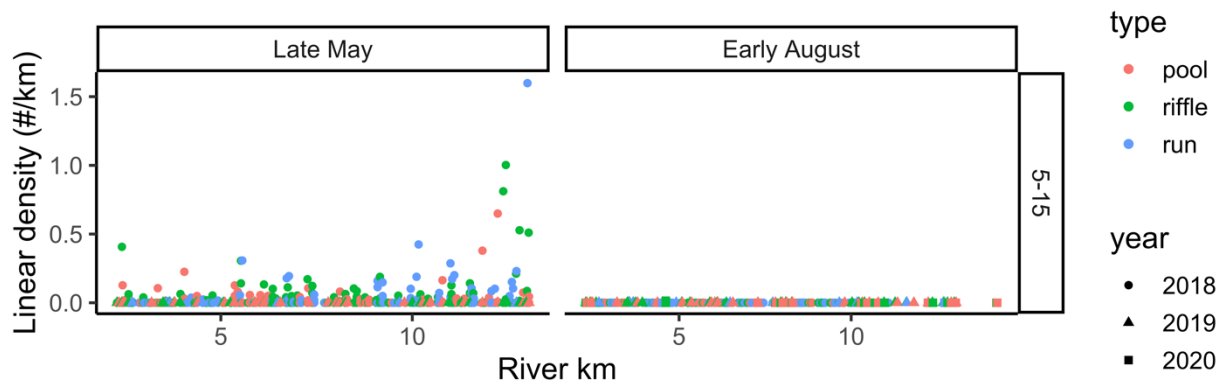
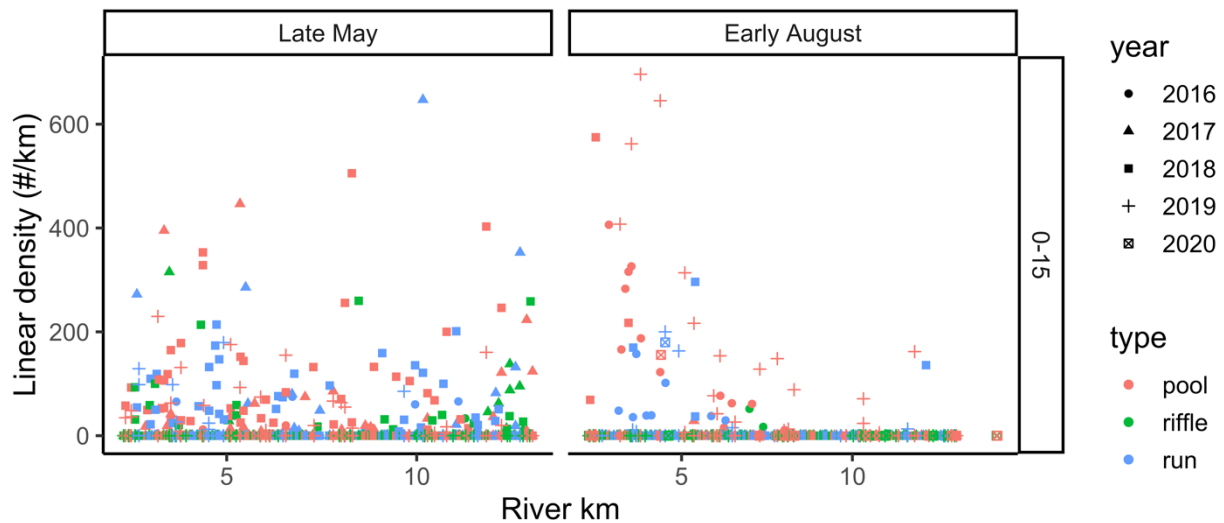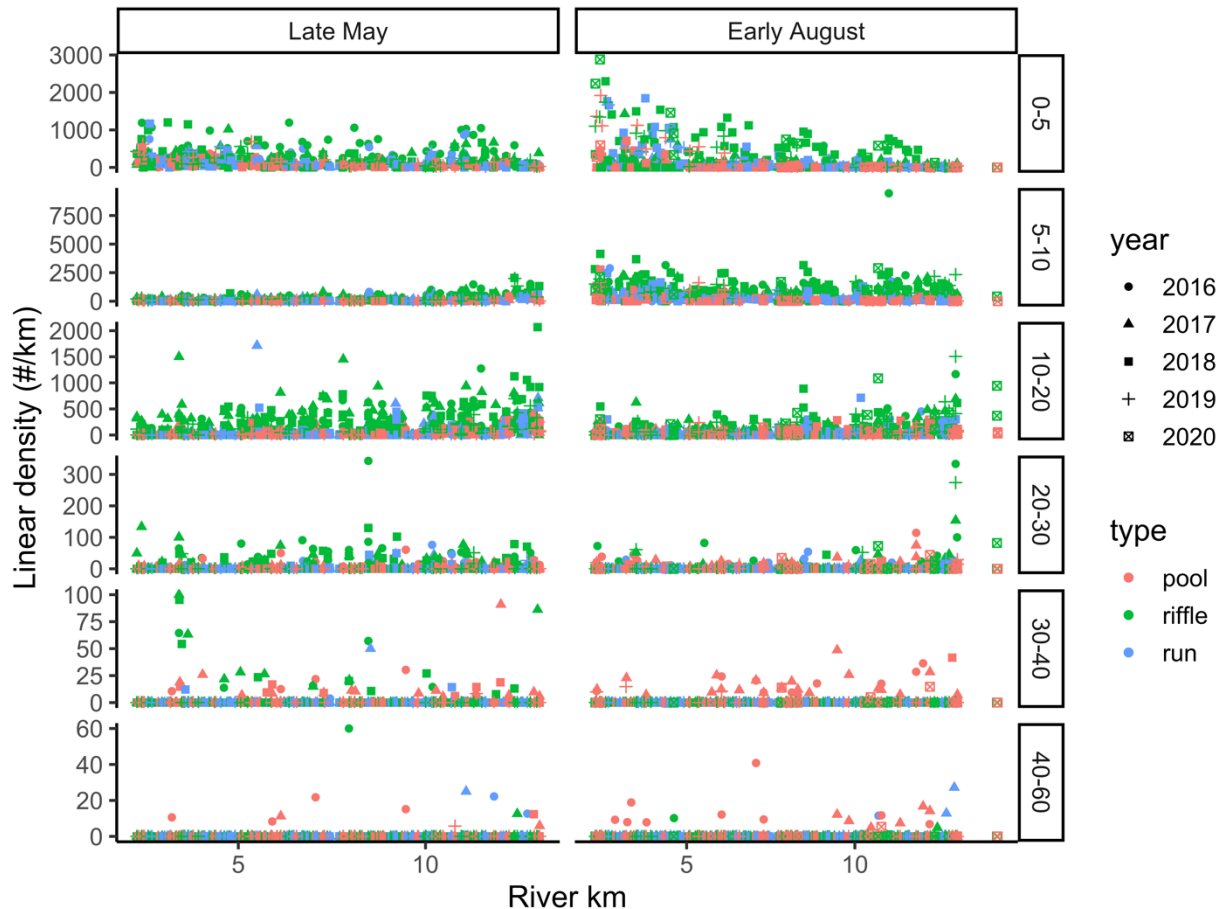*Figure 17:* Linear densities of Steelhead, (*Oncorhynchus mykiss*) calculated by summing the total counts within each unit and dividing by its length. Each point represents one survey. Densities are plotted against River km which increases downstream. Left column of plots show surveys in late May and the right Surveys in early August. Rows of plots correspond to size classes. Years are shown as shapes and habitat types as colors.

Steelhead fry, 0 – 5 cm: Counts of Steelhead fry varied by Counts varied by Season, Year, Habitat type, River km, and the best model included significant interactions between Season x Habitat type, Year x River km, Season x River km, and Season x Year x River km (generalized linear mixed-effect model, Figures 16 & 17, Supplemental Material Table 7). Steelhead fry linear densities were higher in early August than late May. The greatest densities occurred in 2019 and lowest in 2017 (224.9 and 56.8 individuals/ km, Figure 16). Steelhead fry were found most in riffles, then runs, and were least dense in pools (220.5, 119.1, and 74.4 individuals/ km respectively). However, their relative densities decreased as summer progressed in both pools and riffles but increased in runs. Longitudinal density was greater upstream (River km), and densities increased from late May to early August (River km x Season, Figure 17). Longitudinal density also interacted with year (River km x Year) and season within year (Season x River km x Year).

Small Steelhead parr, 5 – 10 cm: Counts of small Steelhead parr varied by Season, Year, Habitat type, River km, and the best model included significant interactions between Season x Habitat type, Year x River km, Season x River km, and Season x Year x River km (generalized linear

mixed-effect model, Figures 16 &17, Supplemental Material Table 7). Linear densities were higher in early August than late May (384.7 and 120.9 individuals / km). The highest densities occurred in 2019 and the lowest in 2017 (313.2 and 171.7 individuals/ km, Figure 16). Small steelhead parr were densest in riffles, then runs, and least dense in pools (618.0, 186.2, and 105.2 individuals/ km). Over the summer small parr proportionally increased slightly in pools and decreased slightly in riffles (Season x Habitat Type). Small parr were denser in downstream units, but denser upstream in Early August (Season x River km, Figure 17). Longitudinal density also interacted with Year (River km x Year) and Season within Year (Season x River km x Year).

Large Steelhead parr, 10 – 20 cm: Counts of small Steelhead parr varied by Season, Year, Habitat type, River km, and the best model included significant interactions between Season x Habitat type, Season x Year, Year x River km, Season x River km, and Season x Year x River km (generalized linear mixed-effect model, Figures 16 & 17, Supplemental Material Table 7). Linear densities were higher in late May than early August (139.0 and 89.9 individuals / km). The highest densities occurred in 2017, and the lowest in 2019 (118.8 and 102.6 individuals/ km, Figure 16). Large parr were most dense in riffles, followed by pools, and least dense in runs (289.3, 64.5, and 49.8 individuals/ km). Over the summer densities decreased in riffles and runs, but increased in pools (Season x Habitat Type, Figure 17). Large parr were denser in downstream units, however, densities upstream decreased in Early August (Figure 17). Densities varied longitudinally by Year, and Season within Year (River km x Year and Season x River km x Year).

Small adults and large potential smolts, 20 – 30 cm: Counts varies by Season, Year, Habitat type, River km, and the best model included significant interactions between Season x Habitat type, Season x Year, Year x River km, Season x River km, and Season x Year x River km (generalized linear mixed-effect model, Figures 16 & 17, Supplemental Material Table 7). Linear densities were higher in late May than early August (7.2 and 5.8 individuals / km). The highest densities occurred in 2016 and the lowest in 2018 (10.6 and 3.1 individuals / km, Figure 16). 20 – 30 cm steelhead were densest in riffles, followed by pools, and least dense in runs. Densities decreased 72.1% in riffles and 44.5% runs over the summer but increased 93.0% in pools (Figure 17). Densities were higher in downstream units, and over the summer this effect was more extreme (River km x Season, Figure 17). Densities also varied longitudinally by Year, and Season within Year (River km x Year and Season x River km x Year).

Adult steelhead/ resident Rainbow trout, 30 – 40 cm: Counts varied by Year, Habitat type, and the best model included significant interactions between Season x Habitat type, Season x Year, and Season x Year x River km (generalized linear mixed-effect model, Figures 16 & 17, Supplemental Material Table 7). The highest densities occurred in 2017 and the lowest in 2019 (3.1 and 0.6 individuals/ km, Figure 16) In late May adult steelhead were densest in riffles, then pools, and least dense in runs (2.8, 2.3, and 0.3 individuals / km). However, in early August no adult steelhead were seen in riffles or runs, all observations occurred in pools (3.6 individuals / km, Figure 17). Counts varied significantly between seasons within years (Season x Year, table 6). Longitudinal densities also varied between Seasons within Years (River km x Season x Year).

Large adult Steelhead, 40 – 60 cm: Counts varied by Year, Habitat type, River km, and Year x River km (generalized linear mixed-effect model, Figures 16 & 17, Supplemental Material Table 7).. The highest densities of this largest size class of steelhead occurred in 2016 and the lowest in 2018 (1.05 and 0.05 individuals/ km, Figure 16). Large adult steelhead were densest in pools, then riffles, then runs.

Three-spined Stickleback, Gasterosteus aculeatus

Three-spined Stickleback were the third most abundant fish species in our survey reach. In our 5 years of surveys 26,827 Three-spined Stickleback were counted, along 34.5 km for an average density of 777.6 individuals/km.
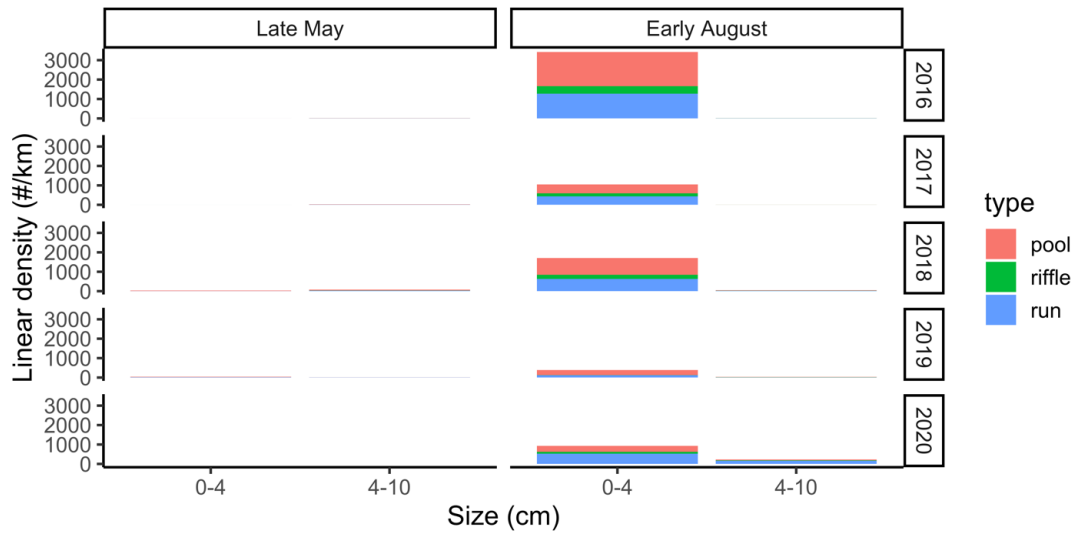
Figure 18. Stacked histograms of linear densities of Three-spined Stickleback, (*Gasterosteus aculeatus*) calculated by summing the total counts within each season of each year and dividing by the total distance surveyed. Size classes are on the x-axis, the left columns of plots depict Late May surveys and right columns show early August surveys, rows of plots correspond to years. Colors depict habitat types. No surveys occurred in Late May of 2020.

Figure 19. Linear densities of Three-spined Stickleback, (*Gasterosteus aculeatus*) calculated by summing the total counts within each unit and dividing by its length. Each point represents one survey. Densities are plotted against River km which increases

22

downstream. Left column of plots show surveys in late May and the right Surveys in early August. Rows of plots correspond to size classes. Years are shown as shapes and habitat types as colors.

Fry and juveniles 0 – 4cm: Counts varied by Season, Year, Habitat type, River km, Season x River km, and Year x River km (generalized linear mixed-effect model, Figures 18 & 19, Supplemental Material Table 4). Across all years a total of 25,771 fry and juvenile stickleback were counted. Densities were two orders of magnitude higher in early August than late May (645.9 and 6.4 individuals / km). The highest counts occurred in 2016 and the lowest in 2019 (624.6 and 97.8 individuals / km, Figure 18). Densities were highest in pools, then runs and least dense in riffles (436.2, 360.2, and 107.1 individuals/ km). Longitudinally, densities were higher downstream (Figure 19), and this became more pronounced in early August. Longitudinal densities also varied with Year (Year x River km)

Adults 4 – 10 cm: Counts varied by Season, Year, Habitat type, River km, Season x Habitat type, Season x River km, and Year x River km (generalized linear mixed-effect model, Figures 18 & 19, Supplemental Material Table 4). A total of 1056 stickleback were counted across all years. Densities were 17% higher in Late May than early August (14.7 and 12.5 individuals / km). The highest densities occurred in 2020 and the lowest in 2017 (26.7 and 5.7 individuals / km). Densities were highest in pools, then runs, and lowest in riffles (20.5, 10.8, and 4.8 individuals/ km respectively). However, over the summer densities increased in 104% in riffles, and decreased in 28 % in pools and 12 % runs. Longitudinally, in late May adult stickleback were slightly denser downstream, but this pattern reversed in early August when they were slightly denser upstream (Figure 19). Longitudinal densities also varied by Year (Year x River km)

Green Sunfish, Lepomis cyanellus

In our 5 years of surveys 206 Green Sunfish were counted, along 34.5 km for an average density of 6.0 individuals/km.
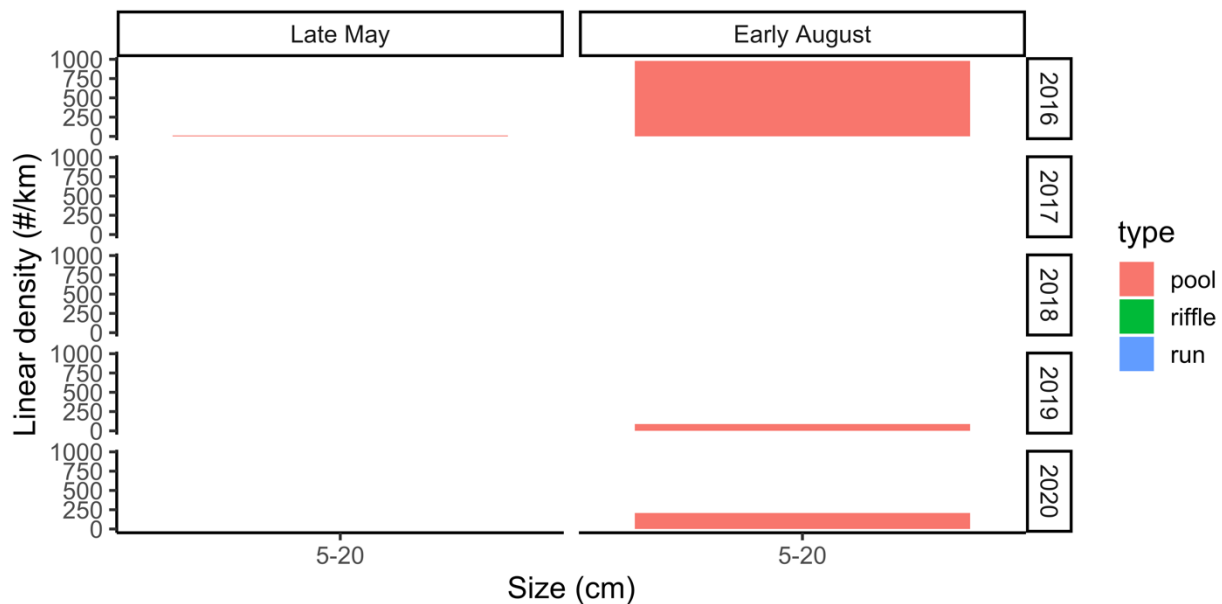
Figure 20. Stacked histograms of linear densities of Green Sunfish, (*Lepomis cyanellus*) calculated by summing the total counts within each season of each year and dividing by the total distance surveyed. Size classes are on the x-axis, the left columns of

Figure 21. Log transformed linear densities of Green Sunfish, (*Lepomis cyanellus*) calculated by summing the total counts within each unit and dividing by its length. Each point represents one survey. Densities are plotted again River km which increases downstream. Left column of plots show surveys in late May and the right Surveys in early August. Rows of plots correspond to size classes. Years are shown as shapes and habitat types as colors.

Juvenile & Adult, 5 – 20 cm: Counts varied by Habitat Type, Year, River km, and Year x River km (generalized linear mixed-effect model, Figures 20 & 21, Supplemental Material Table 9). All sunfish encountered were seen in pools. The highest densities occurred in 2016 when 159 were counted for a density of 7.5 individuals/ km (Figure 20). Densities were higher downstream, but upstream extent of sunfish varied by Year (River km x Year, Figure 21)

Brown Bullhead, Ameiurus nebulosus

One adult brown bullhead was seen tending to 350 fry in 2020. These individuals were in a large pool (Hunter's Pool) at river km 12.3.

Pacific Lamprey, Entosphenus tridentatus

In our 5 years of surveys 944 Pacific Lamprey were counted, along 34.5 km for an average density of 27.4 individuals/km.
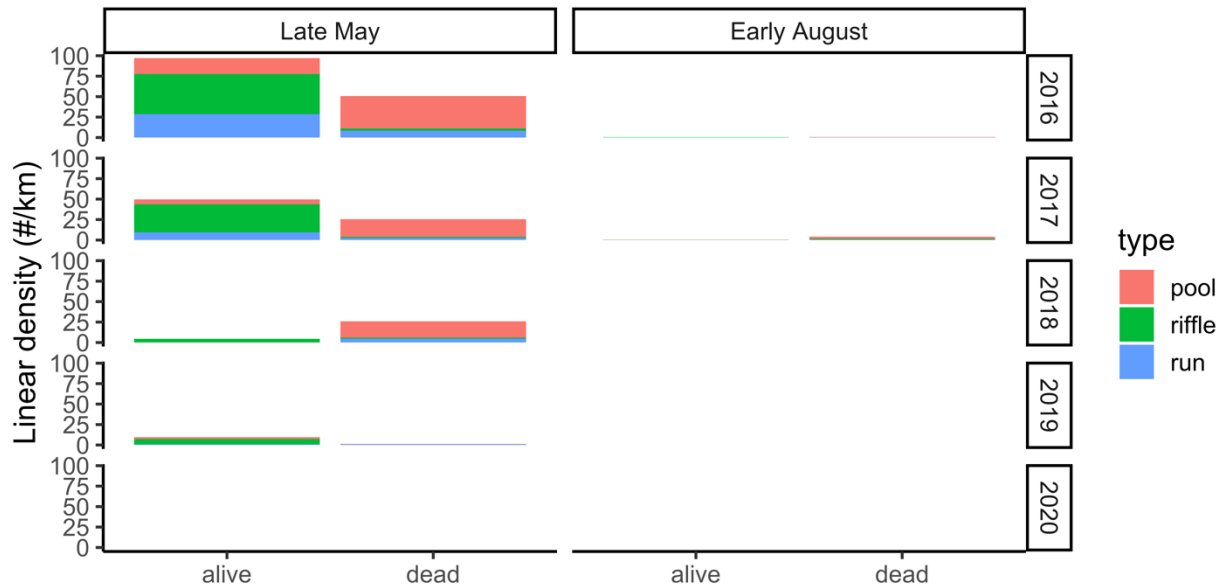
Figure 22. Stacked histograms of linear densities of Pacific Lamprey, (*Entosphenus tridentatus*) calculated by summing the total counts within each season of each year and dividing by the total distance surveyed. Individuals that were live or dead are shown on the x-axis, the left columns of plots depict Late May surveys and right columns show early August surveys, rows of plots correspond to years. Colors depict habitat types. No surveys occurred in Late May of 2020.
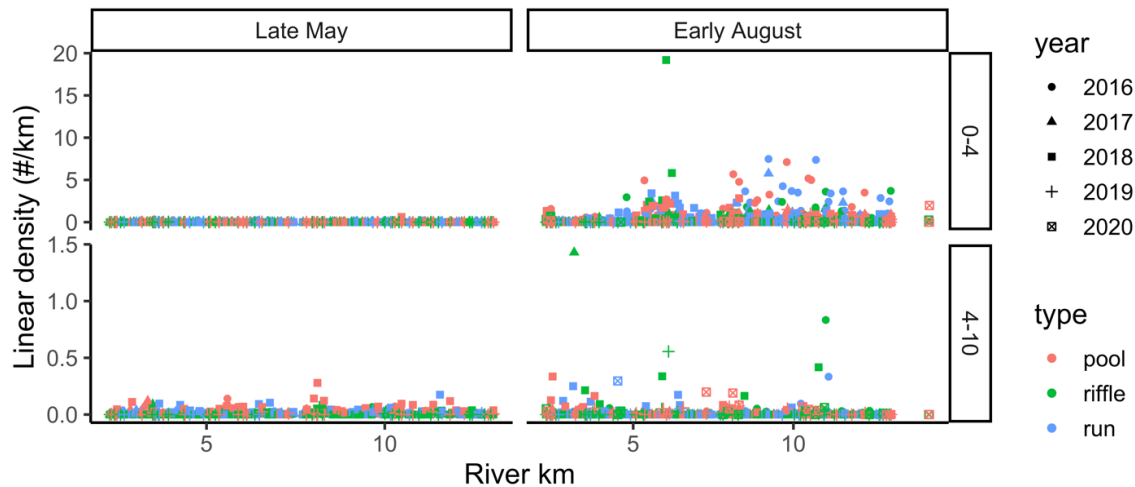

Figure 23. linear densities of Pacific Lamprey, (*Entosphenus tridentatus*) calculated by summing the total counts within each unit and dividing by its length. Each point represents one survey. Densities are plotted against River km which increases downstream. Left column of plots show surveys in late May and the right Surveys in early August. Rows of plots correspond to living or dead lamprey. Years are shown as shapes and habitat types as colors.

Lamprey counts vary by Season, Year and Habitat type (generalized linear mixed-effect model, Figures 22 & 23, Supplemental Material Table 8). 502 live lamprey were counted in late May, only 3 individuals were counted in Early August. The highest lamprey counts occurred in 2016 when 528 individuals (both dead and alive) resulted in a linear density of 12.5 individuals / km, no live lamprey were counted in 2020 (Figure 22). Live lamprey were most dense in riffles, intermediate in runs, and least dense in pools (13.1, 5.9, and 3.3 individuals/ km respectively).

Most dead lamprey were counted in pools, followed by runs, and fewest occurred in riffles (Figure 23).

American Bullfrog, Rana catesbeiana

A total of 1570 bullfrog larva were counted over 5 years. In our 5 years of surveys 1570 American Bullfrog Larvae, along 34.5 km for an average density of 45.5 individuals/km.
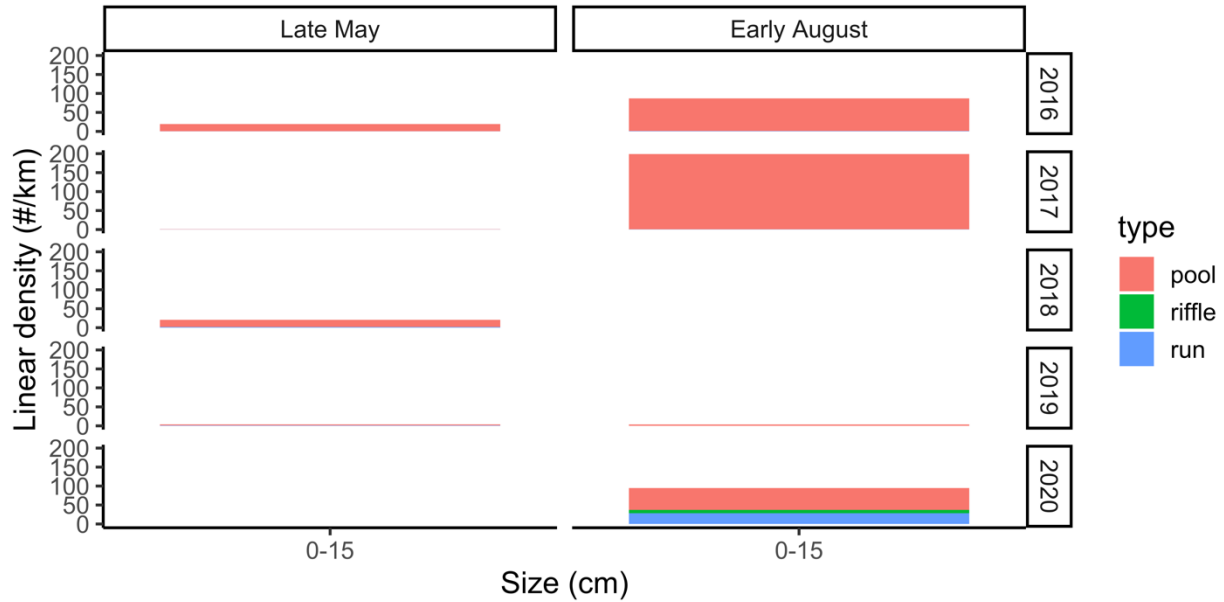
Figure 24. Linear densities of American Bullfrog larva (*Rana catesbeiana*) calculated by summing the total counts within each season of each year and dividing by the total distance surveyed. Size classes are on the x-axis, the left columns of plots depict Late May surveys and right columns show early August surveys, rows of plots correspond to years. Colors depict habitat types. No surveys occurred in Late May of 2020.

Figure 25. Linear densities of American Bullfrog larva (*Rana catesbeiana*) calculated by summing the total counts within each unit and dividing by its length. Each point represents one survey. Densities are plotted against River km which increases downstream. Left column of plots show surveys in late May and the right Surveys in early August. Rows of plots correspond to size classes. Years are shown as shapes and habitat types as colors.

Larva, 5 – 15cm: Counts varied by Season, Year, Habitat type, River km, River km x Season, and River km x Year (generalized linear mixed-effect model, Figures 24 & 25, Supplemental Material Table 10). Linear densities of larva were much higher in early August than late May (34.5 and 4.9 individuals/ km). The highest densities occurred in 2017 and the lowest in 2019 (41.5 and 1.9 individuals / km, Figure 24). 97% of observations occurred in pools (Figure 24). Longitudinally, downstream units were denser (River km, Figure 24), and they became more so over the summer (River km x Season, Figure 25). Longitudinal densities also varied by Year (River km x Year).

Rough-skinned Newt, Taricha granulosa
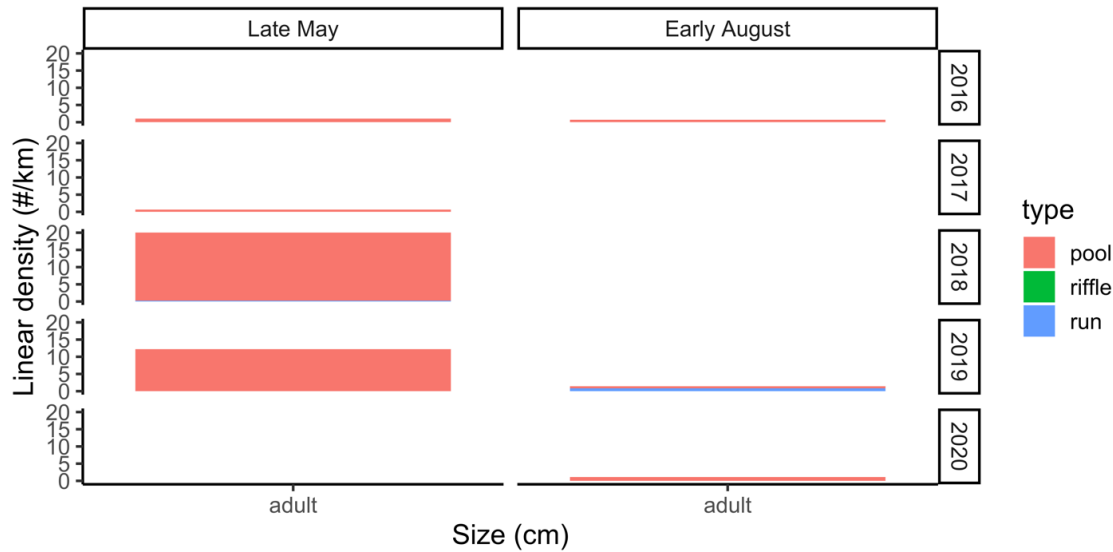
Figure 26. Stacked histograms of linear densities of Rough-skinned Newt (*Taricha granulosa*) calculated by summing the total counts within each season of each year and dividing by the total distance surveyed. Size classes are on the x-axis, the left columns of plots depict Late May surveys and right columns show early August surveys, rows of plots correspond to years. Colors depict habitat types. No surveys occurred in Late May of 2020.
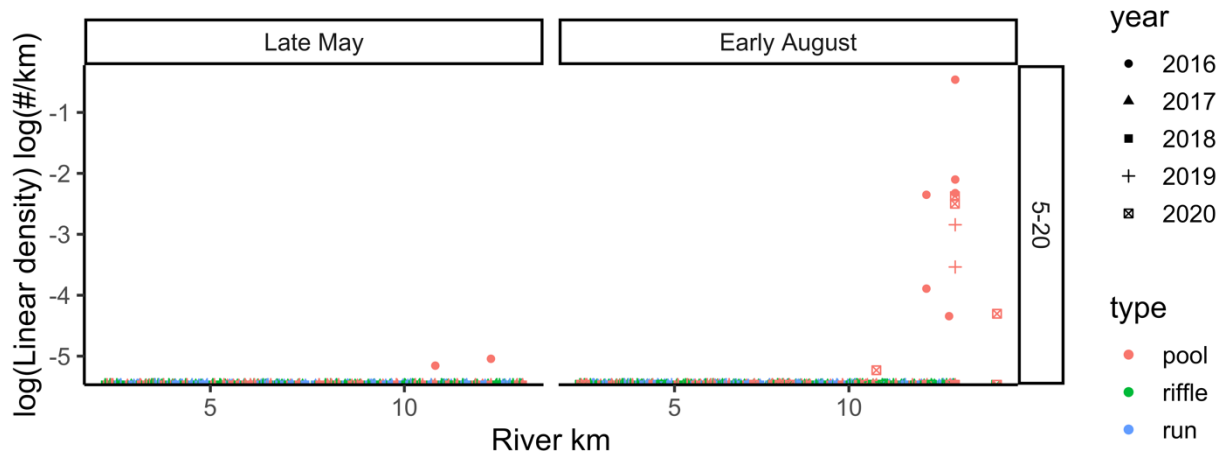

Figure 27. Linear densities of Rough-skinned Newt (*Taricha granulosa)* calculated by summing the total counts within each unit and dividing by its length. Each point represents one survey. Densities are plotted against River km which increases downstream.

Left column of plots show surveys in late May and the right Surveys in early August. Rows of plots correspond to size classes. Years are shown as shapes and habitat types as colors.

Adult, 5-10 cm snout-vent length: 23 adult Rough skinned newts were seen during all five years, 21 we observed in pools, and 2 in runs.

Aquatic Garter Snake, Thamnophis atratus
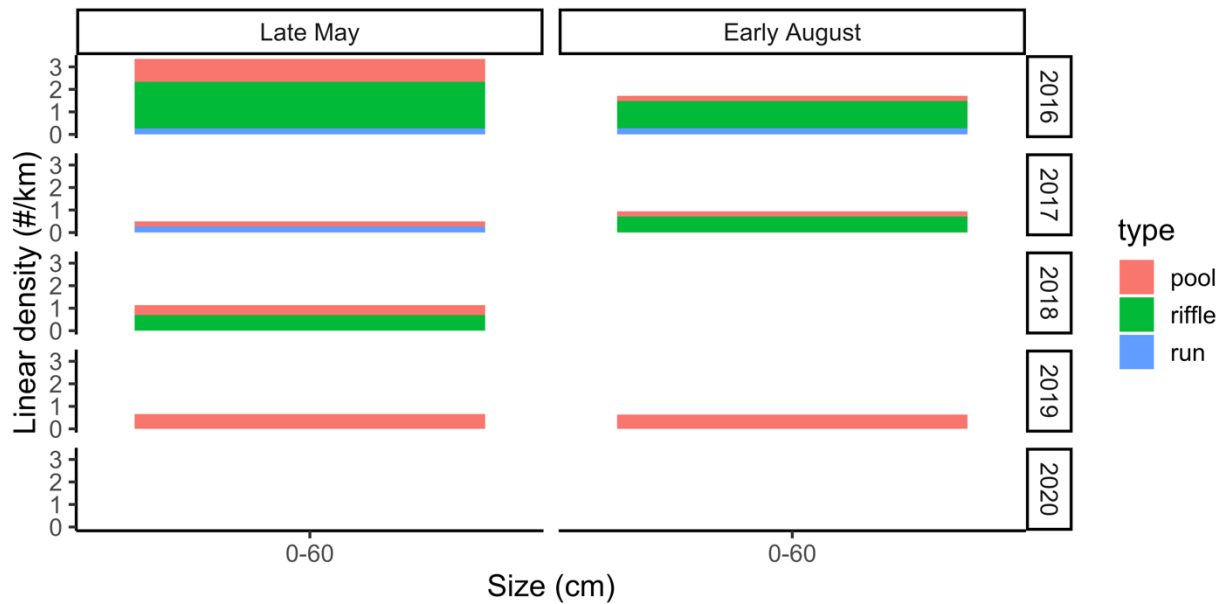
Figure 28 Stacked histograms of linear densities of Aquatic Garter Snake (*Thamnophis atratus)* calculated by summing the total counts within each season of each year and dividing by the total distance surveyed. Size classes are on the x-axis, the left columns of plots depict Late May surveys and right columns show early August surveys, rows of plots correspond to years. Colors depict habitat types. No surveys occurred in Late May of 2020.
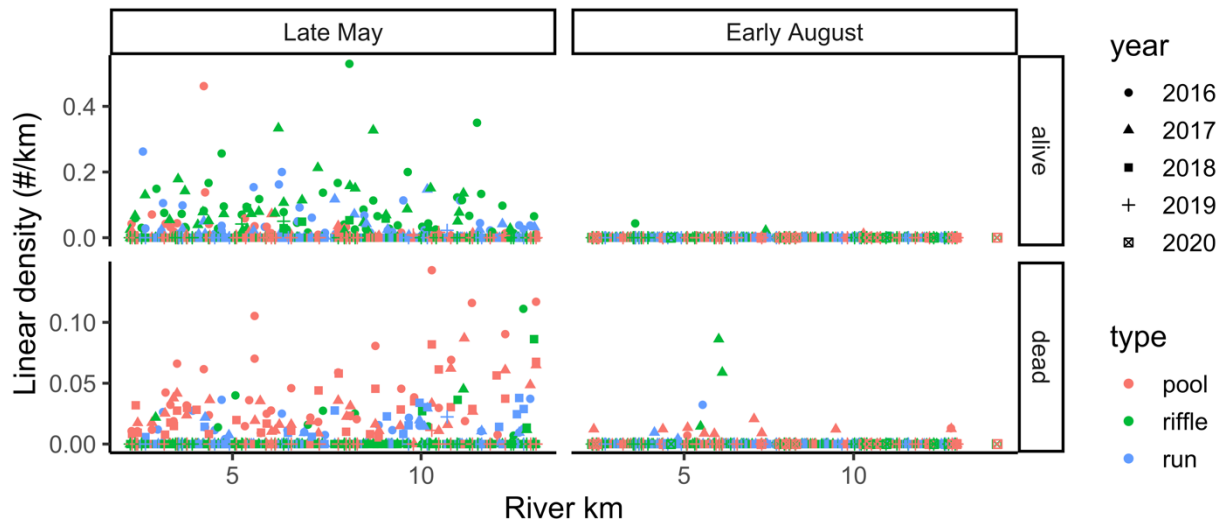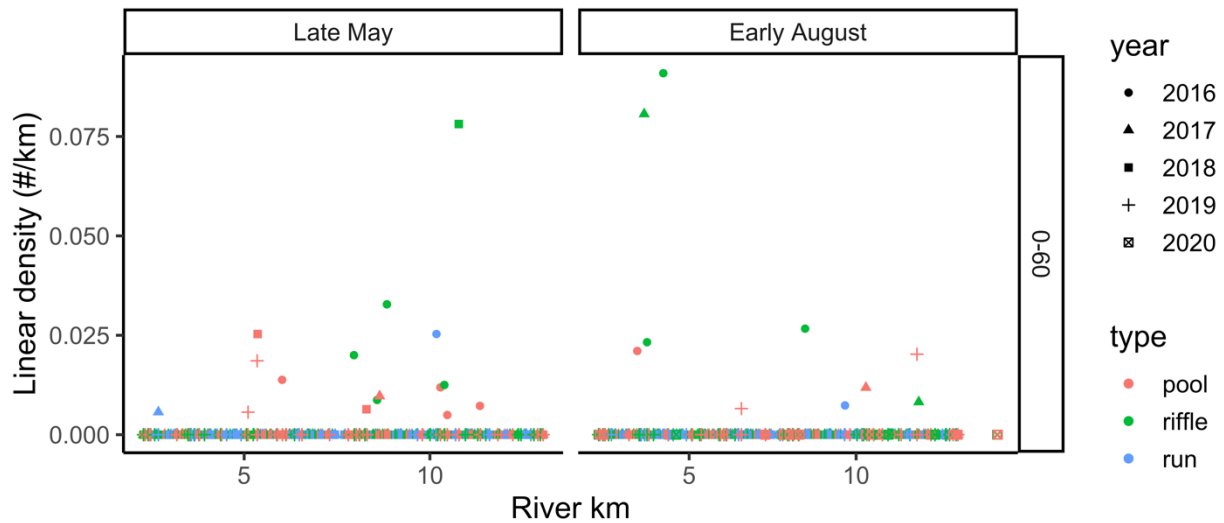

Figure 29. linear densities of Aquatic Garter Snake (*Thamnophis atratus)* calculated by summing the total counts within each unit and dividing by its length. Each point represents one survey. Densities are plotted against River km which increases downstream. Left column of plots show surveys in late May and the right Surveys in early August. Years are shown as shapes and habitat types as colors.

Adults and juveniles, 0 -60 cm: 29 aquatic garter snakes were counted during surveys, Highest count was 16 in 2016. Snakes were most dense in riffles, then pools, and least dense in runs (0.7, 0.4, and 0.1 individuals/ km, Figure 28)

Western Pond Turtle, Actinemys marmorata

In our 5 years of surveys 95 Western Pond Turtles were counted, along 34.5 km for an average density of 2.7 individuals/km.
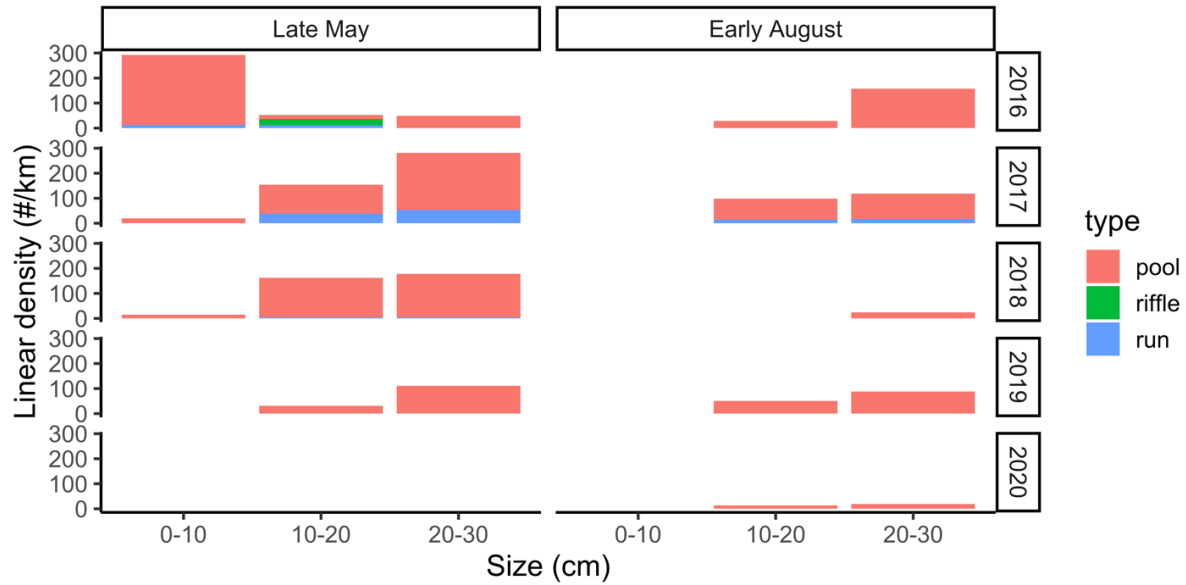
Figure 30. Stacked histograms of linear densities of Wester Pond Turtle (*Actinemys marmorata)* calculated by summing the total counts within each season of each year and dividing by the total distance surveyed. Size classes are on the x-axis, the left columns of plots depict Late May surveys and right columns show early August surveys, rows of plots correspond to years. Colors depict habitat types. No surveys occurred in Late May of 2020.
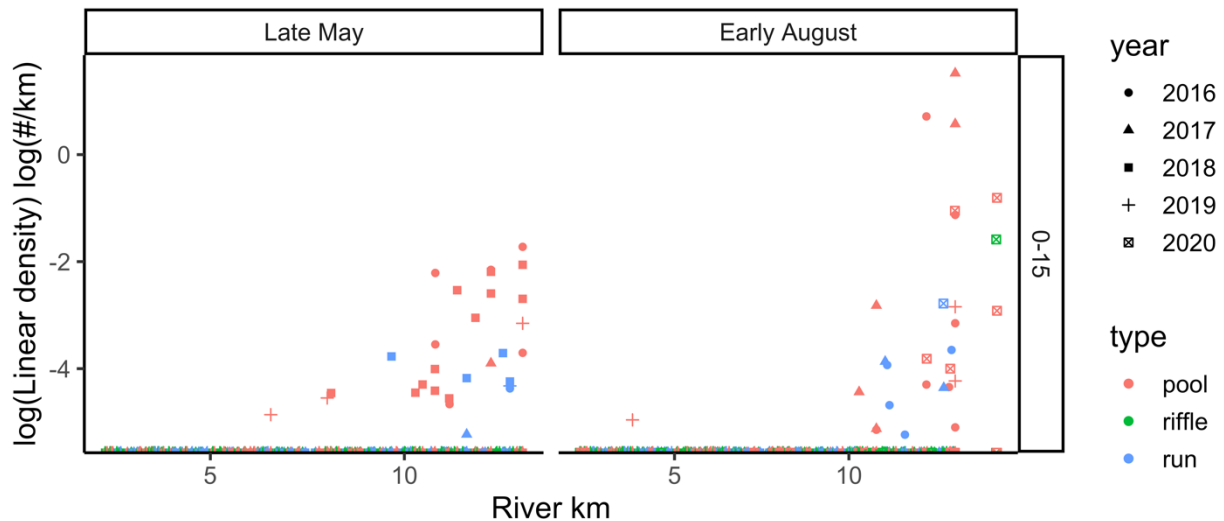
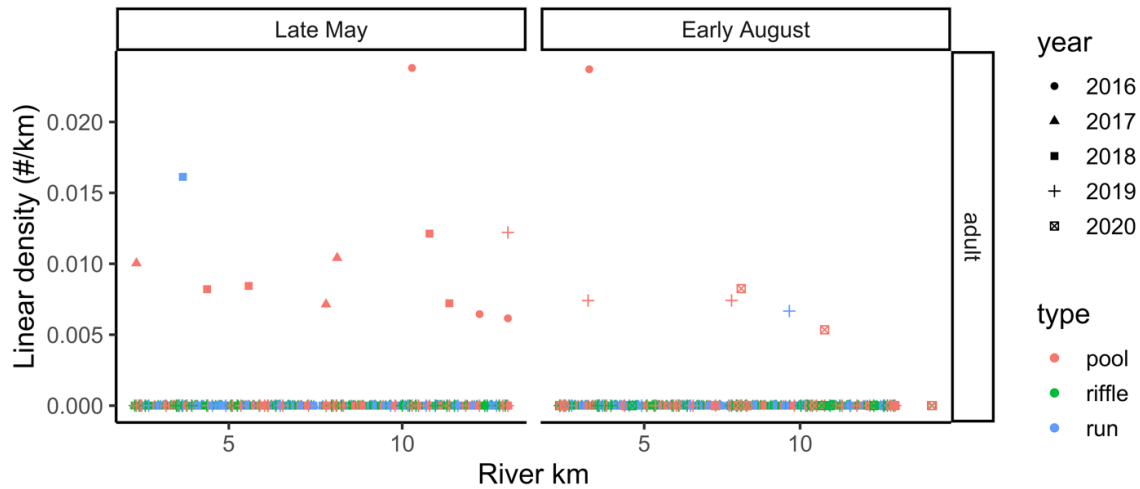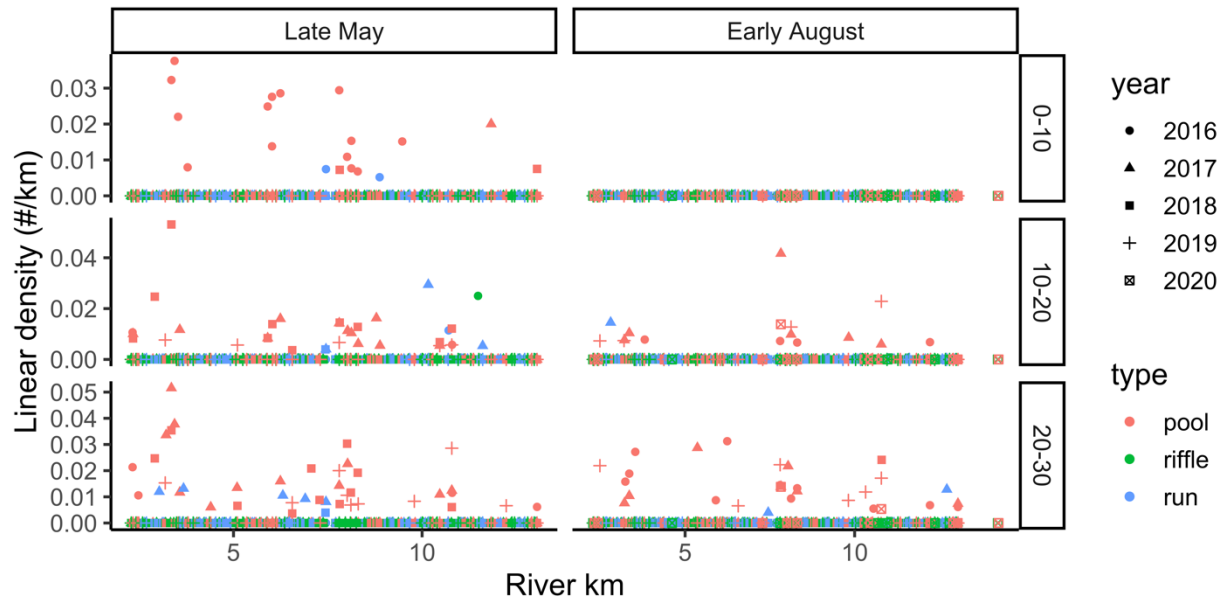*Figure 31. L*inear densities of Wester Pond Turtle (*Actinemys marmorata* calculated by summing the total counts within each unit and dividing by its length. Each point represents one survey. Densities are plotted against River km which increases downstream. Left column of plots show surveys in late May and the right Surveys in early August. Rows of plots correspond to size classes. Years are shown as shapes and habitat types as colors.

Juvenile and adult turtles, 0 – 30cm: Counts of pond turtles varied by Season, Year, and Habitat type. Densities were highest in late May and decreased into August (1.8 and 0.7 individuals/ km). The highest densities occurred in 2016 and the lowest in 2020 (1.6 and 0.8 individuals / km, Figure 30). Pond turtles were most dense in pools, then runs (2.5 and 0.4 individuals / km) and a single individual was seen in a riffle (Figure 30).

Discussion

Counts of all species-size class combinations varied annually. Sixteen of 18 species- size class combinations varied seasonally, and all species varied longitudinally and by habitat type. Often these spatial and temporal effects interacted. Many of the non-native organisms became more abundant downstream in the later summer and preferred pools (Sacramento Pikeminnow, California Roach, Green Sunfish, and American Bullfrog). In contrast, the native species were more abundant upstream in the late summer (smaller size classes of Steelhead, Coho, and Three-spined Stickleback). Understanding how the timing of each species' life history events dictates where and when they are likely to occur is necessary to assess more accurate population numbers and predict the importance of species interactions. Depending on study objectives, monitoring and sampling designs should be scaled appropriately in time and space to reflect life history phenologies, and other factors affecting spatio-temporal dynamics of target species. Below, we expand on each species patterns and suggest how the life histories of the species we encountered drive their distributional dynamics and highlighting future directions of study and monitoring design.

North Coast Range Roach, Hesperoleucus venustus

Eel River roach are non-native, and the population results from introductions from the Russian river (Baumsteiger et al. 2017, Baumsteiger and Moyle 2019). Roach were the most numerous fish in our survey reach. Roach fry typically hatch in May and emerge from sediments in June, likely depending on water temperature during the spring. Fry inhabit the shallow water marginal areas of pools and runs dominated by sedges and growths of the filamentous green algae, *Cladophora glomerata.* Our survey technique certainly systematically undercounts roach fry, since the shallow areas are challenging to see into, and roach fry hide effectively when they are small. Juveniles and adult roach become more abundant throughout the season, though the cause of this could be immigration or increased activity as water temperatures warm. Roach are relatively long-lived and a 10 cm individual is probably between 3 and 8 years (Fry 1936). All roach size-classes were more likely to be in slow water areas (pools and runs) than faster moving habitats. Spawning occurs in riffles and shallow runs throughout the late spring and early summer. Part of the increase in adults in riffles in August could be related to these activities. Longitudinally, roach densities varied with Season, Year, and Season x Year suggesting that the conditions within a year (flow, temperature, and abundance of predators) are important in determining the densities of roach. Also, as the most numerous small fish in the study reach, they

are important prey for many species, and predation pressure almost certainly influences their densities within any year. Roach respond to the presence of predators by shifting their microhabitat use. Brown and Moyle (1991) found roach were more likely to be found in riffles in the presence of pikeminnow. In 2018, we found roach used shallower areas of pools when predators were more dense (Supplemental Material Figure 1) Interestingly, in the lower South Fork and mainstem Eel river, downstream of our study reach, were temperature and forage conditions seem suitable, roach densities are lower than those observed in the headwaters. Abundance of pikeminnow in these downstream reaches seems likely to contribute to these lower densities.

Sacramento Pikeminnow, Ptychocheilus grandis

These non-native large piscivores are seasonally absent from our study reach in the winter and early spring, and migrate upstream each year in late spring or early summer. The timing of this migration varies with spring temperatures, in warmer years they migrate earlier (see Chapter 2). No spawning occurs in the upper reaches of the South Fork, and even the smaller size classes observed in our study reach were capable of consuming small fish. We observed an approximately 12 cm individual catch and consume a 4cm roach. Pikeminnow numbers also varied dramatically year to year, as do their longitudinal densities. Downstream dynamics likely drive this variation. Their migration is likely forage motivated, so relative densities of prey and conspecifics downstream could motivate greater or fewer individuals to migrate. Harvey and Nakamoto (1999) tracked an individual that moved 23km downstream during winter, and it returned to near its original location the following summer. Pikeminnow also moved out of their preferred daytime habitat of pools at night, probably to hunt in adjacent riffles and runs (Harvey and Nakamoto 1999). It is unclear what proportion of the population takes part in such movements, and the spatial extent that migration occurs in the South Fork Eel. Future studies documenting these aspects of the species movement could greatly improve its management.

Sacramento Sucker, Catostomus occidentalis

Sacramento suckers are one of the larger native fish in the study reach. Though Sacramento sucker microhabitat preference varies by life stage (Moyle and Baltz 1985), suckers of all size classes preferred pools. Fry became conspicuous in late May and early June, congregating in the shallow margins of pools, and often schooling with roach fry. Our survey counts suggest suckers migrate predictably upstream each summer in our study reach. Adults and juveniles were more commonly seen in downstream units in Late May and became more abundant in upstream reaches in early August. The timing of this movement coincides with the growth period of the filamentous green alga *Cladophora glomerata.* Suckers were often observed feeding in or resting nestled amongst *Cladophora* filaments. Foraging might be more profitable for these omnivores upstream later in the summer when *Cladophora* is colonized by the nutritious diatom *Epithemia turgida* (Power et al. 2009). They were also much more likely to occur in pools later in the summer. Spawning suckers were observed in 2 years, 2018 and 2019. These observations occurred downstream (~ River km 12.5) were around 10 25 – 50cm individuals congregated in a swiftly flowing reach downstream of the confluence of Ten-mile Creek with pebble substrate, surrounded by bedrock. Like pikeminnow, the density of suckers varied by year and longitudinally, a closer examination of what factors drive this variation would help manage these native fish.

Chinook Salmon, Oncorhynchus tshawytscha

Chinook parr were seen in great numbers in 2018. Reports of adult returns to the mainstem Eel, and lower South Fork Eel, suggest that high counts in 2018 do not reflect large changes in population levels (Eel River Recovery Project Fall Chinook Monitoring, https://www.eelriverrecovery.org/fall-chinook-assessment). More likely is that outmigration of juveniles was delayed this year, perhaps because of delayed spawning in the preceding winter, or cool spring temperatures in 2018 or an interaction of these factors. Chinook smolt outmigrate earlier in warmer years in other systems (Sykes et al. 2009), and 2018 was a relatively cool year (see Chapter 2 Figure 2 A.). The timing of our surveys does not match Chinook phenology well enough to accurately assess populations. Surveys would be more effective earlier in the spring for this species.

Coho Salmon, Oncorhynchus kisutch

The South Fork Eel River is one of the last strongholds for Coho Salmon in California (Yoshiyama and Moyle 2010). Coho counts varied substantially between years, likely reflecting differences in adult returns, and rearing conditions. However, accounts of Coho densities varying annually in some of the tributaries that feed our study reach are intriguing (Pers. Comm. Patrick Higgins, Redwood Creek, Jack of Hearts Creek, and Dutch Charlie Creek). Linking a systematic survey of these tributaries with mainstem observations could help us understand how Coho move between these habitats, and under what conditions mainstem habitat might be particularly important. Coho preferred slower velocity habitats (pools and runs) but were often seen drift foraging in velocities ranging from 30-50 cm/s, which is substantially greater than their reported preference in Washington streams (Beecher et al. 2002). Their densities were greater upstream in early August, probably driven in part by stressful downstream temperatures (Figure 5), but overlap with invasive predators, like Sacramento Pikeminnow, could also negatively influence Coho in downstream units as the summer progresses.

Steelhead, Oncorhynchus mykiss

Our steelhead counts showcase the amazing array of life history diversity in this species (Shapovalov and Taft 1954), Steelhead partition the study reach by size class, habitat type, space and time. Steelhead fry emerge from redds in early spring or late winter. Smaller size classes all preferred riffles. Higher concentrations of the smallest size class upstream in early August could be the result of increased movement into the mainstem from tributaries, and/ or movement downstream from upstream reaches. Depletion in numbers downstream could result from emigration, higher predation downstream, or more rapid growth of these year 0 fish in the warmer temperatures. Increases in the 5 – 10 cm size class over the season likely represent age 0 fish growing into this size class, and movement into the mainstem from tributaries. 10 – 20 cm steelhead distributions drop over the course of the season and are more concentrated downstream. These two surveys seem to capture snapshots of the smoltification and outmigration of this size class. These fish leave their natal tributaries in late spring (Kelson and Carlson 2019) and move into the mainstem. It appears that they spend some time in the mainstem and move downstream over the course of the summer. Though steelhead have been extremely well studied in this area (Kelson and Carlson 2019, Uno and Power 2015, Power et al. 2008, Suttle et al. 2004), the question of how important mainstem habitat is for juvenile steelhead rearing is still

open. Our observations suggest steelhead 10 – 20 and 20 – 30 cm use mainstem habitat from the time they outmigrate from their natal tributaries until late May, and some individuals are present into August. Steelheads' recorded variability in outmigration timing (Kelson and Carlson 2019, Busby et al. 1996) and overall flexibility in life history (Shapovalov and Taft 1954), along with the significant Year x River km interaction for this size class suggests they take advantage of beneficial conditions when they occur. Fish probably vary the amount of time they spend in mainstem depending on such conditions. Unlike smaller size classes, larger Steelhead are found more frequently in pools. Interestingly, their habitat use changes by season, occurring in riffles and pools in late May, but almost entirely in pools by early August. Many of the large pools in our study reach thermally stratify over the course of the summer. Larger fish might seek out the deeper areas of these temperature-stratified habitats to gain access to less stressful temperatures. Steelheads' flexible life history seems to allow them to distribute longitudinally in response to conditions within a given year. Understanding what drives these distributional shifts in mainstem use could help guide restoration efforts by expanding habitat that the fish determine is suitable.

Three-spined Stickleback, Gasterosteus aculeatus

Most stickleback in the upper South Fork Eel River probably live one year, dying after spawning and rearing young (Moyle 2012). Adults are more numerous in late May surveys, and surveys in early August often encountered dead adult stickleback. Fry emerge en-masse in June most years and grow throughout the summer season. The fish overwinter and court in the early spring. After successful courtship and egg deposition, males defend nests made of algae or other organic material, chasing away other fish and fanning the eggs with their pectoral fins. Stickleback tend to have irruptive years with very high densities, and others with lower densities. 2016 was one such irruptive year, when densities were very high. During such years, stickleback are important prey items, the author even saw a large Coast Range Roach, approximately 11cm eat a 2cm stickleback fry.

Green Sunfish, Lepomis cyanellus

Green sunfish are an invasive predator introduced to many western waters. Stocked in many private ponds, they inevitably enter flowing waters when these impoundments fail. In their native range they inhabit ponds, lakes, and slow-moving waterways (Moyle 2002) and can be fearsome predators where introduced (Lemley 1985). Their choice of only inhabiting pools in the upper South Fork Eel is not surprising. It seems likely the Tenmile creek, which is relatively warm water tributary and contains a high density of retention ponds, is a source in the upper South Fork Eel River. In our study reach, Green Sunfish are restricted to the more downstream units, but their upstream extent varied between years. Green sunfish likely prefer the warmer waters of downstream units (Figure 5). Sunfish are only abundant in certain years and are vulnerable to being washed out in high flows (Marchetti and Moyle 2001). The lowest counts occurred in 2017 and 2018, after the 2017 water year winter, which had the highest peak and greatest average flows (Figure 4).

Pacific Lamprey, Entosphenus tridentatus

Pacific lamprey showed large variation between years. In years when they are abundant, there are likely substantial benefits to other aquatic species through deposition of energy and nutrients

in the carcasses, but also through redd building behaviors (see Chapter 3). Live lamprey were found most in riffles, though after spawning their carcasses were displaced from these faster flowing areas and settled in low velocity pools and riffles (Figure 23). This spatial distribution of carcasses makes them most accessible to pool dwelling carrion-feeders. They might be of particular importance to Western Pond Turtles, which where were seen feeding on carcasses at the bottom of pools on multiple occasions.

American Bullfrog, Rana catesbeiana

American bullfrogs are another species that has been introduced throughout the world and are widespread in California (Kupferberg 1997). In the Eel River their larvae take two years to mature. Larvae are particularly vulnerable to high flows as they overwinter and scouring flows can greatly reduce the number that metamorphose into frogs the following summer (Kupferberg 1997). The lowest counts occurred in 2018 late summer surveys. Larvae counted during this survey would have needed to have overwintered the water year 2017, which had the highest peak flows and greatest average flow (Figure 4). Our observations suggest few survived. Like Green Sunfish, bullfrogs only occurred in slow water habitats (pools and runs, Figures 24& 25) in downstream units in our study reach, and their upstream extent varied by year.

Rough-skinned Newt, Taricha granulosa

Though we did not encounter many Rough-skinned newts in our surveys, they are a conspicuous member of the aquatic community in the upper South Fork Eel River. A few exploratory night surveys suggest that newts in this reach are predominantly nocturnal, emerging at night to feed. Densities at night were 10 – 30x higher than daytime surveys. For a more accurate assessment of their population, we suggest surveying at night.

Aquatic Garter Snake, Thamnophis atratus

Aquatic Garter snakes were encountered regularly during surveys. They preferred riffles and the cobble bars of pools to hunt from (Figures 28 & 29). Runs in our study reach are not usually associated with as much exposed rock and sunny patches on the banks for snakes to thermoregulate while hunting in the water. For surveyors seeking to assess aquatic garter snake population levels we feel slowly walking the banks would be more effective than snorkel surveys.

Western Pond Turtle, Actinemys marmorata

Western Pond Turtles were frequently encountered sunning on banks or foraging underwater during surveys. They occurred most frequently in slow water habitats. Though we analyzed all size classes in one statistical model, when examined with more size-class divisions, the smallest size class was far more abundant in 2016 than in any other year. Young turtles likely have very high mortality as they journey from their upslope nests to the river channel. Future turtle work could investigate the movement dynamics of individual turtles, and test other survey methods, like trapping, against snorkel surveys.

Foothill Yellow-legged Frogs, Rana boylii

Conspicuous in their absence from our counts are these river breeding frogs. This is because we avoided areas with large densities of larval yellow-legged frogs, when they were encountered, to avoid causing mortality. Snorkeling is not advisable for surveying this species. For a thorough discussion of survey methods, frog population patterns, and their relation to both physical and biotic conditions, see work by Kupferberg et al. (Kupferberg 1996, Kupferberg 1997, Kupferberg et al. 2009)

Conclusion

In rivers, longitudinal variation in species distributions sets the stage for organismal interactions. To our knowledge the data presented in this study constitutes one of the most extensive survey efforts in space, time, and species of animal counted in a coastal California river. We hope the variation in species in time and space will help inform future conservation, restoration and monitoring programs. Many conservation and restoration groups are interested in restoring the Eel River's iconic salmon runs, and one important aspect of this work will be limiting the negative impacts of invasive animals. Invasive species removal efforts should focus on areas with high overlap with native animals. Such areas could be disproportionally important habitat for native species, especially juvenile salmon. The historical aquatic vertebrate assemblage of the Eel River has shifted with novel species introductions. By investigating the conditions of that promote native species expansion downstream and inhibit invasive species extension upstream, it might be possible for restoration efforts to alter the balance in favor native species, especially at the interface between ranges in space and time.

Literature cited

Baumsteiger, J., and P. B. Moyle. 2019. A reappraisal of the California Roach/Hitch (Cypriniformes, Cyprinidae, Hesperoleucus/Lavinia) species complex. Zootaxa 4543:221–20.

Baumsteiger, J., P. B. Moyle, A. Aguilar, S. M. O'Rourke, and M. R. Miller. 2017. Genomics clarifies taxonomic boundaries in a difficult species complex. PLoS ONE 12:e0189417–22.

Baxter, C. V. 2002, January 23. Fish movement and assemblage dynamics in a Pacific Northwest riverscape.

Beecher, H. A., B. A. Caldwell, and S. B. DeMond. 2002. Evaluation of depth and velocity preferences of juvenile coho salmon in Washington streams. Transactions of the American Fisheries Society 22:785–795.

Bertness, M. D. 1991. Interspecific Interactions among High Marsh Perennials in a New England Salt Marsh. Ecology 72:125–137.

Brown, L. R., and P. B. Moyle. 1991. Changes in habitat and microhabitat partitioning within an assemblage of stream fishes in response to predation by Sacramento squawfish (*Ptychocheilus grandis*). Canadian Journal of Fisheries and Aquatic Sciences 48:849–856.

Brown, L. R., and P. B. Moyle. 1997. Invading species in the Eel River, California: successes, failures, and relationships with resident species. Environmental Biology of Fishes 49:271–291.

Connell, J. H. 1961. The influence of interspecific competition and other factors on the distribution of the barnacle Chthamalus stellatus. Ecology 42:710–723.

Fausch, K. D., S. Nakano, and S. Kitano. 1991. Experimentally induced foraging mode shift by sympatric charrs in a Japanese mountain stream. Behavioral Ecology 8:414–420.

Fry, D. H. 1936. The Life History of Hesperoleucus Venustus. California Fish and Game 22:65–98.

Goodman, D. H., and S. B. Reid. 2012. Pacific Lamprey (Entosphenus tridentatus) assessment and template for conservation measures in California. U.S. Fish and Wildlife Service, Arcata, California.

Whitehorne, I. 2010. Wintering Behavior, Physiology and Site Fidelity in a Partial Migrant, the American Dipper (*Cinclus mexicanus*). Waterbirds 33:461–470.

Kelson, S. J., and S. M. Carlson. 2019. Do precipitation extremes drive growth and migration timing of a Pacific salmonid fish in Mediterranean-climate streams? Ecosphere 10:e02618–17.

Kelson, S. J., M. E. Power, J. C. Finlay, and S. M. Carlson. 2020. Partial migration alters population ecology and food chain length: evidence from a salmonid fish. Ecosphere 11:1–19.

Kupferberg, S. J. 1996. Hydrologic and Geomorphic Factors Affecting Conservation of a River-Breeding Frog (Rana Boylii). Ecological Applications 6:1332–1344.

Kupferberg, S. J. 1997. Bullfrog (*Rana catesbeiana)* Invasion of a California River: The Role of Larval Competition. Ecology 78:1736–1751.

Kupferberg, S. J., A. J. Lind, J. Mount, and S. Yarnell. 2009. Pulsed flow effects on the Foothill Yellow-legged Frog (*Rana boylii*): integration of empirical, experimental and hydrodynamic modeling approaches. California Energy Commision.

Kupferberg, S. J., A. J. Lind, V. Thill, and S. M. Yarnell. 2011. Water Velocity Tolerance in Tadpoles of the Foothill Yellow-legged Frog (Rana boylii): Swimming Performance, Growth, and Survival. Copeia 2011:141–152.

Lemly, A. D. 1985. Suppression of native fish populations by green sunfish in first-order streams of Piedmont North Carolina. Transactions of the American Fisheries Society 114:705–712.

Leopold, L,. B., M. *G.* Wolman, and J. P. Miller.1964. Fluvial processes in geomorphology. W. H. Freeman, San Francisco, Calif. 522

Marchetti, M. P., and P. B. Moyle. 2001. Effects of flow regime on fish assemblages in a regulated California stream. Ecological applications : a publication of the Ecological Society of America 11:530–539.

Moyle, P. B. 2013. Novel Aquatic ecosystems: the new reality for streams in California and other Mediterranean climate regions. River Research and Applications 30:1335–1344.

Moyle, P. B., and D. M. Baltz. 1985. Microhabitat Use by an Assemblage of California Stream Fishes: Developing Criteria for Instream Flow Determinations. Transactions of the American Fisheries Society 114:695–704.

Moyle, P. B., and M. P. Marchetti. 2006. Predicting invasion success: freshwater fishes in California as a model. BioScience.

Paine, R.T., 1974. Intertidal community structure. *Oecologia* 15:93-120.

Power, M. E. 1984a. Habitat quality and the distribution of algae-grazing catfish in a Panamanian stream. The Journal of animal ecology 53:357–374.

Power, M. E. 1984b. Depth distributions of armored catfish: predator-induced resource avoidance? Ecology 65:523–528.

Power, M. E., M. S. Parker, and W. E. Dietrich. 2008. Seasonal reassembly of a river food web: floods, droughts, and impacts of fish. Ecological Monographs 78:263–282.

Power, M. E., R. J. Stout, C. E. Cushing, P. P. Harper, F. R. Hauer, W. J. Matthews, P. B. Moyle, B. Statzner, and I. R. W. De Basgen. 1988. Biotic and abiotic controls in river and stream communities. National American Benthological Society 7:3.

Power, M. E., R. Lowe, P. Furey, J. Welter, M. Limm, J. Finlay, C. Bode, S. Chang, M. Goodrich, and J. Scully. 2009. Algal mats and insect emergence in rivers under Mediterranean climates: towards photogrammetric surveillance. Freshwater Biology 54:2101–2115.

Power, M. E., W. J. Matthews, and A. J. Stewart. 1985. Grazing minnows, piscivorous bass, and stream algae: dynamics of a strong interaction. Ecology 66:1448–1456.

Richards, S. A., M. J. Whittingham, and P. A. Stephens. 2010. Model selection and model averaging in behavioural ecology: the utility of the IT-AIC framework. Behavioral Ecology and Sociobiology 65:77–89.

Shapovalov, L., and A. C. Taft. 1954. The life histories of steelhead rainbow trout (Salmo gairdneri gairdneri) and silver salmon (Oncorhynchus kisutch). California Department of Fish and Game Fish Bulletin 98.

Sinervo, B., F. Mendez-de-la-Cruz, D. B. Miles, B. Heulin, E. Bastiaans, M. Villagran-Santa Cruz, R. Lara-Resendiz, N. Martinez-Mendez, M. L. Calderon-Espinosa, R. N. Meza-Lazaro, H. Gadsden, L. J. Avila, M. Morando, I. J. De la Riva, P. V. Sepulveda, C. F. D. Rocha, N. Ibarguengoytia, C. A. Puntriano, M. Massot, V. Lepetz, T. A. Oksanen, D. G. Chapple, A. M. Bauer, W. R. Branch, J. Clobert, and J. W. Sites. 2010. Erosion of Lizard Diversity by Climate Change and Altered Thermal Niches. Science 328:894–899.

Sousa, W. P. 1984. The Role of Disturbance in Natural Communities. Annual Review of Ecology and Systematics 15:353–391.

Suttle, K. B., M. E. Power, and J. M. Levine. 2004. How fine sediment in riverbeds impairs growth and survival of juvenile salmonids. Ecology 14:969–974.

Sykes, G. E., C. J. Johnson, and J. M. Shrimpton. 2009. Temperature and Flow Effects on Migration Timing of Chinook Salmon Smolts. Transactions of the American Fisheries Society 138:1252–1265.

Uno, H., and M. E. Power. 2015. Mainstem-tributary linkages by mayfly migration help sustain salmonids in a warming river network. Ecology Letters 18:1012–1020.

Vannote, R. L., and G. W. Minshall. 1980. The river continuum concept. Canadian Journal of ….

Wang, T., S. J. Kelson, G. Greer, S. E. Thompson, and S. M. Carlson. 2020. Tributary confluences are dynamic thermal refuges for a juvenile salmonid in a warming river network. River Research and Applications 36:1076–1086.

Wootton, J. T., M. S. Parker, and M. E. Power. 1996. Effects of Disturbance on River Food Webs. Science 273:1558–1561.

Supplemental Material

Supplemental Material. Table 1. Outputs of generalized linear mixed-effect models for North Coast Range Roach (*Hesperoleucus venustus)* distribution in the Upper South Fork Eel River. Levels of categorical factors are listed, and parameter estimates are reported in parentheses. Na's represent parameters not included in the full model, bolded estimates are significantly different from the intercept, p-values <0.05

Size Class (cm)	Intercept	Estimates for parameters in best fit-model determined by AIC							
		Season	Type	Year	River km	Season x Type	River km x Year	River km x Season	River km x Season x Year
0-2	-4.126	Early August *(5.172)*	Riffle *(-2.982)*, Run *(-0.801)*	2017 *(0.278)*, 2018 *(-0.929)*, 2019 *(-1.464)*, 2020 *(-1.069)*	*(-0.053)*	Na	2017 x River km *(0.075)*, 2018 x River km *(0.093)*, 2019 x River km *(0.248)* 2020 x River km *(1.132)*	Na	Na
2-5	-0.342	Early August *(1.224)*	Riffle *(-3.689)* Run *(-0.906)*	2017 *(-1.416)* 2018 *(0.934)* 2019 *(-0.945)* 2020*(0.450)*	*(0.169)*	Early August x Riffle *(2.080)* Early August x Run *(0.226)*	2017 x River km *(-0.049)*, 2018 x River km *(-0.031)*, 2019 x River km *(0.004)* 2020 x River km *(-0.024)*	River km x Early August *(-0.018)*	River km x Early August x 2017 *(0.068)* River km x Early August x 2018 *(-0.075)* River km x Early August x 2019 *(-0.020)*
5-15	-0.632	Early August *(2.135)*	Riffle *(-1.867)* Run *(-1.011)*	2017 *(-0.471)* 2018 *(-1.883)* 2019 *(-0.827)* 2020 *(-1.122)*	*(0.187)*	Early August x Riffle *(0.713)* Early August x Run *(0.378)*	2017 x River km *(-0.041)* 2018 x River km *(0.106)* 2019 x River km *(0.031)* 2020 x River km *(0.023)*	River km x Early August *(-0.124)*	River km x Early August x 2017 *(0.044)* River km x Early August x 2018 *(0.021)* River km x Early August x 2019 *(-0.005)*

38

Supplemental Material. Table 2. Outputs of generalized linear mixed-effect models for Sacramento Pikeminnow (*Ptychocheilus grandis*) distribution in the Upper South Fork Eel River. Levels of categorical factors are listed, and parameter estimates are reported in parentheses. Na's represent parameters not included in the full model, bolded parameters are significantly different from the intercept, p-values <0.05

Size Class (cm)	Intercept	Estimates for parameters in best fit-model determined by AIC				
		Season	Type	Year	River km	River km x Year
10-20	-7.132	Na	Riffle (**-2.469**), Run (**-1.902**)	2018 (-1.469), 2019 (**3.774**), 2020 (-0.720)	0.094	2017 x River km Na, 2018 x River km (**0.331**), 2019 x River km (**0.475**) 2020 x River km (**0.4183**)
20-60	-10.591	Early August (**3.249**)	Na	2017 (**-5.159**) 2018 Na 2019 (-1.401) 2020(-0.724)	(0.111)	2017 x River km (**0.500**), 2018 x River km Na, 2019 x River km (**0.444**) 2020 x River km (**0.355**)

Supplemental Material. Table 3. Outputs of generalized linear mixed-effect models for Sacramento Sucker (*Catostomus occidentalis*) distribution in the Upper South Fork Eel River. Levels of categorical factors are listed, and parameter estimates are reported in parentheses. Na's represent parameters not included in the full model, bolded estimates are significantly different from the intercept, p-values <0.05

Size Class (cm)	Intercept	Estimates for parameters in best fit-model determined by AIC					
		Season	Type	Year	River km	River km x Year	River km x Season
0-10	-9.029	Early August (**4.083**)	Riffle (**-1.123**), Run (**0.620**)	2017 (0.143) 2018 (**-2.487**), 2019 (**-2.409**), 2020 (-1.005)	**0.271**	2017 x River km (**-0.116**) , 2018 x River km (**0.147**), 2019 x River km (**0.202**) 2020 x River km (0.027)	Na
10-20	-18.106	Early August (**7.437**)	Riffle (**-2.299**), Run (**-2.886**)	2017 (**6.680**) 2018 (**5.967**), 2019 (**6.221**), 2020 (**3.198**)	**1.032**	2017 x River km (**-0.638**), 2018 x River km (**-0.445**), 2019 x River km (**-0.574**) 2020 x River km (**-0.358**)	River km x Early August (**-0.417**)
20-60	-16.537	Early August (**4.975**)	Riffle (**-2.236**), Run (**-2.361**)	2017 (**5.866**) 2018 (-0.078), 2019 (**4.379**), 2020 (2.167)	**1.055**	2017 x River km (**-0.532**) , 2018 x River km (-0.019), 2019 x River km (**-0.341**) 2020 x River km (-0.372)	River km x Early August (**-0.406**)

Supplemental Material Table 4. Outputs of generalized linear mixed-effect models for Stickleback (*Gasterosteus aculeatus)* distribution in the Upper South Fork Eel River. Levels of categorical factors are listed, and parameter estimates are reported in parentheses. Na's represent parameters not included in the full model, bolded parameters are significantly different from the intercept, p-values <0.05

Size Class (cm)	Intercept	Estimates for parameters in best fit-model determined by AIC						
		Season	Type	Year	River km	Season x Type	River km x Year	River km x Season
0-5	-4.734	Early August **(3.810)**	Riffle **(-1.498)**, Run (-0.296)	2017 **(-0.702)** 2018 **(0.564)**, 2019 **(-1.791)**, 2020 (-0.047)	**0.082**	Early August x Riffle (Na) / Early August x Run (Na)	2017 x River km **(-0.062** , 2018 x River km **(-0.134)**, 2019 x River km **(-0.026)** 2020 x River km **(-0.195)**	River km x Early August **(0.100)**
5-10	-5.157	Early August **(0.569)**	Riffle **(-2.040)**, Run **(-0.785)**	2017 **(1.063)** 2018 **(2.068)**, 2019 (0.635), 2020 **(3.003)**	**0.130**	Early August x Riffle **(1.186)** / Early August x Run **(0.470)**	2017 x River km **(-0.209)**, 2018 x River km **(-0.123)**, 2019 x River km (-0.073) 2020 x River km **(-0.109)**	River km x Early August **(-0.165)**

Supplemental Material Table 5. Outputs of generalized linear model for Chinook (*Oncorhynchus tshawytscha*) distribution in the Upper South Fork Eel River. Levels of categorical factors are listed, and parameter estimates are reported in parentheses. Na's represent parameters not included in the full model, bolded parameters are significantly different from the intercept, p-values <0.05

Size Class (cm)	Intercept	Estimates for parameters in best fit-model determined by AIC		
		Season	Type	River km
5-15	-5.551	Early August **(-6.565)**	Riffle **(0.598)**, Run **(0.446)**	**0.251**

Supplemental Material Table 6. Outputs of generalized linear mixed-effect models for Coho (*Oncorhynchus kisutch*) distribution in the Upper South Fork Eel River. Levels of categorical factors are listed, and parameter estimates are reported in parentheses. Na's represent parameters not included in the full model, bolded parameters are significantly different from the intercept, p-values <0.05

Size Class (cm)	Intercept	Estimates for parameters in best fit-model determined by AIC								
		Season	Type	Year	River km	Season x Type	Season x Year	River km x Year	River km x Season	River km x Season x Year
0-15	-6.281	*Early August (7.217)*	*Riffle (-1.639), Run (-0.535)*	*2017 (1.990) 2018 (4.284), 2019 (5.244), 2020 (-1.863)*	*0.062*	*Early August x Riffle (-2.301)* *Early August x Run (-0.672)*	*Early August x 2017 (-9.910) Early August x 2018 (-5.638) Early August x 2019 (-6.406)*	*2017 x River km (0.081) , 2018 x River km (-0.104), 2019 x River km (-0.325) 2020 x River km (0.327)*	*River km x Early August (-0.829)*	*River km x Early August x 2017 (0.431) River km x Early August x 2018 (0.043) River km x Early August x 2019 (0.806)*

Supplemental Table 7. Outputs of generalized linear mixed-effect models for Steelhead (*Oncorhynchus mykiss*) distribution in the Upper South Fork Eel River. Levels of categorical factors are listed, and parameter estimates are reported in parentheses. Na's represent parameters not included in the full model, bolded parameters are significantly different from the intercept, p-values <0.05

Size Class (cm)	Intercept	Season	Type	Year	River km	Season x Type	Season x Year	River km x Year	River km x Season	River km x Season x Year
							Estimates for parameters in best fit-model determined by AIC			
0-5	-2.295	*Early August (**1.044**)*	*Riffle (**1.124**), Run (**0.361**)*	*2017 (**-0.685**) 2018 (**0.780**), 2019 (**1.742**), 2020 (**1.442**)*	*-0.001*	*Early August x Riffle (**0.159**)* *Early August x Run (**0.388**)*	na	*2017 x River km(-0.014), 2018 x River km (**-0.185**), 2019 x River km (**-0.243**) 2020 x River km (**0.378**)*	*River km x Early August (**-0.715**)*	*River km x Early August x 2017 (**0.422**) River km x Early August x 2018 (**0.623**) River km x Early August x 2019 (**0.547**)*
5-10	-5.123	*Early August (**3.720**)*	*Riffle (**1.983**), Run (**0.547**)*	*2017 (-0.713) 2018 (**0.491**), 2019 (**0.430**), 2020 (**-0.384**)*	*0.246*	*Early August x Riffle (**-0.206**)* *Early August x Run (0.087)*	na	*2017 x River km (**0.016**), 2018 x River km (**-0.084**), 2019 x River km (**-0.072**) 2020 x River km (0.007)*	*River km x Early August (**-0.293**)*	*River km x Early August x 2017 (0.010) River km x Early August x 2018 (**0.017**) River km x Early August x 2019 (**0.056**)*
10-20	-4.403	*Early August (**0.640**)*	*Riffle (**1.793**), Run (-0.075)*	*2017 (**0.834**) 2018 (**-0.517**), 2019 (**-0.929**), 2020 (**0.743**)*	*0.176*	*Early August x Riffle (**-0.803**)* *Early August x Run (**-0.206**)*	*Early August x 2017(**-1.119**) Early August x 2018 (**0.451**) Early August x 2019 (**1.689**)*	*2017 x River km (**-0.054**), 2018 x River km (**0.066**), 2019 x River km (**0.042**) 2020 x River km (0.017)*	*River km x Early August (**-0.077**)*	*River km x Early August x 2017 (**0.087**) River km x Early August x 2018 (-0.036) River km x Early August x 2019 (**-0.061**)*
20-30	-5.562	*Early Augus t*	*Riffle*	*2017 (-0.443) 2018 (**-1.609**),*	*0.088*	*Early August x Riffle (**-1.522**)*	na	*2017 x River km (-0.057),*	*River km x Early*	*River km x Early August x 2017 (**0.076**)*

		t (0.167)	*(1.319), Run (-0.471)*	*2019 (-1.738), 2020 (-0.002)*		*Early August x Run (-0.882)*		*2018 x River km (0.091), 2019 x River km (0.052) 2020 x River km (0.007)*	*August (0.029)*	*River km x Early August x 2018 (-0.330) River km x Early August x 2019 (0.091)*
30-40	-5.907	*Na*	*Riffle (0.170), Run (-2.054)*	*2017 (-0.360) 2018 (-0.306), 2019 (-2.043), 2020 (-0.273)*	-0.038	*Early August x Riffle (-22.105) Early August x Run (-21.072)*	*Early August x 2017(1.606) Early August x 2018 (-33.101) Early August x 2019 (5.061)*	*na*	*na*	*River km x Early August x 2017 (-0.050) River km x Late May x 2017 (0.121) River km x Early August x 2018 (2.620) River km x Late May x 2018 (0.066) River km x Early August x 2019 (-0.712) River km x Late May x 2019 (0.058) River km x Early August x 2020 (-0.024)*
40-60	-6.965	*Na*	*Riffle (-0.319), Run (-0.793)*	*2017 (-6.016) 2018 (-48.958), 2019 (-4.665), 2020 (-3.903)*	0.030	*na*	*na*	*2017 x River km (0.512), 2018 x River km (3.827), 2019 x River km (0.307) 2020 x River km (0.252)*	*na*	*na*

Supplemental Material Table 8. Outputs of generalized linear mixed-effect models for Pacific Lamprey (*Entosphenus tridentatus*) distribution in the Upper South Fork Eel River. Levels of categorical factors are listed, and parameter estimates are reported in parentheses. Na's represent parameters not included in the full model, bolded parameters are significantly different from the intercept, p-values <0.05

Size Class (cm)	Intercept	Estimates for parameters in best fit-model determined by AIC	
		Type	River km
Alive	-5.291	Riffle (*1.421*), Run (*0.577*)	-0.059

Supplemental Material Table 9. Outputs of generalized linear mixed-effect models for Green sunfish (*Lepomis cyanellus*) distribution in the Upper South Fork Eel River. Levels of categorical factors are listed, and parameter estimates are reported in parentheses. Na's represent parameters not included in the full model, bolded parameters are significantly different from the intercept, p-values <0.05

Size Class (cm)	Intercept	Estimates for parameters in best fit-model determine by AIC		
		Year	River km	River km x Year
5-20	-68.846	2019 (*-3033.148*), 2020 (*54.200*)	5.173	2019 x River km (*232.324*) 2020 x River km (*-4.294*)

Supplemental Material Table 10. Outputs of generalized linear mixed-effect models for Bullfrog (*Rana catesbeiana*) distribution in the Upper South Fork Eel River. Levels of categorical factors are listed, and parameter estimates are reported in parentheses. Na's represent parameters not included in the full model, bolded parameters are significantly different from the intercept, p-values <0.05

Size Class (cm)	Intercept	Estimates for parameters in best fit-model determined by AIC					
		Season	Type	Year	River km	River km x Year	River km x Season
0-20	-9.033	Early August (*-7.631*)	Riffle (*-4.997*), Run (*-3.487*)	2017 (*-59.480*) 2018 (-0.075), 2019 (-0.797), 2020 (-0.393)	*0.514*	2017 x River km (*4.671*) , 2018 x River km (-0.117), 2019 x River km (-0.169) 2020 x River km (-.104)	River km x Early August (*0.769*)

Supplemental Material Table 1. Outputs of generalized linear mixed-effect models for Western Pond Turtle (*Actinemys marmorata*) distribution in the Upper South Fork Eel River. Levels of categorical factors are listed, and parameter estimates are reported in parentheses. Na's represent parameters not included in the full model, bolded parameters are significantly different from the intercept, p-values <0.05

Size Class (cm)	Intercept	Estimates for parameters in best fit-model determine by AIC			
		Season	*Type*	*Year*	*River km*
0-30	-16.461	*Early August* **(-4.51)**	*Riffle* **(-3.873)**, *Run* **(-5.707)**	*2017 (-0.973)* *2018* **(-2.292)**, *2019 (-1.776)*, *2020 (-0.656)*	*-0.818*
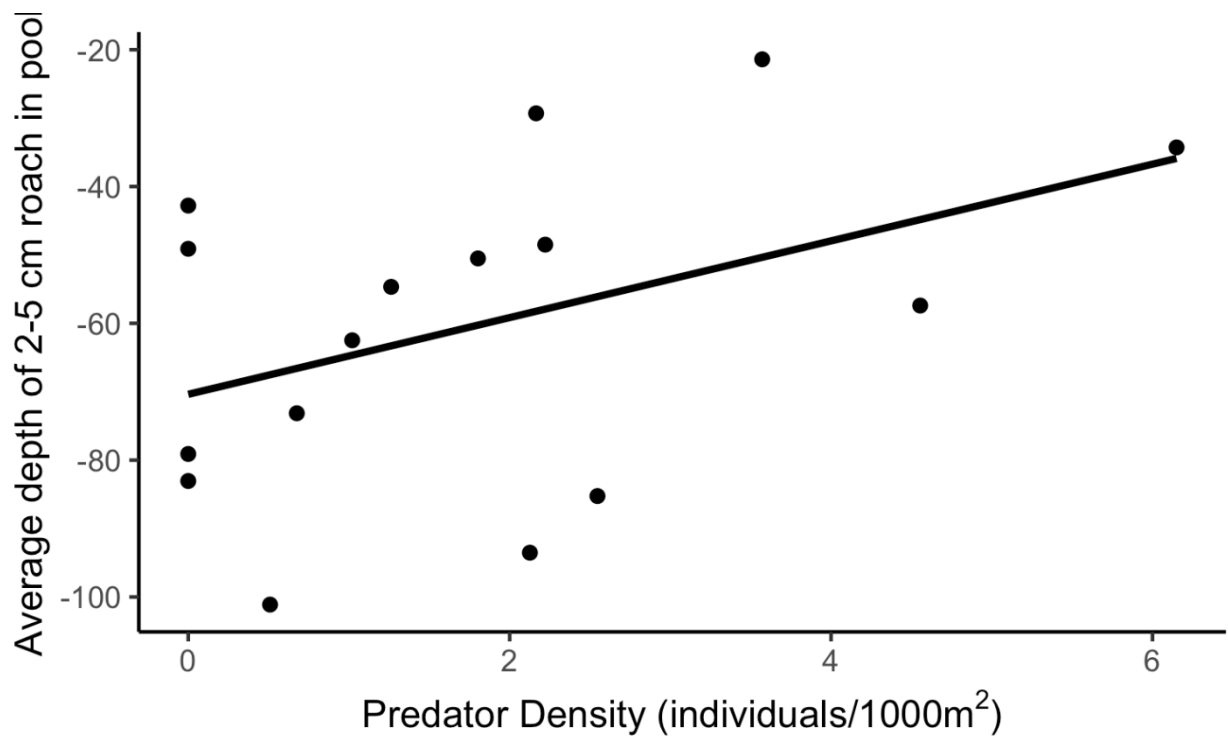
SM Figure 1: Roach depths in 18 large pools in 2018 that spanned a range of predator densities. Predators were Steelhead or Sacramento Pikeminnow larger than 20cm and counted by snorkel survey. Average depths were calculated by taking a weighted average of scan samples along transects that extended 5m from the bank.

Transition from Chapters 1 to 2

During the survey work described in Chapter 1, we noted the absence of Sacramento Pikeminnow from the upstream reaches of or study reach in spring. Before these observations, no description of migration by Sacramento Pikeminnow existed. However, their impacts as introduced competitors (Reese and Harvey 2002) and predators (Brown and Moyle 1991) had been described. In 2015, I monitored 8 pools within the Angelo Coast Range Reserve and noted that pikeminnow seemed to move upstream as temperatures warmed. This motivated the more careful studies described in Chapter 2 to determine how this migration might be influenced by warmer future conditions, and identify what factors drive pikeminnow to migrate in the South Fork Eel. Conceptually, lessons can be learned from these dynamics as many systems undergo changes in physical conditions. In response to these altered physical conditions species phenologies and ranges change. In addition, their interactions with other organisms also change; this is especially important as we seek to understand the impacts of non-native species and mitigate their impacts on natives.

Chapter 2. Spring temperature predicts timing of seasonal upstream migration of invasive Sacramento pikeminnow (*Ptychocheilus grandis)* in a salmon-bearing river

Abstract

Rapid climate change and invasive species introductions are major threats to ecological communities across the globe, and freshwaters are particularly vulnerable and impacted. We document the first instance of an invasive piscine predator, the Sacramento pikeminnow (*Ptychocheilus grandis),* migrating within its introduced range, the South Fork Eel River. Through a combination of snorkel surveys and temperature monitoring in 2015-2019 we show upstream migration by pikeminnow during spring and early summer occurred earlier in years when river water was warmer. Pikeminnow were more likely to occur in pools where their primary prey, North Coast Range Roach (*Hesperoleucus venustus)* were more abundant and dense, suggesting that feeding motivates seasonal pikeminnow migration. We developed a statistical temperature model to forecast the timing and extent of upstream migration by pikeminnow under combinations of discharge and air temperature that were not observed. This model was calibrated with our field observations that showed that river temperature decreased with river flow and increased downstream, and with air temperature. In years with low flow and high air temperature, we predict pikeminnow will move upstream earlier and overlap there with native fishes for a longer period of time. Pikeminnow consume or compete with all the native fishes of the South Fork Eel River, including culturally and economically important salmonids. Understanding the conditions which limit overlap between pikeminnow and threatened salmonids in important refuge habitat can direct habitat restoration efforts and aid the recovery of these native fishes. Additionally, insight into the phenology of life history events, like migration, exposes invasive pikeminnow to potential control. We suggest that capturing individuals as they move upstream or downstream or decreasing water withdrawals to keep river temperatures cool to limit co-occurrence of pikeminnow and rearing salmonids could minimize the negative impact of pikeminnow on native fishes. Invasive pikeminnow will likely have larger impacts in the South Fork Eel River with global warming and increasing drought severity. As with other invasive organisms, understanding pikeminnow life history and phenology can focus control efforts to take advantage of vulnerable life stages and seasonal time windows to benefit native species.

Introduction:

Compounded perturbations can exert large, synergistic, and unexpected effects on communities (Paine et al. 1998). Fresh water ecosystems are extremely threatened by climate change (Jackson et al. 2001, Rahel and Olden 2008), and among the Earth's most heavily invaded ecosystems (Strayer 2010). Here, we consider how warming, due to

climate change and human water extraction, influences the seasonal timing and consequent impacts of an invasive fish that migrates within its introduced range.

In animal migrations, large numbers of conspecific individuals, sometimes entire populations, periodically move en masse to track spatially shifting resources (Dingle 2014, Lucas and Buras 2001). Fishes migrate, sometimes thousands of kilometers (Tyus and McAda 1984, Quinn 2005), to spawn, feed, or to avoid stressful or dangerous conditions (Northcote 1978). Timing of migrations vary, often with environmental conditions like river temperature (Quinn et al. 1997), the onset of seasonal rains (Kelson 2018, Campbell et al. 2006), elevated flows (Lucas and Batley 1996), floodplain inundation (Correa et al. 2007), and melting ice (Hughes and Reynolds 1994). As climate continues to change, temperatures will get warmer, storms more intense, and the timing of rains will shift (Pierce et al. 2018). These changes will alter the timing of fish migrations in fresh waters. For example, in a partially migratory population of European roach (*Rutilus rutilus)*, warmer temperatures advanced the timing of spring migration and delayed fall migration between a Swedish lake and its surrounding streams (Brodersen et al. 2011). In North America, Chinook salmon (*Oncorhynchus tshawytscha)* smolts out-migrated earlier in years with warmer spring temperatures (Sykes et al. 2009). In the Columbia River, adult sockeye salmon (*Oncorhynchus nerka)* spawning migrations occurred earlier and earlier over a half-century as water temperatures warmed (Quinn et al. 1997). Understanding the influence of temperature on migration timing is increasingly important for managing a variety of fish species.

Pikeminnows (Genus *Ptychocheilus*) are North America's largest predatory minnows. Here we describe what to our knowledge is the first instance of migration observed in the Sacramento Pikeminnow (*Ptychocheilus grandis*). Two other species of *Ptychocheilus* are known to make long-distance, potadromous migrations to spawning locations (Tyus and McAda 1984, Gadomski et al. 2001). Here we document the seasonal migration of *P. grandis* in the South Fork Eel River of northwestern California, including timing of arrival upstream as a function of water temperature (Obj 1). We then explored whether pikeminnow migrate to breed (by exploring pikeminnow size structure) or to feed (by exploring pikeminnow abundance in pools with different prey densities) (Obj 2). Finally, we developed a predictive temperature model based on river flow, air temperature, distance downstream. We then used this model together with information on pikeminnow distribution as a function of temperature to explore the influence of four climate scenarios (combinations of high and low flow crossed with high and low temperature) on pikeminnow distributions (Obj 3). We conclude that pikeminnow are migrating upstream as upstream waters warm to a temperature conducive to feeding, which has implications for native fish conservation and restoration efforts.

Methods

Study site and historical background

The Eel River in northwestern California (drainage area 9546 km^2) historically supported large populations of culturally and economically important Pacific salmon (Steelhead *Oncorhynchus mykiss,* Coho, *Oncorhynchus kisutch,* and Chinook, *Oncorhynchus*

tshawytscha) (Yoshiyama and Moyle 2010). Annual runs of over a million individuals and the fisheries they supported collapsed due to overfishing and habitat destruction via deforestation, with the most severe effects resulting from bank erosion and channel widening during the great floods of 1955 and 1964 (Yoshiyama and Moyle 2010).

There are currently signs of salmonid recovery, particularly in the more forested reaches of the South Fork Eel River, likely due to recovery of mature riparian forests that provide shade, cover and deeper, more heterogeneous channel habitats (Power et al. 2015). Unfortunately, salmonid recovery in the Eel River could be derailed by interactions of climate warming, water extraction for marijuana cultivation (Bauer et al. 2015, Carah et al. 2015), and the invasive, mobile, warm-water piscivore, the Sacramento pikeminnow (*Ptychocheilus grandis*)(Harvey and Nakamoto 1999).

Sacramento pikeminnow are native to the Sacramento San-Juaquin river systems, Clear Lake, and a few coastal drainages in California (Brown and Moyle 1991). Pikeminnow were introduced to the Eel River in 1979, and in less than a decade, became widespread in the basin (Brown and Moyle 1991). The initial introduction has been traced back to just 3-4 individuals from Clear Lake (Kinziger et al. 2013). Pikeminnow in the Eel River now threaten recovering populations of cold-adapted salmonids (threatened winter-run steelhead (Northern California Steelhead DPS), threatened coho salmon (Southern Oregon / Northern California Coast Coho Salmon ESU), and Fall chinook) and other native species through both competition and predation (Nakamoto and Harvey 2003).

We studied a 10-km reach of the Upper South Fork Eel River, in and around the Angelo Coast Range Reserve, a UC Natural Reserve System reserve managed by the University of California, Berkeley in Mendocino Co., Northern California (Figure 1).   Our study reach extended from the Angelo Reserve's Environmental Science Center (39.7189°N, 123.6529°W) downstream to Hunter's Pool (39.7579°, 123.6368°W).
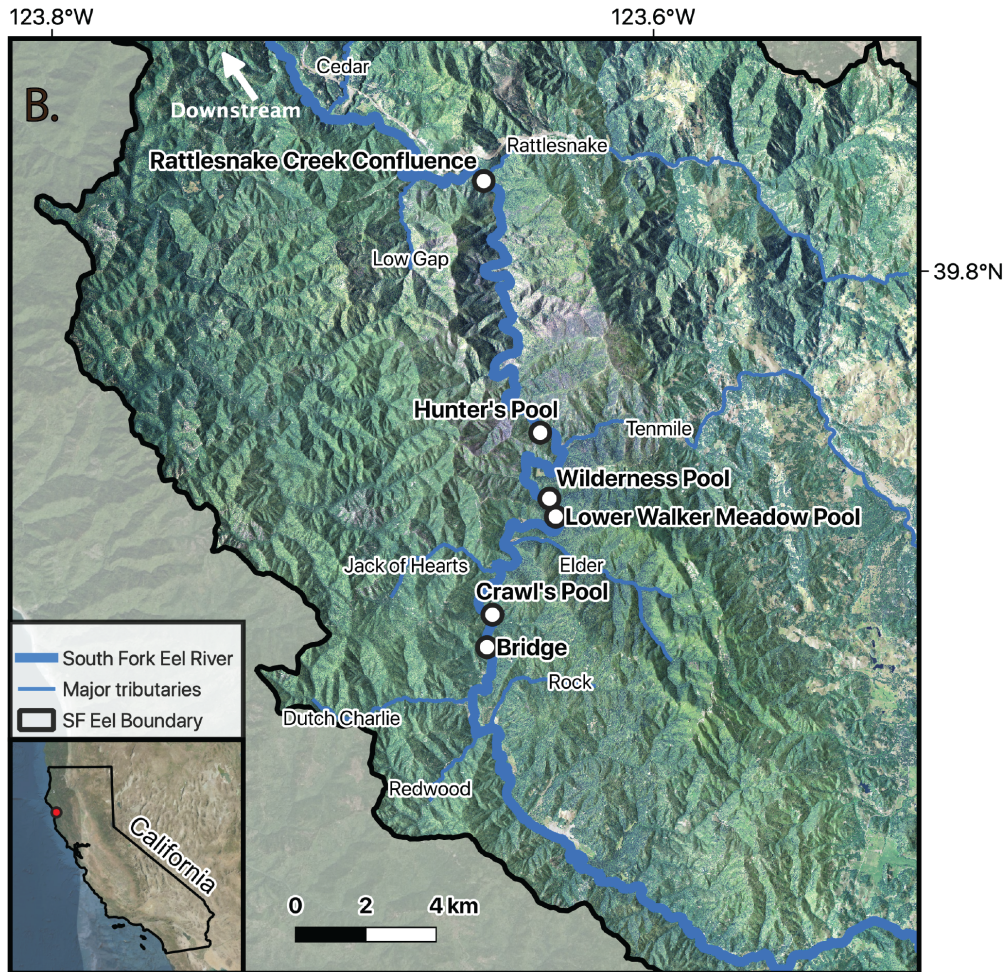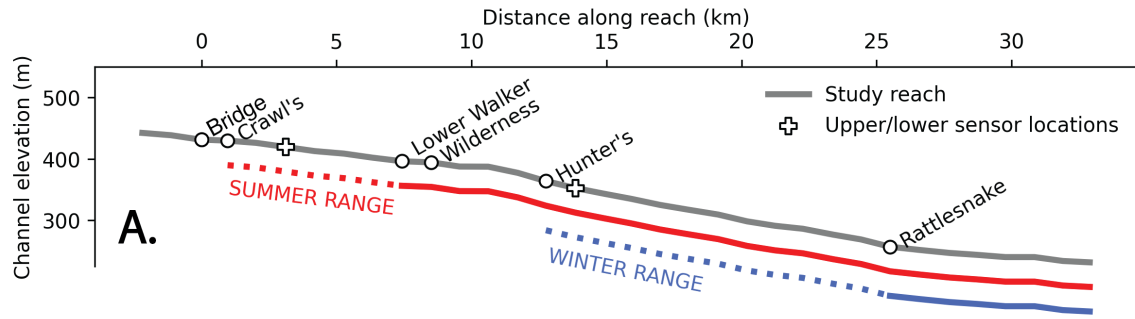
Figure 1 **A.** Long profile of the study reach. Gray line shows the river channel, red and blue lines below channel show winter (blue) and summer (red) range of pikeminnow. Dashed sections show uncertainty(winter) or variability(summer). Extent of summer range varies between Lower Walker Pool and Crawl's Pool. Upstream extent of winter range is between Hunter's Pool and Rattlesnake Creek Confluence, exact position uncertain due to difficulty accessing this region and high winter flows. River kilometer 0 was designated as the Wilderness Lodge Rd. Bridge across the South Fork Eel River, crosses designate the upper and lower borders of where we measured temperature. **B.** Map of the same section of upper South Fork Eel River and its tributaries shown in long profile. Relevant pools are shown in both long profile and map.

Documenting the pikeminnow migration, including the extent of upriver movement and timing

In 2015, we surveyed 8 pools in a 10.7 km stretch of the South Fork Eel across the summer as part of a preliminary study to characterize fish distributions. During the course of our sampling, we observed the arrival of pikeminnow to the reach and subsequent departure. Hypothesizing a seasonal upstream movement, we repeated the survey and expanded the effort in four additional years (i.e., data collected from 2015-2019). Specifically, in 2015, eight large non-contiguous pools in the Angelo Coast Range Reserve were surveyed by a single diver during summer (Appendix S1: Table 1). Each pool was visited roughly every 10 days for 15 weeks throughout the summer season. Surveys began in mid-May and continued through mid-August. The surveyor swam an S pattern, moving slowly up the river right bank, down through the thalweg of the pool, then up the river left bank. From 2016-2018 each hydraulic unit (pools, riffles, and runs) in our entire 10-km study reach study reach was surveyed by two divers; units were surveyed once at the end of May and once in the beginning of August. In 2019, approximately 30% of the total units were surveyed, including those pools targeted in 2015; as in 2016-2018, we surveyed these units once in late May and once in early August. In surveys that involved two divers, the surveyors swam upstream along the edges of the unit, counting animals and communicating to avoid double counting. If the unit was too wide, or the visibility was too poor for divers to see the middle, one of the divers swam downstream, surveying the middle, after reaching the upstream limit of the unit. During these surveys, all vertebrates sighted were counted, with their body lengths estimated in categories (Appendix S1: Table 2). These data allowed us to document pikeminnow distributions in early and late summer (Obj 1).

We complemented the above distributional survey with intensive monitoring of a single pool to detect the *timing* of pikeminnow arrival to the upper South Fork Eel River, including both biological observations and temperature measurements. Specifically, for all 5 years, 2015-2019, we used the single diver survey pattern described above to monitor one large pool (Wilderness Pool, 39.74075° N, 123.6333° W, river km 7.90, Figure 1) daily, from mid-May until the date of first detection of pikeminnow. Any pikeminnow encountered were counted and their sizes were estimated to the nearest 5cm. After pikeminnow were detected in Wilderness Pool, more infrequent surveys continued. We collected temperature via a single logger deployed at the tail of the pool in a well-mixed location. We used linear regressions with arrival time (Julian day) as a response variable and 4 temperature metrics (mean, minimum, standard deviation, and degree-days) for May 15th to July 1st (Table 2) as explanatory variables. Cumulative degree-days were calculated as the hourly deviation from 15°C (a temperature at or below which pikeminnow are less effective competitors (Reese and Harvey 2002) and predators (Vondracek 1987)), and summed for the total period of interest (Appendix S1: Equation 1). These data allowed us to explore the influence of temperature on migration timing (Obj. 1).

Why do pikeminnow migrate?

We explored potential drivers of migration, including spawning and feeding. To test the hypothesis that the pikeminnow migration is for spawning, we collected data on body

size for all pikeminnow encountered (assuming presence of year 0 pikeminnow ,0-7cm (Brown and Moyle 1997), to reflect recent spawning in the region).

Another hypothesis is that this pikeminnow migration might be motivated by foraging opportunities. To test whether pikeminnow were more likely to occur in pools with higher counts and densities of their prey, we focused on 2015, the year when we surveyed pools throughout the summer, and the most abundant and ubiquitous potential prey fish: roach (see Chapter 1). We also collected information on measured, widths and length of pools to calculate pool area, and used area to calculate roach density (fish / m^2). All the pools we surveyed were greater than 2.5 m deep. To explore the relationship between pikeminnow and roach, we used two generalized linear mixed-effect models with binomial distributions. Our response variable in both models was pikeminnow presence or absence, river kilometer was included as a fixed-effect. One model included a fixed-effect of roach pool-wide abundance and the other included a fixed-effect of roach density. Both models included random-effects of pool and survey date (Table 2).

Exploring climate scenarios and implications for pikeminnow distributions
To explore how environmental factors influenced our observed river temperature, we used a linear mixed-effect model to evaluate a range of environmental predictors. We expected water temperature to depend on air temperature (°C), river discharge (m^3/s), and longitudinal river position (km downstream from an upstream bridge benchmark (Figure 1)). The latter was correlated with channel width and hence with areal exposure of the channel surface to direct solar radiation.

To parameterize this model, we measured stream temperature hourly from mid-May through mid-September at 7-18 sites along the 10-km study reach from 2015-2019 (Appendix S1: Table S1). Deeper pools in the South Fork Eel River thermally stratify each summer, so temperature sensors were placed in the river thalweg at the outflow of pools, where water was well mixed. Temperature sensors were either vacuum-sealed Maxim ibuttons (DS1990) or Onset HOBO Temperature Pendant Logger (MX2201, MX2202). Stream discharge in the South Fork Eel River was estimated using a flow rating curve (Power et al. 2008) with river stage recorded in a United State Geological Survey stilling well located at the southern end of the Angelo Coast Range Reserve (Branscomb South Fork Eel gage ID 11475500, now operated by UC Berkeley Angelo Reserve researchers, data available at http://angelo.berkeley.edu/data/meteorological-data/).

Our linear mixed-effect model included the natural logarithm of mean air temperature, mean discharge, and longitudinal river position (km), as environmental predictors and fixed-effects. Our response variable was mean temperature along our study reach (river km 2.35 – 13.04, Figure 1) from May 15- July 1st for 2015-2019, we chose this time period to capture much of the interannual variation in seasonal river warming (Figure 2A). The model included a random-effect of year. We then used the parameter estimates from the mixed-effect model (Table 2) to predict river temperatures for combinations of environmental conditions we did not observe. We generated 4 scenarios for the period May 15 – July 1; combinations of two mean flows (0.5 and 8 m^3/s) and two mean air

temperatures (16 and 20 °C). These conditions are representative of combinations of cool and warm springs and low and high-flow years. We constrained our predicted river temperatures to the same reach where temperature was measured.

We then used the conditions under which pikeminnow arrived at Wilderness Pool between years to predict the location of upstream extent of pikeminnow on July 1. Upstream extent was calculated by locating the position of a mean temperature of 16.3°C, in each of the four scenarios we created predicting river temperature using combinations of flow and air temperature not observed. This temperature corresponds to the mean temperature at Wilderness Pool from May 15 to the date of pikeminnow arrival observed from 2015-2019 (Table 1). Predicting upstream extent not only allows us to predict a total area of impact of pikeminnow under certain discharge and air temperature conditions, but also presence or absence at a location by the date specified, here July 1.

We used R statistical software (R Development Core Team, 2018, version 3.14) and the Python programming language (https://www.python.org/) for all analyses and data management.

Results

Seasonal Migration of Pikeminnow

Snorkel surveys revealed Sacramento pikeminnow migrated upstream in the South Fork Eel River during all five years of the study period (2015 – 2019, Figure 1). The extent of upstream movement varied from year to year: 2015 was the shortest (5.5 km upstream from our most downstream pool surveyed (Hunter's Pool, River km 13.04)), and 2018 the longest (9.3 km upstream from Hunter's Pool). Pikeminnow were absent from the most downstream survey pool during the first surveys each spring and overwinter at an unknown location downstream of our study reach, between the Angelo Coast Range Reserve and the Rattlesnake Creek Confluence (Figure 1A). In 2018, we surveyed farther downstream during the winter season to try and identify the source of the upriver migrants. Pikeminnow were detected around Rattlesnake Creek in late February and in early March, suggesting they are present throughout the winter at this location, but the actual distance of migration is still uncertain, since individual fish were not tracked.

Our intensive sampling of Wilderness Pool revealed that Pikeminnow arrival times differed between years by up to 49 days but generally occurred in late spring/early summer (Figure 2 A). Pikeminnow arrived earliest to this site in the warmest year, 2015, on June 6th, and latest in the coolest year, 2019 on August 4th. Arrival date (measured as Julian date) varied significantly with mean temperature at this pool (Table 2, Figure 2 B). While arrival timing varied across years, the temperature conditions the week before *P. grandis* arrived in the pool were similar across years. Mean temperature for the week preceding arrival was 20°C (s.d. 0.75°C), mean maximum weekly average temperature (MWAT) across years was 21.7°C (s.d. 0.6°C). Mean accumulated degree-days above 15°C from May 15th to the date of arrival across years was 36.0 (s.d. 6.0) and mean temperature over this time interval was 16.3°C (s.d. 0.78°C). We used the mean temperature (16.3°C) as the threshold value in our modeling.
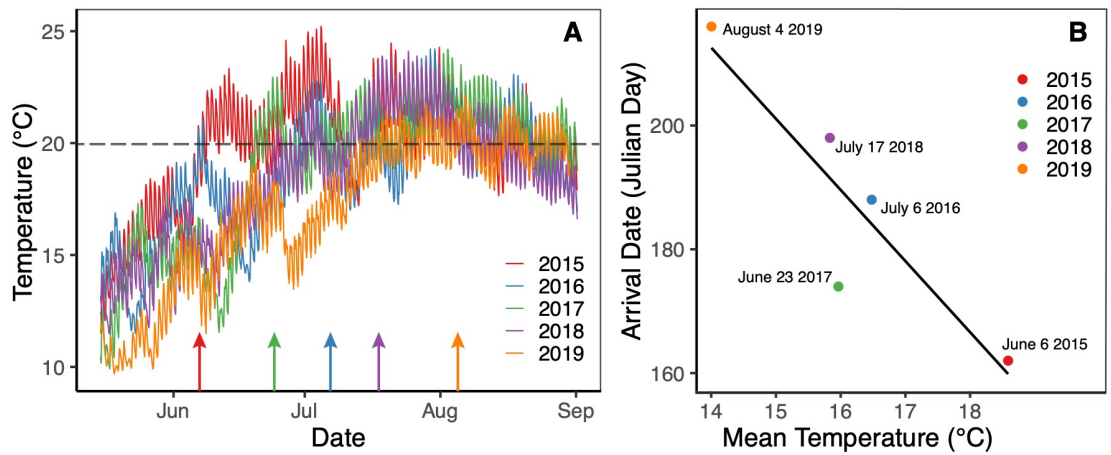
Figure 2. A. Hourly temperature for the 5 study years at a pool in the South Fork Eel River in the Angelo Coast Range Reserve, Mendocino Co. CA. Horizontal dashed at 19.98°C, the mean temperate of the pool during the week before pikeminnow arrive across years. Arrows on x-axis depict date of arrival each year, years are color coded. B. Linear regression (R^2 = 0.798, p = 0.041) of mean (computed from May 15th to July 1st) of daily mean temperatures versus date of arrival (Julian day) of *Ptychocheilus grandis* at Wilderness Pool in the South Fork Eel River, Angelo Coast Range Reserve, Mendocino Co. CA.

Why do pikeminnow migrate?

Across all our surveys – including the reach-scale snorkel surveys and the intensive surveying of Wilderness Pool, we never observed pikeminnow fry. In fact, no pikeminnow smaller than 13cm total length were ever seen in the survey reach. The most abundant size classes were 30-40cm and 25-30cm. This pattern suggests the upriver migration we documented in Sacramento pikeminnow is not a spawning migration.

Another possibility is that the seasonal upriver migration as temperatures warm is to take advantage of prey resources as habitats prey densities peak and temperatures warm. In support of this hypothesis, we found that pikeminnow were more likely to occur in pools with high roach abundance and density (Generalized linear mixed-effects models, p = 0.03, p= 0.04 respectively, Figure 3, Table 2). Pikeminnow were also more likely to occur in pools farther downstream (p = 0.02, Table 2). Despite co-occurrence, pikeminnow and roach were not seen schooling together in this reach, as occurs farther downstream.
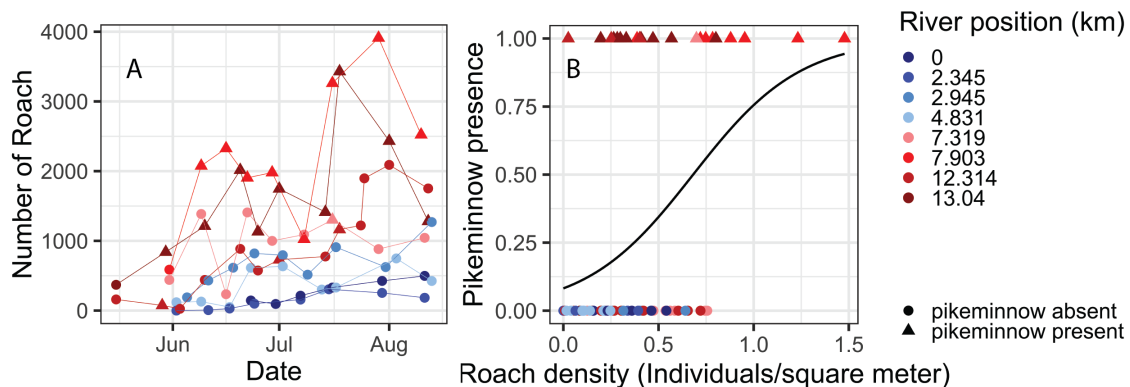

55

Figure 3. A. Coast Range Roach (*Hesperoleucus venustus)* abundance in 8 large pools in the South Fork Eel River within the Angelo Coast Range Reserve, Mendocino, Co. CA during 2015. Counts from visual snorkel surveys plotted against date. Pools are listed by their river positions in km, lower values are more upstream are large pools and are shown in cooler colors. Each point is one snorkel survey, triangles depict surveys where Sacramento pikeminnow, *Ptychocheilus grandis,* where detected, circles when absent. B. logistic regression of the Roach density and pikeminnow presence. Pool colors and pikeminnow symbols are the same as panel A. In a generalized linear mixed-effect models, roach number, roach density, and river position (increasing downstream) significantly increased the probability of pikeminnow presence (Table 2).

Climate scenario modeling and implications for pikeminnow distributions

During the 5 years of this study, summer temperature and river conditions varied dramatically. An four drought in Northern California ended in December 2015 (Hahm et al.2019, Goulden & Bales 2019). During this year, river temperatures warmed rapidly and by July, had reached the highest recorded values of any year (Figure 2 A). In contrast, 2019 was exceptionally wet and cool. A late spring spate kept flows high, above the 95th percentile of flows measured from 1950-2019 throughout the summer (USGS 11475800, Leggett, CA). Water temperatures warmed more slowly in 2019 and remained cooler than in other years. Years 2016-2018 were intermediate in temperature (Figure 2A). Various temperature metrics were summarized for Wilderness pool (Table 1).

In our linear mixed-effect model mean air temperature, river position, and the natural logarithm of mean flow over the May 15 – July 1 window significantly explained mean river temperature, during the same period. As expected, river temperatures correlated with air temperatures, were inversely related to river discharge, and increased downstream. These three environmental predictors explained 96% of the observed variation in mean temperature and were significant or marginally significant (Table 2). When we used the parameter estimates to create four predictive scenarios combining two discharges and two air temperatures, river temperatures were hottest throughout the reach when discharge was low (0.5 m^3/s) and mean air temp was high (20°C, Figure 4 A). In contrast, when discharge was high (8 m^3/s) and air temperatures were cool (16°C) river temperatures were coolest (Figure 4 D). Intermediate temperatures were predicted in both our low discharge, low temperature (Figure 4 B) and high discharge high temperature (Figure 4 C) scenarios.
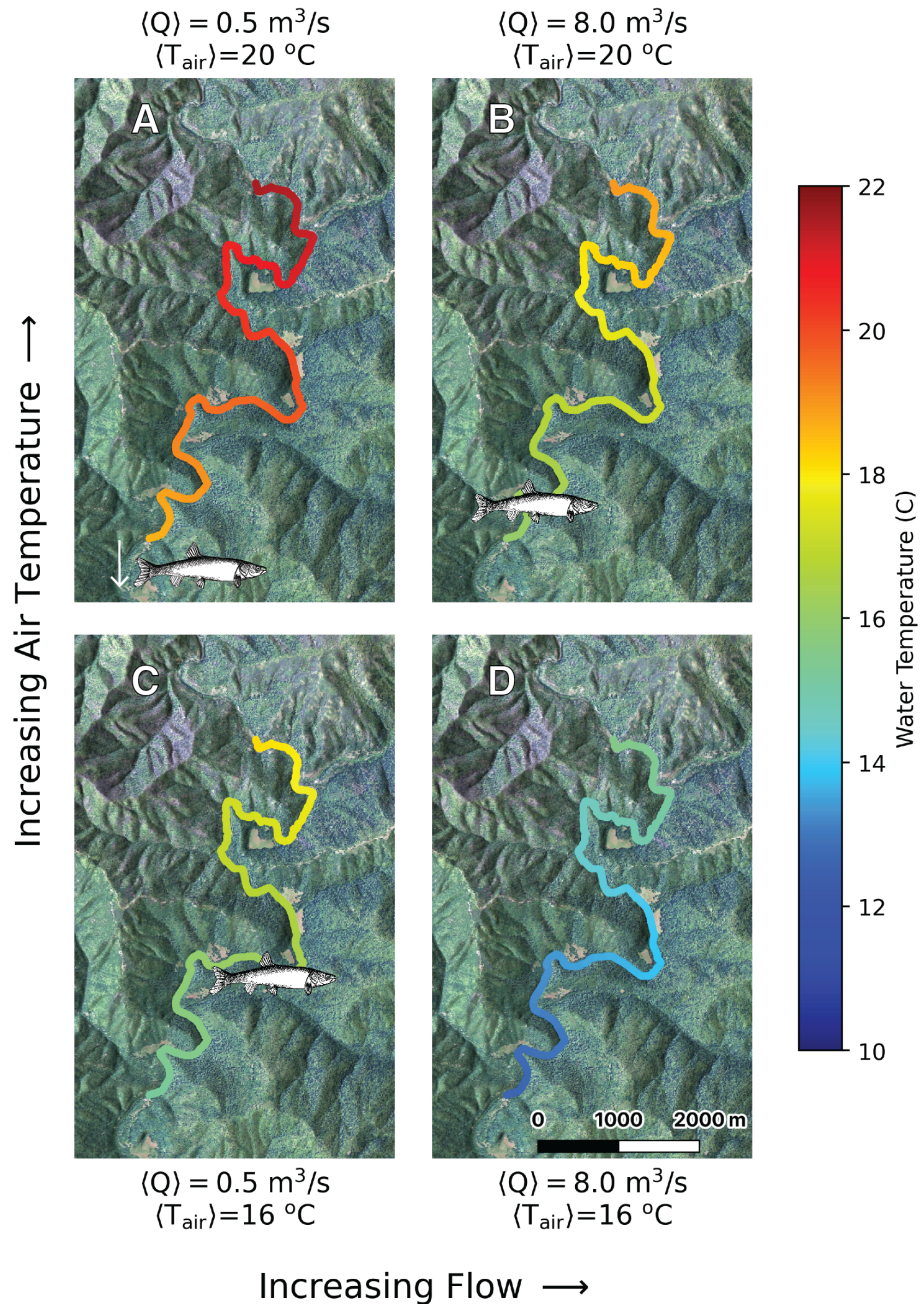
Figure 4. Gridded maps with river channel colored as predicted mean temperature from May 15- July 1 in 4 scenarios. Scenarios are combinations of two mean flow conditions (0.5 and 8.0 m³/s, x-axis) and two air mean temperatures (16 and 20 °C, y-axis). Mean river temperatures are calculated from the parameter estimates of a linear mixed-effect model. Temperatures are predicted for the reach in which temperature was measured. The pikeminnow icon shows where channel mean temperature is 16.3°C, which was the mean temperature from May 15- date of pikeminnow arrival at Wilderness pool from 2015-2019 and is an estimate of pikeminnows upstream distribution July 1 in each scenario. In scenario A the whole reach is above 16.3 °C, and scenario D the 16.3 temp threshold, and presumably the upstream limit of pikeminnow migration for such years, is below our study reach.

In our four temperature scenarios (Figure 4) we identified the position of the 16.3°C temperature threshold that represents our estimate of upstream extent of pikeminnow on July 1. This predicted threshold was farthest upstream when discharge was low (0.5 m³/s) and mean air temp was high (20°C, Figure 4 A). In contrast, when discharge was high (8 m³/s) and air temperatures were cool (16°C) river temperatures were coolest and did not exceed 16.3°C in the entire 10.8 km study reach. In this case, we predict that no pikeminnow would arrive in our study reach by July 1 (Figure 4 D). In both our low discharge/ low temperature (Figure 4 B) and high discharge/ high temperature (Figure 4 C), pikeminnow were predicted to reach intermediate positions (9.9 km and 6.8 km respectively) by July 1.

Table 1. Temperature metrics, flow and pikeminnow arrival time for Wilderness Pool for 2015-2019. Flow data from USGS Gauge 11475800, Leggett, CA

Environmental factor	Year					5-year mean
	2015	2016	2017	2018	2019	
Mean temperature °C 1 week before pikeminnow arrival	19.4	20.8	19.0	20.6	20.1	20.0
Mean temperature °C from May 15 – pikeminnow arrival date	16.8	16.9	15.1	16.9	16.0	16.3
Mean temperature °C from May 15 – July 1	18.6	16.5	16.0	15.8	14.0	16.1
Degree-day May 15 – pikeminnow arrival date	31.0	40.8	28.3	39.1	41.2	36.1
Degree-day May 15 – July 1	168.6	69.6	45.3	39.1	-46.9	55.1
Maximum weekly average temperature (MWAT, °C), 1 week before pikeminnow arrival	21.6	22.2	21.1	22.4	21.2	21.7
Mean flow (m³/s) May 15- July 1	0.597	1.226	2.028	1.614	7.357	2.564
Arrival date	June 11	July 6	June 23	July 17	August 4	July 5
Julian day	162	188	174	198	216	187

Table 2. Summary of model outputs of various temperature metrics, all metrics calculated from May 15th – July 1st for 2015- 2019 at Wilderness Pool in the South Fork Eel River, Angelo Coast Range Reserve, Mendocino Co. CA. Model types are abbreviated lm for linear model, lmm for linear mixed-effect model, glmm for generalized linear mixed-effect model. ΔAIC calculated by subtracting the AIC of a reduced model without the specified explanatory variable from the AIC of the full model will all explanatory variables.

Response Variable	Explanatory Variable	Model type	Intercept	Parameter estimate	Adj. R^2	p-value	ΔAIC
Pikeminnow arrival (Julian day)	Degree day	lm	38.37	- 0.25	0.81	0.04	NA
Pikeminnow arrival (Julian day)	Mean temperature (°C)	lm	196.75	- 11.49	0.81	0.04	NA
Pikeminnow arrival (Julian day)	Minimum temperature (°C)	lm	108.07	- 8.68	0.15	0.53	NA
Pikeminnow arrival (Julian day)	Temperature standard deviation	lm	112.47	- 33.00	0.34	0.24	NA
Mean river temperature (°C)	Log (mean flow) (m^3/s)	lmm	0.13	- 0.93	0.96	0.06	-8.85
Mean river temperature (°C)	Mean air temperature (°C)	lmm	0.13	0.86	0.96	0.05	- 9.43
Mean river temperature (°C)	River position (km)	lmm	0.13	0.27	0.96	<0.001	- 163.13
Pikeminnow presence /absence	River position (km)	glmm (binomial)	- 7.29	0.5159	NA	0.01	- 4.28
Pikeminnow presence /absence	Roach abundance	glmm (binomial)	- 7.29	0.0015	NA	0.03	- 3.02
Pikeminnow presence /absence	Roach density	glmm (binomial)	- 8.63	3.7015	NA	0.04	-2.25
Pikeminnow presence /absence	River position (km)	glmm (binomial)	- 8.63	0.6661	NA	0.02	- 4.09

Discussion

To our knowledge, this is the first documentation of Sacramento Pikeminnow *(P. grandis)* migration. The seasonal upstream migration began in early summer at the downstream end of their introduced range in the mainstem and South Fork Eel River (Figure 1). River temperature in our study reach was strongly influenced by discharge, air temperature and river position (which correlates with solar radiation and drainage area) (Table 1, Figure 4), and pikeminnow migration timing varied significantly with mean spring river temperature (Figure 2B). At the location that was monitored daily (Wilderness Pool) each year from 2015 to 2019, pikeminnow arrived earlier in warmer years under similar thermal condition (mean weekly temperature, maximum weekly average temperature, Table 1, Figure 2 A, B).

Northcote (1978) described three drivers for fish migration: reproduction, feeding, and refuge. Three lines of evidence suggest that for pikeminnow feeding rather than refuge-seeking or reproduction motivate migration. First, no pikeminnow smaller than 15 cm has ever been seen in our study reach (personal observations and B. Harvey, pers. comm. to Mary Power), suggesting spawning does not occur in this upstream reach. The pikeminnow that seasonally occupy the Angelo Coast Range Reserve are in the sub-adult to adult length range of 15cm - 50cm. Second, timing of pikeminnow arrival coincides with large seasonal increases in the density of their most numerous prey, North Coast Range Roach *(Hesperoleucus venustus,* Figure 3, see also Chapter 1: Figure 6.), due to both roach reproduction and concentration during river recession. Pikeminnow in the South Fork Eel consume these roach (Nakamoto and Harvey 2003). Third, in early and mid-summer *P. grandis* are more likely to be found in large pools where roach are abundant and dense (Figure 3), where their recent arrival may not have allowed sufficient time for reduction in prey numbers.

Temperature likely triggers pikeminnow migration indirectly, by influencing their prey, and directly through their physiology. Temperatures could alter North Coast Range Roach abundance and body size within and between years. Warming strongly influences spawning time (Webb and McLay 1996) and developmental rates (Herzig and Winkler 1986) in cyprinids, as well as growth rates (*P. Georgakakos,* in preparation) of the North Coast Range Roach. If, as we suggest, pikeminnow follow a pulse of roach recruitment, pikeminnow arrival time might track growth and numerical responses of roach, which in turn are responding to temperature. Experimental studies of increases in roach somatic growth rates under warmer temperatures (*P. Georgakakos*, in preparation) are consistent with this interpretation. Additionally, as summer progresses and river waters warm, the upper reaches of pikeminnows' range become more physiologically favorable. Pikeminnow compete more effectively with steelhaed (Reese and Harvey 2002) and can digest more prey in warmer temperatures (Vondracek 1987). Both foraging opportunities from more concentrated prey and the physiological benefits of warmer water likely motivate pikeminnow migration upstream in the South Fork Eel River.

Other pikeminnows, like the Colorado Pikeminnow (*Ptychocheilus lucius),* are known to migrate seasonally to access desirable spawning locations (Tyus and McAda 1984). In

other fishes, migrations can be driven by a combination of factors. For example, pikeperch (*Stizostedion lucioperca)* in River Gudenaa, Denmark, migrate upstream in the spring to spawning locations, and downstream to sites where prey concentrate in the fall (Koed et al. 2000). Similarly, European roach (*Rutilus rutilus*) migrate from lakes to spawn in tributary streams, then as flows increase, roach return to slower water refuge areas after spawning (Vøllestad and L'Abée-Lund 1987). It seems likely that the downstream migration of the Eel River pikeminnow is associated with high fall flows when individuals may seek slow-water refuges downstream.

We predicted river temperature in four scenarios combining "hot" or "cool" spring air temperatures with "low" and "high" flows (Figure 4). If our management goal is to limit stress to native salmonids in this reach, withdrawals prescriptions for a given summer should vary depending on these factors. In years with cool springs and high flows, water temperatures should remain cool throughout the reach, despite sustainable water withdrawals (Figure 4 D). In contrast, years with hot spring air temperatures and low flow, any water withdrawals will elevate temperatures to adverse thresholds. In this case, water withdrawals should be very limited, not only to reduce river temperature for salmonids, but to delay pikeminnow migration and make conditions less physiologically favorable for them (Figure 4 A). These two extreme scenarios are perhaps the most straightforward to manage. Intermediate scenarios with combinations of warm air temperatures and high flow (Figure 4 B) or low air temperature and low flow (Figure 4 C) are more complicated. We suggest prioritizing water for environmental flows in these conditions. Managers could pick a threshold temperature, such as 16.3 (see Figure 4) and adjust withdrawal prescriptions based on the conditions of the year. While our temperature model works well for our study reach, additional temperature data from downstream locations would be needed to model downstream reaches where parameter estimates would likely change. Additional parameters such as watershed lithology, and accounting for autocorrelation of explanatory variables at larger scales would likely be needed to maintain model accuracy. With our relatively limited scope, we show the feasibility of our approach for mechanistically understanding how environmental drivers can predict temperature in a given year and therefore, the timing of pikeminnow migration and arrival.

Our temperature-flow model predicted that pikeminnow would migrate farthest upstream in a low discharge (0.5 m^3/s), high mean air temperature (20°C) year (Figure 4 A). Unexpectedly, the observed pikeminnow migration in 2015, the year most similar to these conditions (mean air temperature 18.9°C, mean discharge 0.59 m^3/s), terminated at the most downstream location of any year of survey from 2015-2018. In summer 2015, the whole study reach was above the 16.3°C threshold we designated as thermally suitable for pikeminnow, by July 1. The shorter migration that year suggests a different factor blocked their upstream spread. A good candidate would be a barrier to passage imposed by low flows. In 2015, flow was so low (less than half of any other year, Table 1) that some areas upstream were likely impassable, potentially limiting upstream extent of movement, despite suitable thermal conditions. Future models predicting pikeminnow migration extent in river reaches should incorporate threshold effects of flow reduction

on passage, as well as temperature regimes under different discharge-air temperature scenarios.

The South Fork Eel River is the most important salmon-bearing tributary in the Eel and one of the last strongholds of Coho Salmon in California (Yoshiyama and Moyle 2010). Size-matched pikeminnow decreased steelhead growth when experimentally competed at 20-23°C but not at 15-18°C (Reese and Harvey 2002), demonstrating that juvenile and sub-adult pikeminnow can outcompete steelhead of their own size, but only under warmer conditions. As adults, pikeminnow consume all the fishes of the South Fork Eel River at some point in their life history (Nakamoto and Harvey 2003). Pikeminnow predation is likely more intense at higher temperatures, as gut passage time was lowest and digestion rate fastest at 20°C versus 15, 10 and 5°C (Vondracek 1987). In addition to these competitive and predatory effects, pikeminnow can also alter the behavior of potential prey fish, which have been observed to shift their habitat use when pikeminnow are present, often spending more time in riffles and shallower areas that pikeminnow do not frequent (Brown and Moyle 1991, Brown and Brasher 1995). Pikeminnows' impacts on upstream prey are more prolonged in warmer years when earlier arrivals in upstream reaches prolong their co-occurrence, and higher temperatures likely intensify their impacts. Timing also determines which species and life history stages of prey they potentially affect. For example, in the South Fork Eel, of the three native Pacific salmonids that regularly spawn and rear in the river, Chinook (*O. tshawytscha*) smolt earliest, and few Chinook smolt linger in the upper South Fork Eel after May of each year. In contrast, both coho (*O. kisutch)* and steelhead (*O. mykiss*) over-summer as fry and parr in this reach. These different life history phenologies suggest that seasonal migration by pikeminnow likely influences coho and steelhead more than chinook in this reach. Timing is also important for the total impact of pikeminnow each summer. Pikeminnow are gape-limited predators, and can consume fish approximately one-third of their body length (Nakamoto and Harvey 2003). Earlier arrival times reduce the chance that over-summering salmonid fry can outgrow the gape limitation of smaller pikeminnow.

Understanding the factors that drive pikeminnow migration, directly or indirectly, will help us predict variation over space and time in the distribution and abundance of this introduced predator, and the resulting impacts on the ecological communities and habitats they traverse. Migrants often transfer energy and nutrient transfers between ecosystems (Polis et al. 2004). Spawning migrations and subsequent death of semelparous Pacific salmons (*Oncorhynchus spp.)* are particularly well studied examples of such subsidies. Fish migration entirely within freshwater -potadromy- is less frequently documented, and such migrants' impacts are often behaviorally mediated. Migratory fishes disperse seeds (Correa et al. 2007), alter rates of nutrient cycling (Flecker 1996), and in contrast to salmonids, migrating *P. grandis* exert predatory and competitive impacts on communities they traverse (Brown and Moyle 1991, Reese and Harvey 2002).

Like Sacramento pikeminnow in the Eel River, other invasive species often experience different seasonal environmental regimes in their non-native environments. Understanding how temperature, moisture, flow velocities, or other seasonal factors

control behavior, movement patterns and the timing of life history events in other invasive species will help us anticipate and manage their impacts on native species and ecosystems under global change. For example, cane toads (*Rhinella marina*) are more active and move greater distances in wet seasons, when they will likely have greater impacts, but possibly would be easier to trap (Brown et al. 2011). Invasive fire ants (*Linepithema humile)* are less active in winter months, when they retreat from satellite nests, and concentrate in fewer larger nest sites, where they may become more vulnerable to control (Heller and Gordon 2006). Understanding how organisms, particularly non-natives, react to environmental factors that change the timing of major life history events will help us control and manage these organisms. Responses of invasive species to environmental change warrant particular attention, in order to minimize their impacts on native organisms. Alterations in spatial distributions, movement, or timing of life history events, for both native and exotic invasive species, set the stage for altered biotic interactions and management strategies in our wetter wet, hotter hot, or drier dry futures.

Acknowledgements

Literature cited

Bauer, S., J. Olson, A. Cockrill, M. van Hattem, L. Miller, M. Tauzer, and G. Leppig. 2015. Impacts of Surface Water Diversions for Marijuana Cultivation on Aquatic Habitat in Four Northwestern California Watersheds. PLoS ONE 10:e0120016–25.

Brodersen, J., A. Nicolle, P. A. Nilsson, C. Skov, C. Brönmark, and L.-A. Hansson. 2011. Interplay between temperature, fish partial migration and trophic dynamics. Oikos 120:1838–1846.

Brown, G. P., C. Kelehear, and R. Shine. 2011. Effects of seasonal aridity on the ecology and behaviour of invasive cane toads in the Australian wet-dry tropics. Functional Ecology 25:1339–1347.

Brown, L. R., and A. M. Brasher. 1995. Effect of predation by Sacramento squawfish (*Ptychocheilus grandis*) on habitat choice of California roach (*Lavinia symmetricus*) and rainbow trout (*Oncorhynchus mykiss*) in artificial streams. Canadian Journal of Fisheries and Aquatic Sciences 52:1639–1646.

Brown, L. R., and P. B. Moyle. 1991. Changes in habitat and microhabitat partitioning within an assemblage of stream fishes in response to predation by Sacramento

squawfish (*Ptychocheilus grandis*). Canadian Journal of Fisheries and Aquatic Sciences 48:849–856.

Brown, L. R., and P. B. Moyle. 1997. Invading species in the Eel River, California: successes, failures, and relationships with resident species. Environmental Biology of Fishes 49:271–291.

Campbell, I. C., C. Poole, W. Giesen, and J. Valbo-Jorgensen. 2006. Species diversity and ecology of Tonle Sap Great Lake, Cambodia. Aquatic Sciences 68:355–373.

Carah, J. K., J. K. Howard, S. E. Thompson, A. G. Short Gianotti, S. D. Bauer, S. M. Carlson, D. N. Dralle, M. W. Gabriel, L. L. Hulette, B. J. Johnson, C. A. Knight, S. J. Kupferberg, S. L. Martin, R. L. Naylor, and M. E. Power. 2015. High Time for Conservation: Adding the Environment to the Debate on Marijuana Liberalization. BioScience 65:822–829.

Correa, S. B., K. O. Winemiller, H. Lopez-Fernandez, and M. Galetti. 2007. Evolutionary perspectives on seed consumption and dispersal by fishes. BioScience 57:748–756.

Flecker, A. S. 1996. Ecosystem Engineering by a Dominant Detritivore in a Diverse Tropical Stream. Ecology 77:1845–1854.

Flecker, A. S., P. B. McIntyre, J. W. Moore, J. T. Anderson, B. W. Taylor, and R. O. Hall Jr. 2010. Migratory fishes as material and process subsidies in riverine ecosystems. American Fisheries Society Symposium 73:559–592.

Gadomski, D. M., C. A. Barfoot, J. B. T. O. the, 2001. 2001. Early life history of the northern pikeminnow in the lower Columbia River basin. Taylor & Francis 130:250–262.

Goulden, M. L., and R. C. Bales. 2019. California forest die-off linked to multi-year deep soil drying in 2012–2015 drought. Nature Geoscience 12:632–637.

Hahm, W. J., D. N. Dralle, D. M. Rempe, A. B. Bryk, S. E. Thompson, T. E. Dawson, and W. E. Dietrich. 2019. Low Subsurface Water Storage Capacity Relative to Annual Rainfall Decouples Mediterranean Plant Productivity and Water Use From Rainfall Variability. Geophysical Research Letters 46:6544–6553.

Harvey, B. C., and R. J. Nakamoto. 1999. Diel and seasonal movements by adult Sacramento pikeminnow (*Ptychocheilus grandis*) in the Eel River, northwestern California. Ecology of Freshwater Fish 8:209–215.

Helfield, J. M., and R. J. Naiman. 2001. Effects of salmon-derived nitrogen on riparian forest growth and implications for stream productivity. Journal of Animal Ecology 82:2403–2409.

Heller, N. E., and D. M. Gordon. 2006. Seasonal spatial dynamics and causes of nest movement in colonies of the invasive Argentine ant (*Linepithema humile*). Ecological Entomology 31:499–510.

Herzig, A., and H. Winkler. 1986. The influence of temperature on the embryonic development of three cyprinid fishes, *Abramis brama, Chalcalburnus chalcoides mento* and *Vimba vimba*. Journal of Fish Biology 28:171–181.

Hughes, N. F., and J. B. Reynolds. 1994. Why Do Arctic Grayling (*Thymallus-Arcticus*) Get Bigger as You Go Upstream. Canadian Journal of Fisheries and Aquatic Sciences 51:2154–2163.

Jackson, R. B., S. R. Carpenter, C. N. Dahm, D. M. McKnight, R. J. Naiman, S. L. Postel, and S. W. Running. 2001. Water in a Changing World. Ecological Applications 11:1027–1045.

Johnston, N. T., E. A. MacIsaac, P. J. Tschaplinski, and K. J. Hall. 2004. Effects of the abundance of spawning sockeye salmon (*Oncorhynchus nerka*) on nutrients and algal biomass in forested streams. Canadian Journal of Fisheries and Aquatic Sciences 61:384–403.

Kinziger, A. P., R. J. Nakamoto, and B. C. Harvey. 2013. Local-scale invasion pathways and small founder numbers in introduced Sacramento pikeminnow (Ptychocheilus grandis). Conservation Genetics 15:1–9.

Letters, D. S. G. R., 2015. 2015. A tale of two California droughts: Lessons amidst record warmth and dryness in a region of complex physical and human geography. Geophysical Research Letters 42:9999–10003.

Lucas, M. C., and E. Batley. 1996. Seasonal movements and behaviour of adult barbel *Barbus barbus*, a riverine cyprinid fish: implications for river management. Journal of Applied Ecology 33:1345.

Lund, J., J. Medellin-Azuara, J. Durand, and K. Stone. 2018. Lessons from California's 2012–2016 drought. Journal of Water Resources and Planning Management 144:04018067.

Montgomery, D. R., J. M. Buffington, N. P. Peterson, D. Schuett-Hames, and T. P. Quinn. 1996. Stream-bed scour, egg burial depths, and the influence of salmonid spawning on bed surface mobility and embryo survival. Canadian Journal of Fisheries and Aquatic Sciences 53:1061–1070.

Moore, J. W., and D. E. Schindler. 2008. Biotic disturbance and benthic community dynamics in salmon-bearing streams. Journal of Animal Ecology 77:275–284.

Nakamoto, R. J., and B. C. Harvey. 2003. Spatial, seasonal, and size-dependent variation in the diet of Sacramento pikeminnow in the Eel River, northwestern California. California Fish and Game 89:30–45.

Paine, R. T., M. J. Tegner, and E. A. Johnson. 1998. Compounded perturbations yield ecological surprises. Ecosystems 1:535–545.

Payne, L. X., and J. W. Moore. 2006. Mobile scavengers create hotspots of freshwater productivity. Oikos 115:69–80.

Pierce, D. W., J. F. Kalansky, and D. R. Cayan. 2018. Climate, drought, and sea level rise scenarios for California's fourth climate change assessment.

Polis, G. A., M. E. Power, and G. R. Huxel. 2004. Food webs at the landscape level. University of Chicago Press.

Power, M. E., K. Bouma-Gregson, P. Higgins, and S. M. Carlson. 2015. The Thirsty Eel: Summer and Winter Flow Thresholds that Tilt the Eel River of Northwestern California from Salmon-Supporting to Cyanobacterially Degraded States. Copeia 103:200–211.

Power, M. E., M. S. Parker, and W. E. Dietrich. 2008. Seasonal reassembly of a river food web: floods, droughts, and impacts of fish. Ecological Monographs 78:263–282.

Quinn, T. P., S. Hodgson, C. P. C. J. of, 1997. 1997. Temperature, flow, and the migration of adult sockeye salmon (Oncorhynchus nerka) in the Columbia River. Canadian Journal of Fisheries and Aquatic Sciences 54:1349–1360.

Rahel, F. J., and J. D. Olden. 2008. Assessing the Effects of Climate Change on Aquatic Invasive Species. Conservation Biology 22:521–533.

Reese, C. D., and B. C. Harvey. 2002. Temperature-dependent interactions between juvenile steelhead and Sacramento pikeminnow in laboratory streams. Transactions of the American Fisheries Society 131:599–606.

Schindler, D. E., M. D. Scheuerell, J. W. Moore, S. M. Gende, T. B. Francis, and W. J. Palen. 2003. Pacific salmon and the ecology of coastal ecosystems. Frontiers in Ecology and the Environment 1:31–37.

Strayer, D. L. 2010. Alien species in fresh waters: ecological effects, interactions with other stressors, and prospects for the future. Freshwater Biology 55:152–174.

Sykes, G. E., C. J. Johnson, and J. M. Shrimpton. 2009. Temperature and Flow Effects on Migration Timing of Chinook Salmon Smolts. Transactions of the American Fisheries Society 138:1252–1265.

Tyus, H. M., and C. W. McAda. 1984. Migration, movements and habitat preferences of Colorado squawfish, *Ptychocheilus lucius*, in the Green, White and Yampa rivers, Colorado and Utah. Journal of Animal Ecology 29:289–299.

Vondracek, B. 1987. Digestion rates and gastric evacuation times in relation to temperature of the Sacramento Squafish, *Ptychocheilus Grandis*. Fishery Bulletin 85:159–163.

Vøllestad, L. A., and J. H. L'Abée-Lund. 1987. Reproductive biology of stream-spawning roach, Rutilus rutilus. Environmental Biology of Fishes 18:219–227.

Walters, A. W., R. T. Barnes, and D. M. Post. 2009. Anadromous alewives (*Alosa pseudoharengus*) contribute marine-derived nutrients to coastal stream food webs. Canadian Journal of Fisheries and Aquatic Sciences 66:439–448.

Webb, J. H., and H. A. McLay. 1996. Variation in the time of spawning of Atlantic salmon (*Salmo salar*) and its relationship to temperature in the Aberdeenshire Dee, Scotland. Canadian Journal of Fisheries and Aquatic Sciences 53:2739–2744.

Wipfli, M. S., and C. V. Baxter. 2010. Linking Ecosystems, Food Webs, and Fish Production: Subsidies in Salmonid Watersheds. Fisheries 35:373–387.

Yoshiyama, R. M., and P. B. Moyle. 2010. Historical review of Eel River anadromous salmonids, with emphasis on Chinook salmon, coho salmon and steelhead. Report for California Trout. Center for Watershed Science.

Supplementary Material

Formula 1. Cumulative degree-days above 15°C

$$DegreeDay\ (°C \bullet 24hr) = \sum_{Date\ Time_{Start}}^{Date\ Time_{End}} \frac{T_{hourly} - 15}{24hrs}$$

Table 1. Location and river position of survey pools and temperature sensors

Location description	Latitude (N)	Longitude (W)	River position (km)	Study activity and year
Wilderness Lodge Rd. Bridge	39.70293°	123.6540°	0	River kilometer zero marker
Science Center	39.71890°	123.6529°	2.346	Bi-weekly snorkel survey (2015, Figure 3)
Temperature sensor 1	39.719031°	-123.6524°	2.395	Most upstream temperature sensor 2016, 2017, 2018, 2019
Temperature sensor 2	39.719046°	-123.6519°	2.435	Temperature sensor 2015, 2016, 2017
Edell's Pool	39.72205°	123.6500°	2.945	Bi-weekly snorkel survey (2015, Figure 3)
Temperature sensor 3	39.723954°	-123.6484°	3.385	Temperature sensor 2016, 2017, 2018, 2019
Temperature sensor 4	39.723308°	-123.6470°	3.528	Temperature sensor 2016, 2017
Temperature sensor 5	39.723452°	-123.6458°	3.623	Temperature sensor 2016, 2017, 2018, 2019
Temperature sensor 6	39.725865°	-123.6447°	3.994	Temperature sensor 2016, 2017, 2018, 2019
Temperature sensor 7	39.727961°	-123.6469°	4.313	Temperature sensor 2016, 2017, 2018, 2019
Temperature sensor 8	39.728778°	-123.6486°	4.499	Temperature sensor 2016, 2017, 2018, 2019
Pete's Pool	39.73101°	123.6474°	4.831	Bi-weekly snorkel survey (2015, Figure 3)
Temperature sensor 9	39.732800°	-123.6464°	5.025	Temperature sensor 2015, 2016, 2018, 2019
Temperature sensor 10	39.735932°	-123.6316°	7.233	Temperature sensor 2015, 2016, 2017, 2018, 2019
Lower Walker Meadow Pool	39.73638°	123.6314°	7.319	Bi-weekly snorkel survey (2015, Figure 3)
Temperature sensor 11	39.739735°	-123.6321°	7.703	Temperature sensor 2016, 2017
Temperature sensor 12	39.740260°	-123.632420°	7.760	Temperature sensor 2016, 2017, 2018, 2019
Wilderness Pool	39.74075°	123.6333°	7.903	Bi-weekly snorkel survey (2015, Figure 3), Daily snorkel survey for pikeminnow arrival 2015-2019, Figure 2)

Temperature sensor 13	39.741369°	-123.6342°	7.982	Temperature sensor 2016, 2017, 2018, 2019
Temperature sensor 14	39.742392°	-123.6379°	8.443	Temperature sensor 2016, 2017, 2018
Whitehouse Pool	39.74767°	123.6337°	10.842	Bi-weekly snorkel survey (2015, Figure 3)
Temperature sensor 15	39.747625°	-123.6330°	10.992	Temperature sensor 2015, 2016, 2017, 2019
Temperature sensor 16	39.753939°	-123.6315°	12.116	Temperature sensor 2016, 2018, 2019
Tenmile Confluence Pool	39.75497°	123.6314°	12.314	Bi-weekly snorkel survey (2015, Figure 3)
Temperature sensor 17	39.755764°	-123.6313°	12.345	Temperature sensor 2015, 2016, 2017, 2018, 2019
Hunter's Pool	39.75790°	123.6368°	13.040	Bi-weekly snorkel survey (2015, Figure 3)
Temperature sensor 18	39.758944°	-123.6372°	13.192	Most downstream temperature sensor 2015, 2016, 2017, 2018, 2019

Table 2. All vertebrates encountered during snorkel surveys. Species-specific size classes used to categorize organisms during snorkel surveys.

Species	Size classes (cm)	Measurement type
Hesperoleucus venustus, North Coast Range Roach	(0-2), (2-5), (5-10), (10-15)	Total length
Ptychocheilus grandis, Sacramento pikeminnow	(0-5), (5-10), (10-15), (15-20), (20-25), (25-30), (30-40), (40-60)	Total length
Notemigonus crysoleucus, golden shiner	(0-5), (5-10), (10-15), (15-20)	Total length
Catostomus occidentalis, Sacramento sucker	(0-5), (5-10), (10-15), (15-20), (20-25), (25-30), (30-40), (40-60)	Total length
Oncorhynchus tshawytscha, chinook salmon	(0-5), (5-10), (10-15), (15-20)	Total length
Oncorhynchus kisutch, coho salmon	(0-5), (5-10) (10-15), (15-20)	Total length
Oncorhynchus mykiss, steelhead	(0-5), (5-10) (10-15), (15-20), (20-25), (25-30), (30-40), (40-60)	Total length
Gasterosteus aculeatus, three-spined stickleback	(0-2), (2-5), (5-10)	Total length
Entosphenus tridentatus, Pacific lamprey	(0-10), (10-40), (40-100)	Total length
Lepomis cyanellus, green sunfish	(0-5), (5-10), (10-15), (15-20), (20-30)	Total length
Lepomis macrochirus, bluegill	(0-5), (5-10), (10-15), (15-20), (20-30)	Total length

Species	Size classes (cm)	Measurement
Micropterus salmoides, largemouth bass	(0-5), (5-10), (10-15), (15-20), (20-30), (30-40)	Total length
Amerius sp., bullhead catfish	(0-5), (5-10), (10-15), (15-20), (20-30)	Total length
Thamnophis atratus, aquatic garter snake	(0-20), (20-40), (40-60), (60-80)	Total length
Actinemys marmorata, western pond turtle	(0-5), (5-10), (10-20), (20-30)	Carapace length
Rana boylii, foothill yellow-legged frog	Larvae (0-2), (2-5) Frog (0-3), (3-10)	Larva: Total length Frog: snout-vent length
Rana catesbeiana, bullfrog	Larvae (0-2), (2-5), (5-10), (10-15) Frog (0-3), (3-15)	Larva (with tail): Total length Frog (no-tail): snout-vent length
Taricha granulosa, rough-skinned newt	Larvae: (0-4) Adult: (0-5), (5-10)	Larva (no back limbs): Total length Adult (has back limbs): snout-vent length

Transition from Chapter 2 to 3

In addition to the negative effects described in Chapter 2, native species might be detrimentally impacted by a reduction in positive interaction that occurred in the historic ecological state. During the survey work described in Chapter 1, I encountered Pacific Lamprey *(Entosphenus tridentatus)* constructing redds in late May. While observing lamprey constructing redds in the shallow outflow of a pool, I saw several juvenile steelhead *(O. mykiss)* congregated at the downstream end of an active redd. These fish appeared to be drift foraging on invertebrates that the lamprey dislodged during their redd building activities. Gabe Rossi had similar observations from redds in Elder Creek during the same year. This motivated a collaboration to determine the profitability of foraging behind lamprey redds for juvenile salmonids. Sarah Kupferberg added observations of Foothill Yellow-legged Frogs (*R. boylii)* using redds as egg mass depositions sites after hearing about our steelhead observations. These observations built into a narrative of positive influences of Pacific Lamprey, and how the decline in their numbers from historical levels could influence other members of the aquatic community.

Chapter 3. Pacific Lamprey facilitate juvenile salmonids and Foothill Yellow-legged Frogs

Abstract

Migrating organisms can exert strong influences on the ecosystems they traverse, physically altering habitats and delivering subsidies of resources. While the effect of migrants on nutrient and trophic dynamics are well studied, their role in species interactions that shape population and community dynamics is less understood. In Northwestern California great numbers of Pacific Lamprey (*Entosphenus tridentatus*) swim into coastal rivers annually to spawn. While engineering their redds, lamprey mobilize and rearrange large amounts of sediment and disturb the macroinvertebrates living in and on the benthos. In California's Eel River we investigated (1) how bioturbation during lamprey redd construction influenced invertebrate drift, (2) whether juvenile Steelhead (*Oncorhynchus mykiss*) foraged more behind active redds, (3) how redd building influenced foraging profitability (as estimated from bioenergetic models), and (4) the effects of built lamprey redds on local water velocity. On average, 113% more invertebrates were collected in drift samples downstream of lamprey that were actively building redds and biomass of drifting invertebrates was 125% more concentrated, relative to drift in adjacent lateral positions not influenced by lamprey redd construction. Additionally, different taxa were more abundant in drift samples downstream of lamprey: Simuliids, Chironomids, and Elmids were more numerous. Juvenile Steelhead foraged on average 76% more frequently while drift feeding downstream of redd building lamprey, and results of our bioenergetics models suggest that these locations were more profitable for growth than adjacent areas. Foothill yellow-legged frogs (*Rana boylii)* deposited their egg masses in completed lamprey redds, capitalizing on the flow refuge that both decreased scour risk and added depth that kept clutches submerged as spring flow receded. Salmonid fry also held positions in the low-velocity areas within redds. Our findings emphasize the importance of semelparous migratory organisms as ecological interactors that can benefit other native species in addition to subsidizing spawning areas with nutrients and energy from their carcasses. The historical abundance of lamprey in coastal California rivers suggests these interactions could influence population dynamics of salmonids and foothill yellow-legged frogs. Our insights support the need to continue efforts to restore Pacific Lamprey to their historic ranges and abundance.

"And the other is Gary Nabhan's idea. In one of his books he says that animals don't go extinct because someone shoots the last one, or a bulldozer scrapes away the last habitat. They go extinct because the web of relationships that sustain them unravels. He then put it in anthropomorphic terms and said, they go extinct because of a lack of ecological companionship."

Jim Lichatowitch (2013)

Introduction

Animals' migrations are among the most spectacular ecological events across the globe. Sadly, in recent history fewer individuals take part in the most iconic migrations (Wilcove and Wikelski 2008). Monarch butterfly populations have dwindled (Brower et al. 2011), migratory North American avifauna are estimated to have diminished by 2.5 billion individuals since 1970 (Rosenberg et al. 2019), and mammal migrations are greatly reduced worldwide (Harris et al. 2009). Not least, numbers of anadromous fish migrating from the ocean to freshwater streams pale in comparison to their historic abundances (Brown et al. 1994, Mattocks et al. 2017). The decline of animal migrations has been well documented, with cascading effects on trophic and nutrient dynamics (Quinn et al. 2009).   Equally important are the losses of species interactions that shape population and community dynamics in landscapes traversed during migrations (Flecker et al. 2010). This loss of interactions and changes or reduction in their strength is challenging to quantify, but important as we try to predict how declines of migratory animals will influence ecological communities.

Migrants exert strong effects on the ecosystems they traverse, physically altering habitats (e.g. Gerlanc and Kaufman 2003), delivering trophic subsidies (e.g. Uno and Power 2015), and interacting with other species (Flecker et al. 2010, Uno and Power 2015). Their movements connect geographically distant systems, and large influxes of animals can seasonally alter food web dynamics (Polis et al. 1997). Migrants, like Pacific Salmon (*Oncorhynchus spp.)* in North America transfer energy and nutrients to recipient systems (Johnston et al. 2004, Walters et al. 2009), and to the surrounding habitats (Helfield and Naiman 2001) when they return to spawn. In addition to these energy and nutrient subsidies, migrants also alter local conditions and processes through behaviors (Flecker et al. 2010). Migratory fishes mobilize fine sediments (Montgomery et al. 1996), reduce production of periphyton and invertebrates by building redds (Moore and Schindler 2008), disperse seeds (Correa et al. 2007), and alter rates of nutrient cycling (Flecker 1996).

Anadromous Pacific Lamprey (*Entosphenus tridentatus)*, are semelparous, and not only subsidize their spawning grounds with the energy and nutrients from their carcasses, but also interact with other aquatic organisms as they build redds. As recently as the late 19th century, large numbers of Pacific Lamprey regularly returned to rivers of Western North America to spawn. Descriptions of layers of individuals writhing up Willamette Falls attest to their plentiful numbers in these years (Macdonald 1894). These observations of large numbers of breeding lamprey have largely disappeared, and though poorly quantified, current observations and evidence suggest widespread Pacific lamprey population decline and range contraction across the Pacific basin (Stillwater Sciences 2010, Goodman and Reid 2012, Close et al. 2002). Lamprey declines have not attracted the same degree of conservation attention as declines of Pacific salmon, likely due to the lack of commercial interest. This has been changing, however, because of the cultural importance of lamprey to indigenous people along the Pacific Coast (Close et al. 2002). In 2003, conservation groups, including Native American tribes, initiated an effort to list four species of western lampreys under the Endangered Species Act (Nawa et al. 2003). This effort was eventually rejected, citing lack of evidence quantifying decline (USFWS 2004). More recently, tribal interests and natural resource agencies came together to

create the Pacific Lamprey Conservation Initiative, which aims to assess lamprey populations, reduce threats to lamprey, and improve their habitats and population status (USFWS 2012). This initiative represents a major change in management focus and sparked a growth in studies on aspects of lamprey dynamics and ecology, which include studies documenting lamprey swimming ability (Frick et al. 2017), detection of occupancy during surveys (Reid and Goodman 2015), performance in passing constructed fishways (Goodman and Reid 2017), effects of temperature on migration (Keefer et al. 2009), the influence of ocean conditions (Clemens et al. 2019), and susceptibility to climate change (Wang et al. 2020). Goodman and Reid (2015) summarized many studies in a management plan to conserve Pacific Lamprey in California coastal streams. Collectively, this body of work lays the foundation needed to build effective management and conservation plans for Pacific Lamprey.

The overall goal of our work is to contribute knowledge on lamprey ecology by describing ecological interactions, specifically, positive interactions associated with redd building between lamprey and other members of aquatic food-webs. In particular, we: 1) quantify lamprey redd building's influence on stream invertebrate drift, 2) evaluate the ability of juvenile steelhead (*Oncorhynchus mykiss*) to capitalize on increased drift associated with redd building, 3) estimate the influence of this seasonal subsidy on steelhead growth using a bioenergetics model and consider the effects of this subsidy on steelhead populations; and 4) document the use of redd depressions and associated velocity and depth refugia by both breeding Foothill Yellow-legged Frogs (Rana boylii) and juvenile salmonids. We hypothesized that (H1) lamprey redd building would increase invertebrate drift due to bioturbation of the stream benthos; which would (H1a) increase the foraging rate of juvenile steelhead directly proximate to lamprey redds and (H1b) increase the foraging profitability of these areas relative to nearby foraging locations. We also hypothesized that (H2) the physical structure of the redds would alter stream hydraulics (Stone 2006) in a manner that would create velocity and depth refugia for other aquatic species such as Steelhead trout fry and Foothill Yellow-legged Frogs.

Methods

Study site and ecological community

We studied the effects of lamprey redds and their construction on juvenile Steelhead and Foothill Yellow-legged Frogs in the upper South Fork Eel River in and around the University of California, Berkeley's Angelo Coast Range Reserve (Mendocino Co.). Our study reach, near the Angelo Reserve, spanned 10km and extended from the Angelo Reserve's Environmental Science Center (39.7189°N, 123.6529°W) downstream to Hunter's Pool (39.7579°N, 123.6368°W). Additionally, we studied Lamprey redds in the South Fork Eel River at the Benbow State Recreation Area in Humboldt Co., California (40.0659°N, 123.7906°W).

Food web phenology and life history timing of study species

The South Fork Eel supports populations of Steelhead, Pacific Lamprey, and Foothill Yellow-legged Frogs. During typical springs in this Mediterranean river, flow recedes,

temperatures increase, and light levels increase. These physical changes coincide with the timing of key life history events in all three species that set the stage for the ecological interactions we describe. Steelhead fry emerged from nests in the spring, where eggs were deposited by spawning adults in the late winter, and actively forage while avoiding larger conspecifics. The previous year's cohort has grown into parr roughly 60-100mm (Moyle 2002), and the increased temperature, invertebrate abundance, and algal production, makes spring an important period for trout growth (Gasith and Resh 1999, Power et al. 2013). Steelhead trout's flexible life history results in individuals from 1-4 years old present in the river, which range from 100-200mm, and continue to forage and grow as they move towards smoltification or remain residents (Moyle 2002). Individuals that will smolt in a given year move from natal tributaries into the mainstem (Kelson and Carlson 2019) and aggregate into loose schools as they move downstream. Foothill yellow-legged frogs also migrate in April from tributaries to historic lek sites on the mainstem. Frog lek sites occur where cobble and gravel sediments deposit, such as pool tail outs, and thus often coincide with the same mesohabitats typical of lamprey spawning grounds (Mayfield et al. 2014). Female frogs deposit one clutch of eggs per year that contains 1000-2000 eggs, and laying location is an important decision. This annual choice determines offspring survival from egg masses that are vulnerable to scour, stranding, predators, and disease (Kupferberg 1996). Eggs must stay submerged for the two to three weeks (depending on temperature) to hatch into mobile tadpoles that graze diatoms in low flow, high productivity areas.

Adult Pacific Lamprey migrate upstream to spawn in late winter and early spring. Adults of both sexes excavate redds using two distinct behaviors. To move larger sediments (5-15cm diameter), they attach their suctorial mouth to the target object and flail their bodies vigorously to dislodge the object, which is usually displaced downstream. To move finer sediments, individuals attach by mouth to an "anchor", an object large enough to remain stationary, often a boulder, then rotate their bodies 90° around their lateral axis and rapidly flutter their caudal fin against the bed. This second behavior dislodges fine sediments which drift downstream with the current. Lamprey exhibit similar behavior when spawning; the male wraps itself around the female, who flutters her caudal fin while releasing eggs that settle in the downstream portion of the redd. Juveniles emerge and filter feed for three to seven years before metamorphosing into parasitic adults that migrate to the ocean (Close et al. 2002).

Lamprey numbers and density

Counts of lamprey in the South Fork Eel River in the Angelo Coast Range Reserve ranged from 524 individuals in 2016 to 126 in 2018, with even lower densities estimated at 37 individuals, based on their densities in the 51.7% of units surveyed in 2019. In 2017, we counted 253 lamprey (Supplemental Material Table 1, see Chapter 1 for methods). Tracking abundance, lamprey densities were highest in 2016 (49.2 (individuals/ km), and lowest in 2019, 3.4 (individuals/km).

Site/pair description

To test hypothesis H1, we used a paired study design focused on lamprey redds actively under construction (Figure 1). Paired sites consisted of both a 'Lamprey' treatment that was downstream of the active redd and influenced by redd building activities, and an adjacent physically similar lateral position lacking redd-making activity ('No-Lamprey' treatment).
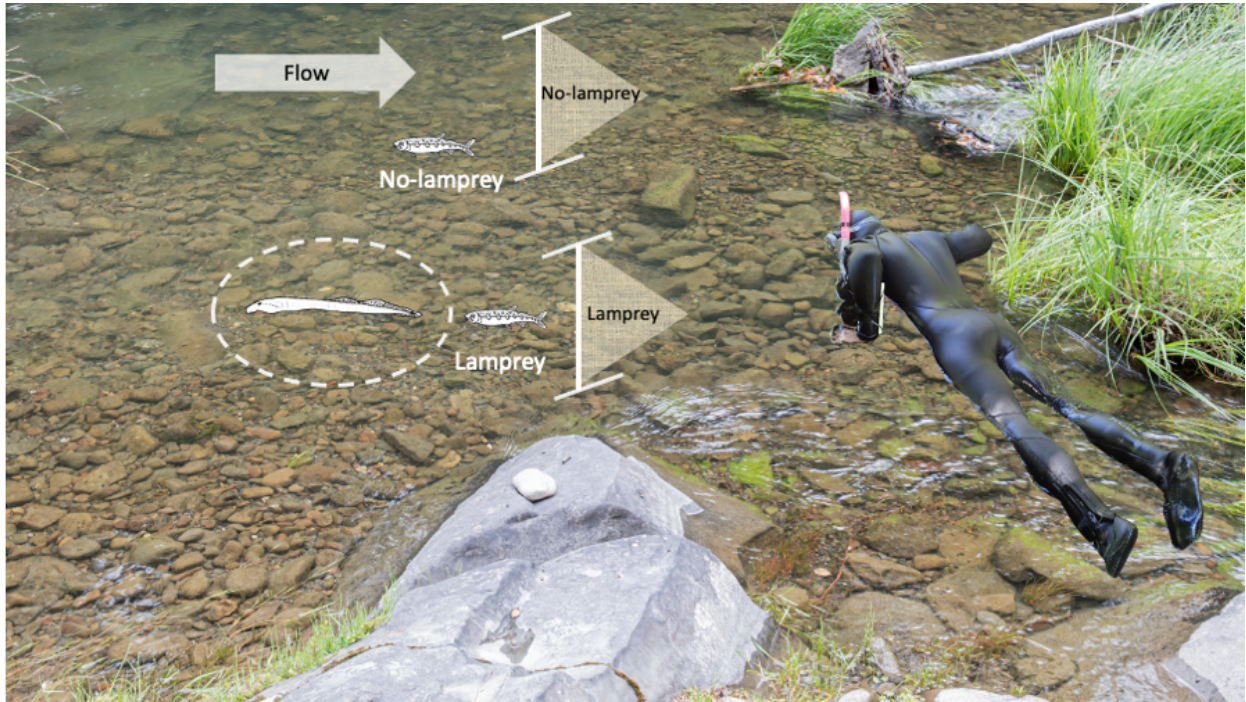

Figure 1: Depiction of our study design. The dashed line depicts a hypothetical redd being constructed by a lamprey. Two Juvenile *O.mykiss* and drift nets are depicted in this location, the steelhead and net directly downstream of the lamprey constitute the 'Lamprey' treatment. The adjacent *O. mykiss* represent the 'No-Lamprey' treatment. The snorkeler, stationary while observing steelhead foraging behavior, is depicted in a typical location. Though shown together here, nets were never deployed while steelhead behavior was being observed.

H1: The Effect of Lamprey Redd Building on Stream Invertebrate Drift

We collected drifting invertebrates from 5 sites with redd building lamprey (Figure 1). Drift nets (10cm x 10cm and 500-μm mesh) were set near the river bottom, just above the substrate to avoid collecting crawling invertebrates. Stream drift is often measured near the water surface (Baxter et al. 2017). Because our objective was to measure the effect of redd building on invertebrate drift, however, we sampled just above the bed. At each site, one drift net was set 1.5m downstream of redd building lamprey ('Lamprey' treatment), and another was deployed simultaneously in an adjacent lateral position ('No-Lamprey' treatment). Nets were separated laterally by at least 2 m to avoid collecting any invertebrates dislodged by redd building activities in the no-lamprey treatment nets. Nets were deployed for 2hrs in the afternoon from 1400-1800. After nets were removed, water velocity was measured with a Marsh -McBirnery flow meter (Model 2000-11) at 3 positions at the mouth of the nets; these measurements were averaged. Water velocity entering the drift net times the area of the net mouth was used to calculate discharge

intercepted and to compute drift concentration (Baxter et al. 2017). Invertebrates were rinsed from the nets into trays and elutriated into falcon tubes where they were stored in 95% ethanol. In the laboratory, invertebrates were separated from other material collected in drift, measured to the nearest millimeter and identified to the lowest taxonomic unit possible using 10x magnification. Biomass (mg dry mass) was estimated from published length to dry mass relationships (Benke et al. 1999, Sabo et al. 2002). Drift flux (mg/hr) was computed by summing the mass of drifting invertebrates captured in the drift net and dividing the total mass by the duration of the drift sample. We calculated concentration by dividing biomass or number of invertebrates by water velocity (m/s) * time net deployment (120 minutes) * net area (100cm^2) (Baxter et al. 2017). We used paired t-tests (linear mixed-effect model with random effect of pair) to test for differences in biomass concentration and concentration of invertebrates. We tested whether there were differences in the number of drifting invertebrates with a generalized linear mixed-model with a Poisson distribution and a random effect of pair.

To determine whether the composition of drift differed between lamprey and no-lamprey treatments, we used a Permutational Multivariate Analysis of Variance (PERMANOVA) with Bray-Curtis distance, implemented in the 'vegan' package. We also tested to see whether there were differences in the size distributions of the 5 most numerous taxa, using X^2 tests, and linear mixed effect models, to test if redd building influenced invertebrates in different developmental stages differentially. We plotted the community composition using Non-metric Dimensional Scaling (NMDS).

H1a: The Effect of Lamprey Redd Building on Juvenile Steelhead Foraging Rate

After locating an active redd, a snorkeler submerged in the riffle approximately 5m downstream or to the side of the redd (Figure 1) and waited 10 minutes to let animals acclimate to their presence. Individual steelhead were observed for 5 minutes, and the number of foraging attempts were recorded. We considered a foraging attempt to be a change from upstream orientation, often accompanied by a short sally from the starting position, and subsequent return to the same or similar location with upstream orientation (Nakano et al. 1999). All observed steelhead were estimated to be between 11 and 14 cm in total length. Observations of a juvenile steelhead feeding on drift directly downstream of the redd building lamprey ('Lamprey' treatment) were paired with 'control' observations of a juvenile steelhead feeding in the same riffle, but adjacent (further than 1 m) from the redd building lamprey ('No-Lamprey' treatment). A total of 11 pairs or 22 total fish were observed. We used a paired t-test (linear model with random effect of pair) to test for differences in the number of foraging attempts between fish in the lamprey and no-lamprey treatments.

H1b: The Effect of Lamprey Redd Building Juvenile Steelhead Growth Potential

We modeled the net rate of energy intake (NREI) as an indicator of drift foraging profitability at each of the 5 paired sites where we collected drift. To estimate NREI we used a drift foraging bioenergetics model based on Caldwell et al. (2018) and Rosenfeld and Taylor (2009). The model uses drift concentration, foraging volume (a function of fish size, water velocity, and prey size see Rosenfeld and Taylor (2009)), fish size, and

prey size to quantify gross energetic intake rate (Caldwell et al. 2018). This gross energetic intake is a product of capture probability, drift concentration, and discharge through foraging volume. Energetic losses are subtracted from these energetic gains; losses include swimming costs which vary with fish size and focal point velocity (Rosenfeld and Taylor 2009, Caldwell et al. 2018). Water temperature was incorporated into the swimming costs (Rosenfeld and Taylor 2009); however, we assumed a constant energy assimilation efficiency of 0.6 (Tucker and Rasmussen 1999). Fish foraging time was set to 12 hours a day. For fish focal point velocity, we used our flow measurements at the mouth of the drift nets. The NREI (joules $\times$ second^{-1}) is the net energy acquired by juvenile fish for growth (gross energy intake – swimming and metabolic costs). Following Rosenfeld and Taylor (2009) and (Naman et al. 2019), we used NREI to estimate growth rate. Energy, in joules, was converted to biomass (dry weight) using a family (Salmonidae) specific relationship. This method accounts for differences in fish sizes (Post and Parkinson 2001). We used these estimated gains in weight to calculate the percentage of biomass added for steelhead ranging from 10-20cm. We tested whether there were differences in both NREI (joules/day) and potential growth (grams/day) with linear mixed-effect models. Both models included lamprey treatment and fish size as fixed-effects and a random effect of site.

H2: Physical structure and hydraulic influence of redds as velocity and flow refugia

We measured the dimensions (to the nearest cm) of a total of 70 redds in 2017 and 2018 (length, parallel to flow; width, perpendicular to flow; depth of excavation, and depth beneath the water's surface). We also measured velocity in and around a total of 16 lamprey redds in 2018 and 2020. Flow measurements were taken at 4 locations, inside the deepest area in redd depression, outside the redd both left and right, and just upstream of the redd. Measurements were taken with a Marsh-McBirney flow meter (Model 2000-11) ~ 2.5 cm above the bed, as close to the bottom as possible. Comparisons were made with a linear mixed-effect model, with fixed-effects of location around the redd and a random-effect of redd.

During annual frog breeding censuses (2015-2020) we kept a tally of instances when lamprey and frog spawning coincided. In 2018 we measured water depth to the nearest 0.5 cm at a weekly interval where frogs oviposited inside lamprey redds. We calculated the depth and velocity differences between clutches inside vs. outside of redds and translated the depth difference into a time relevant for frog spawn desiccation by examining the rate of depth decrease at marked clutches. We extrapolated the additional number of days clutches would remain inundated. We compared the survival to hatching in 2018 when eggs were laid inside redds versus years when oviposition in redds did not occur.

We compared the sediment composition of the streambed at frog lek sites where oviposition occurred in lamprey redds to sites where redds were not used for oviposition. We conducted Wolman pebble counts using a sample frame (Bunte and Abt 2001) and calculated the median grain size.

Data management and statistical analysis
All data were manipulated and analyzed in R (R core team R version 3.5.1.), using the CRAN packages, tidyverse, lubridate, vegan, lme4, and lmerTest.

Results

The Effect of Lamprey Redd Building on Stream Invertebrate Drift

Amount and concentration of drift
In our 5 paired drift samples invertebrate biomass was on average 89% more concentrated (Figure 2B, paired t-test, N = 5, p = .038) in the lamprey treatments. Numbers of drifting invertebrates were 113% greater (Fig. 2a, GLMM, N = 5, p <0.0001) and drifting invertebrate biomass was 125% more concentrated in the lamprey treatment compared to the no-lamprey treatment (paired t-test, N = 5, p = 0.01).

Composition of drift
In addition to total number and biomass of drifting invertebrates there were differences in the composition of taxa drifting between treatments (Figure 3, Figure 4, p = 0.01, PERMANOVA). 382 invertebrates representing 23 taxa were identified and measured from our 5 pairs of drift samples. The four most numerous taxa were simuliids, chironomids, baetids, and elmids, which made up 91% of the total number of invertebrates (Figure 4 A), and 79 % of biomass (Figure 3 B). Of these, simuliids, chironomids and baetids were the main drivers of variation in the PERMANOVA (Figure 5, simuliidae 20.1%, chironomidae 13.8%, baetidae 7.1). These soft-bodied taxa were more abundant in Lamprey samples (Figure 4). Simuliids, chironomids and baetids occurred in all drift samples. Elmids, adult dipterans, and hydropsychids occurred in 3-5 samples. All other taxa were collected in 2 or fewer samples. Perlids, ephemerellids, and acari were collected in one sample each, and all in lamprey treatments. One lepidostomatid, psephenid, tipulid, and heptageniid were collected, and only in no-lamprey samples.

Size frequency distributions of invertebrates
 We found no difference in the size frequency distributions of any of the 4 most common taxa (SM figure 1, Simuliidae, Chironomidae, Baetidae, and Elmidae. P > 0.05, X^2 tests, sm. fig 2.). However, both baetids and elmids show a trend towards larger individuals in the lamprey treatment (elmid lamprey treatment mean = 2.96mm, no-lamprey = 1.10mm, baetid lamprey treatment mean = 2.39mm, no-lamprey = 1.97mm). Differences in the sample means were marginally significant for baetids (paired t, p = 0.07) and not significant for elmids (paired t, elmid p= 0.16). Size frequency distributions were not significantly different (X^2, baetid 0.40, elmid p = 0.66). This could result from a relatively small sample size, rather than lack of effect.
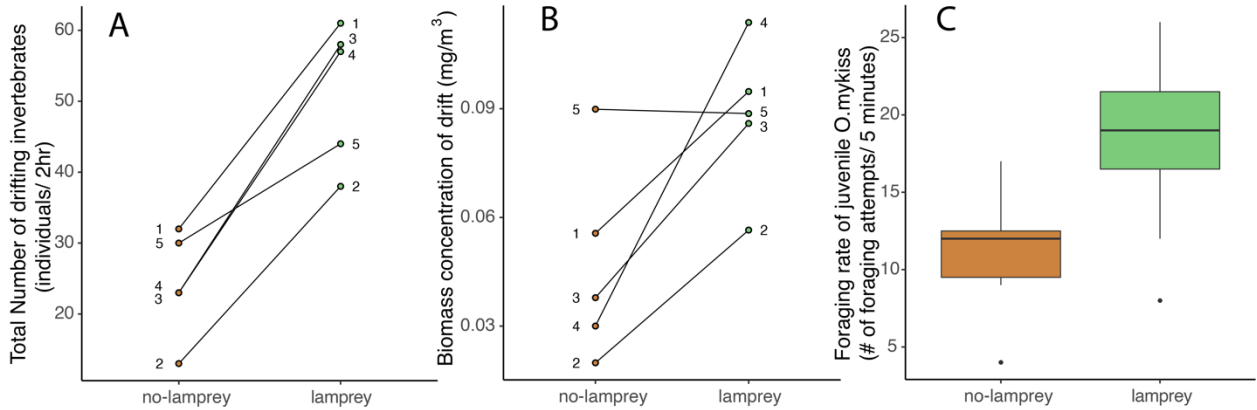
Figure 2: **A.** Number of invertebrates collected in drift samples in both lamprey and no-lamprey treatments. Lines connect paired samples. Significantly more invertebrates were sampled in lamprey treatments (GLMM, N = 5, p <.0001) **B.** Biomass concentration of drifting invertebrates (mg/m^3) from drift samples in both lamprey and no-lamprey treatments. Lines connect paired samples. Drift biomass was significantly more concentrated in lamprey samples (paired t-test, N = 5, p = .038). **C.** Number foraging attempts by juvenile *O. mykiss* in 5 minutes behind lamprey and No-lamprey sites. Midline is the median, box edges are 25 and 75 percentiles, and whiskers show 5 and 95 percentiles.

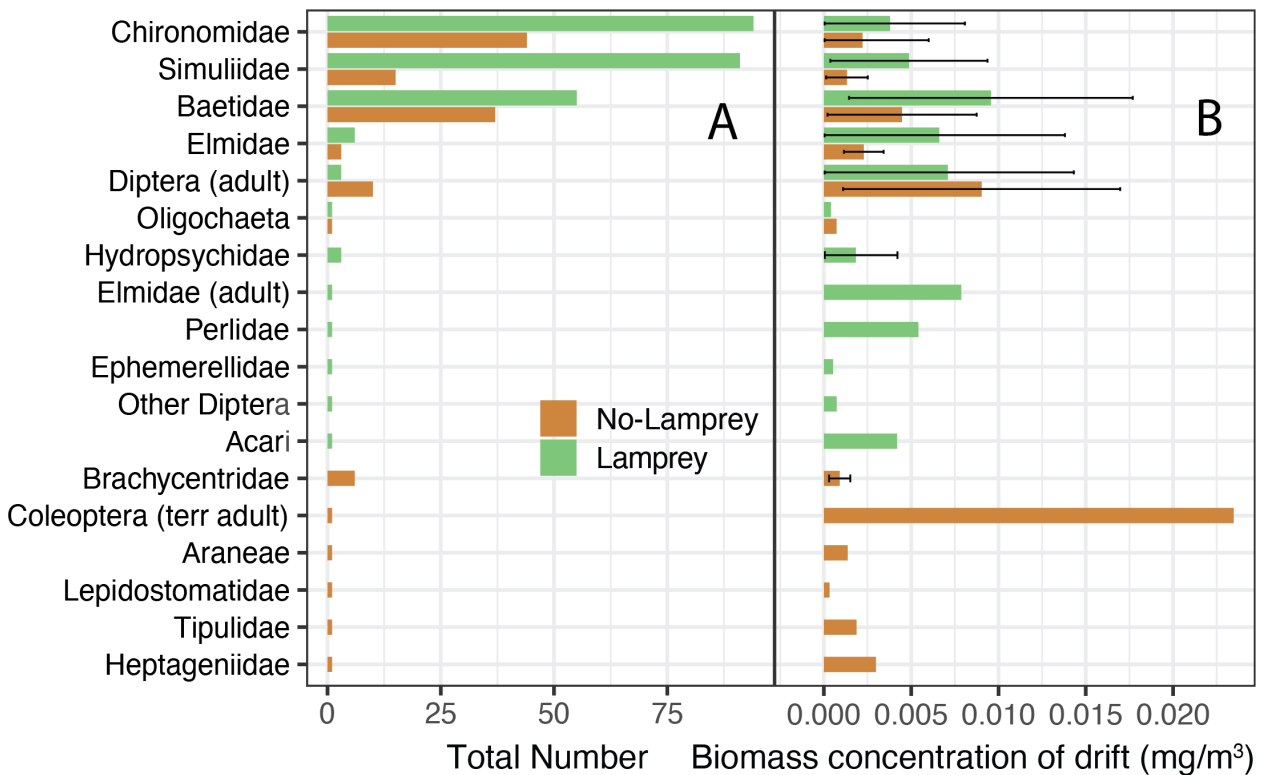*Figure 3:* Bar plots of total number of invertebrates (larvae of aquatic insects, unless otherwise indicated) **A.** and biomass concentration **B.** for each taxon collected. Unless otherwise specified life stages are larva. All data from 5 pairs of drift samples. Error bars in panel b are standard deviations bounded at zero and were calculated for taxa that occurred in at least three samples for a given treatment.
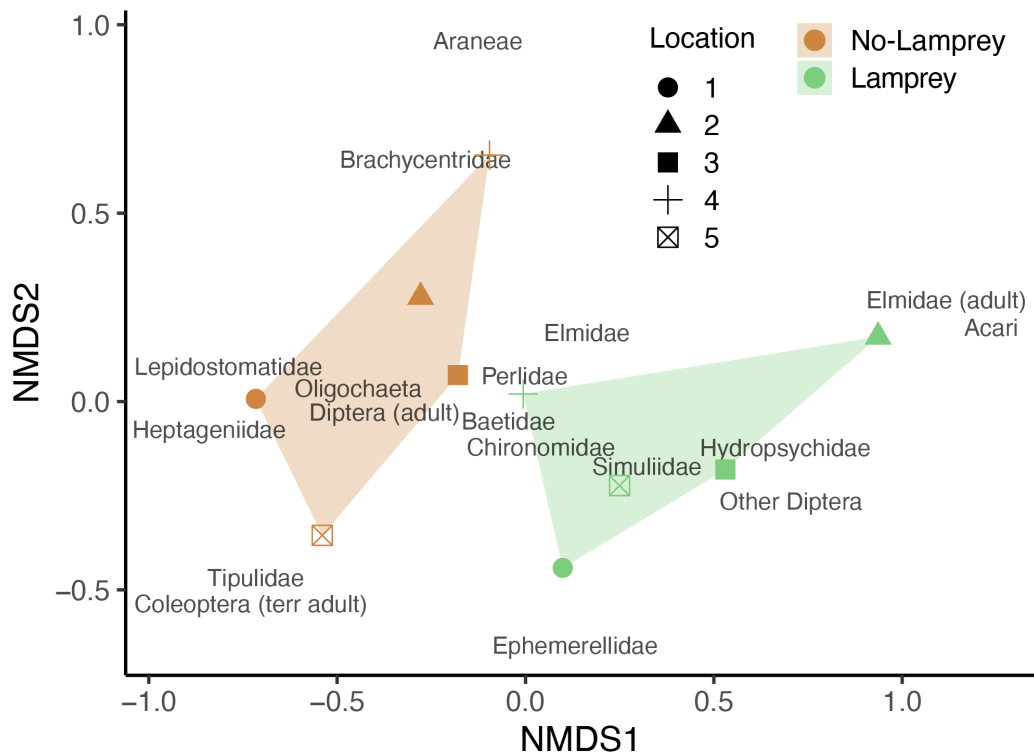
79

Figure 4: Non-metric Dimensional Scaling (NMDS) of lamprey drift samples from Lamprey (green) and No-lamprey (tan) treatments. Drift collected for paired samples at 5 locations. Polygons are convex hulls are the smallest multidimensional space that enclose all points in each treatment. Samples that are more similar are more proximate in multivariate space. Taxa names are placed on the ordination in the direction that they drive samples. Drift collected in each treatment is significantly different from each other (p = 0.01, PERMANOVA).

The Effect Of Lamprey Redd Building Juvenile Steelhead Foraging Rate

Steelhead in the lamprey treatment foraged on average 76% more than those in the no-lamprey treatment (Figure 2 C., N = 11, paired t-test, p = 2.76e-05) means 10.55 and 8 (forages/ 5 minutes), respectively.

The Effect Of Lamprey Redd Building Juvenile Steelhead Growth Potential

Mean NREI (Joules per day) was 25.1-27.5% higher behind lamprey than in adjacent sites (Figure 5a, LMM, N = 5, p <0.001). This varied with fish size; 25.1% for 10 cm *O. mykiss* 27.5% for 20 cm *O. mykiss*. NREI across all samples trended lower for larger fish as a result of larger swimming costs, but because of our relatively low sample size (5 sites) and large amount of variation between sites fish size was not significant. Potential growth ranged from 0.40-1.13g (Table 2, Figure 5 B) per day across fish sizes and lamprey treatments. Lamprey had a positive effect on potential growth (Figure 5 B,

LMM, N= 5 p <0.001) and smaller size classes had higher potential growth rates (Figure 5 B, mean of 1.02 g/day for 10 cm fish, 0.46 g/day for 20cm fish across treatments, LMM, N= 5 p <0.001). When scaled to body weight, potential growth increases behind lamprey building redds were greatest in smaller size classes of trout, with 10 cm trout potentially adding an additional 2.0% of their body mass per day, on average, when foraging behind lamprey building redds for a total of 9.8 % increase in mass per day. The largest modeled size class of trout (20cm) showed the smallest proportional potential gains, adding 0.5% to their body mass each day, on average, when foraging behind lamprey building nests. This was an average of 0.1% higher than the no-Lamprey estimates (Table 2, Figure 5 B).
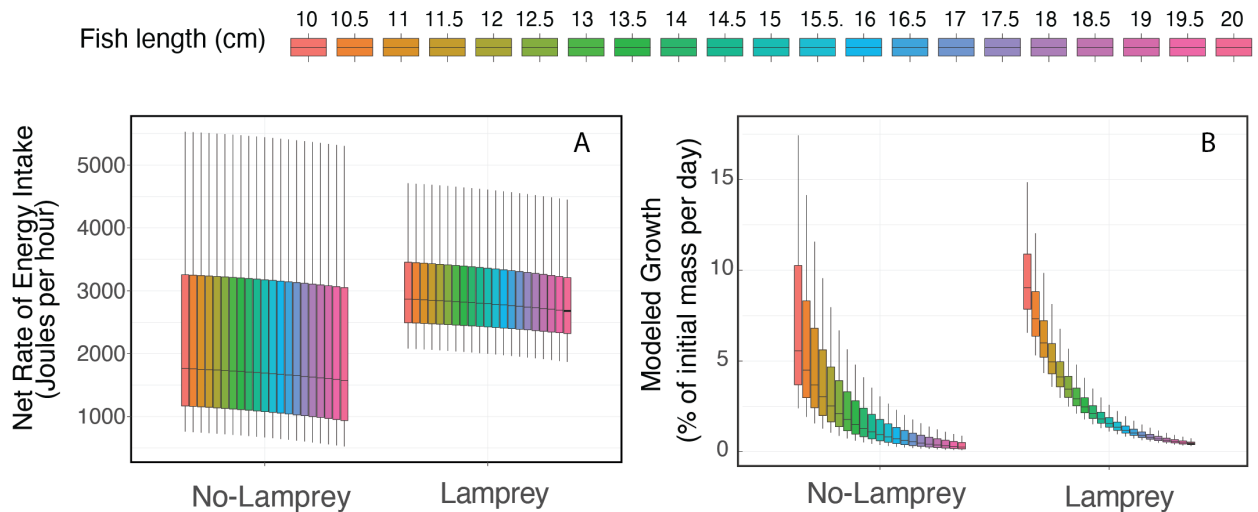

Figure 5: Boxplots of outputs bioenergetics models for foraging juvenile steelhead trout. Ranges represent estimates at the 5 paired sites where we collected invertebrate drift and measured velocity. Treatments were lamprey and No-Lamprey, colors depict steelhead of different sizes, ranging from 10-20cm. Boxplot midlines are medians, box edges are 25 and 75 percentiles, and whiskers show 5 and 95 percentiles. **A.** Estimates of Net Rate of Energy Intake (NREI) in Joules per hour. **B.** Estimates of growth potential.

Physical structure and hydraulic influence of redds as velocity and flow refugia

Lamprey redds (n=70) had mean depth of excavation = 11.4 ± 0.4 cm and area = 0.278 ± 0.011 m^2. Water velocity measured at the river bottom inside of lamprey redds was significantly lower (mean 0.03 m/s) than that measured outside of the redd on the left, right, and upstream; respective means 0.15, 0.12, and 0.12 m/s (Figure 6, linear mixed-effect model, p = 0.01). In five of our 17 velocity measured redds, water at the deepest position was flowing upstream, as a result of a vertical eddy formed inside the redd. Observations of particles in the water column, suggest this is a common occurrence.

The deepest portion of completed redds were used by a number of species, presumably as flow and depth refugia. Between 2015 and 2020 we observed a total of 81 clutches of Foothill Yellow-legged Frog eggs attached to rocks around the inside perimeter of lamprey redds. This number represents a tiny fraction of the total reproductive output by frogs in the two study reaches (Table S2), but at specific sites where the river bottom was fairly homogenous and in years when water was shallower than the preferred oviposition depth of 20 cm (Kupferberg 1996), most or all of the clutches within a given lek were

laid inside redds. For a set of clutches measured in 2018, we found those laid in redds were on average 13.1cm deeper than those laid outside of redds at the same lek (t-test, p < 0.001) and in locations that would have been too swift for oviposition had the redds not been there (average velocity in redd 0.03m/s, outside 12.8m/s, linear mixed-effect model, N = , p < 0.001, Figure 6a). At a lek where 26 out of 31 clutches were laid in redds in 2018, mortality due to desiccation prior to hatching rate was 3.2%, much lower than years when clutches also experienced receding flows but redds were either not present or not used at that site (2017, 48.0%; 2019, 22.8%; 2020 30.4%).
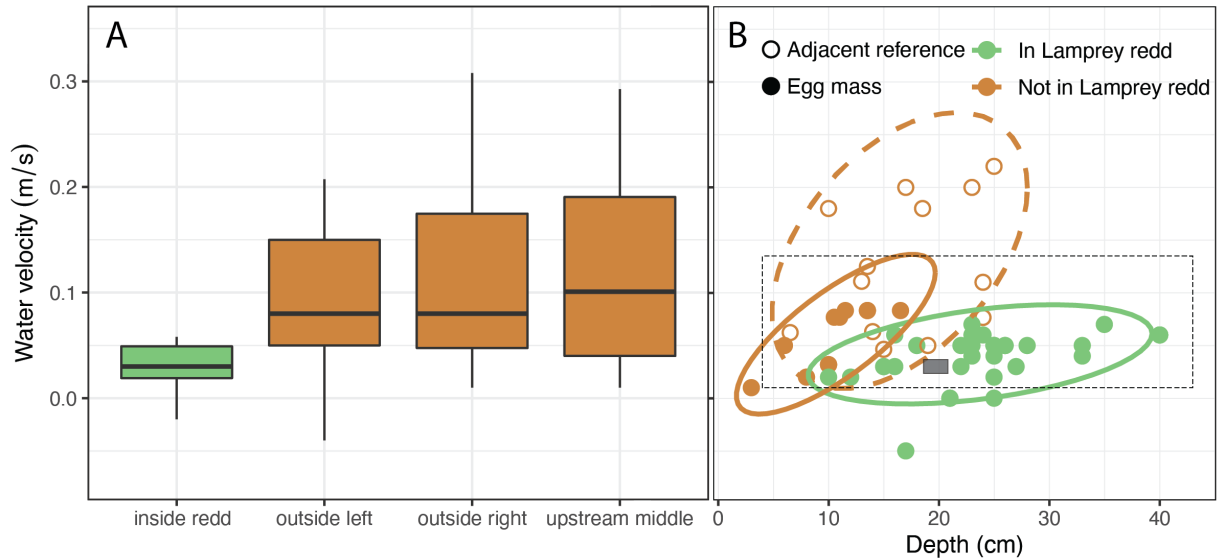

Figure 6: **A.** Water velocity measured near the river bottom at four positions (x-axis) inside and near 16 lamprey redds. One outlier (0.8 m/s) for the outside left position is not shown. **B.** Water velocities and depths of 43 egg masses shown with closed circles (32 inside lamprey redd, green, and 11 outside lamprey redds, tan) and 32 adjacent reference points shown with open circles. Ellipses depict 95% confidence intervals calculated for egg masses not in redds (solid tan ellipse), egg masses in lamprey redds (solid green ellipse) and adjacent reference points (dashed tan ellipse). Rectangles depict conditions suitable for egg masses from Kupferberg (1996). Dashed large rectangle shows the range of conditions where eggs were found, and the small shaded gray rectangle encloses the 99% confidence interval for where egg masses were found.

Discussion

Our observations support the hypotheses that lamprey alter the concentration of drift (H1a) and thus increase the foraging profitability of juvenile steelhead (H1b) through their redd building behaviors. We also found support for the hypothesis (H2) that lampreys' redds created velocity refugia for aquatic species. Collectively these observations suggest a number of important species interactions that may alter population dynamics of species that interact with spawning lamprey.

The Effect of Lamprey Redd Building on Stream Invertebrate Drift

Invertebrate drift biomass and concentration

Drifting invertebrates were more numerous and more concentrated downstream of redd building lamprey (Figure 3 A & B). Bioturbation of the river benthos during redd building by salmon has been shown to dislodge invertebrates (Peterson and Foote 2000, Moore et al. 2004). These dislodged invertebrates are vulnerable to predation by fish downstream, once ejected from the interstitial matrix of river sediments they usually inhabit (Scheuerell et al. 2007). This increase in drifting invertebrates is limited in time and space, but potentially impactful for both the invertebrates and organisms that consume them. Here we document a similar pattern due to redd building by Pacific Lamprey dislodging benthic invertebrates. Similarly, sea Lamprey (*Petromyzon marinus*) impact the invertebrate communities in streams where they spawn. Sea Lamprey carcasses are consumed by invertebrates and can increase secondary production (Weaver et al. 2018). Also, invertebrates were more numerous in the mounds downstream of redds created by spawning Sea Lamprey excavating redds (Hogg et al. 2014). This could be a result of displacement, forced drift, and subsequent settling, or as the authors suggest, altered habitat characteristics that make downstream mound more attractive to invertebrates. It seems likely that Sea Lamprey, and more broadly, most redd building fishes that excavate sediments, also dislodge invertebrates that are then more susceptible to predation by other water column foraging aquatic insectivores (Scheuerell et al. 2007).

Redd building behaviors and drift composition

Lamprey dislodge invertebrates when they move larger sediments with their mouths and smaller sediments by beating the benthos with their tails. Both types of redd building behaviors can dislodge benthic invertebrates and might differentially impact certain invertebrates. Invertebrates typically found attached to or crawling on cobbles like simuliids or baetids are probably dislodged when lamprey move larger sediments, which would account for their substantial increases in our drift samples found downstream of Lamprey actively constructing redds. All three taxa which were significantly more common in drift behind lamprey redds (simuliids, baetids, and chironomids) were soft-bodied and highly vulnerable as salmonid prey. This beneficial increase in vulnerable taxa to foraging salmonids was not captured in the bioenergetics model – in which gross energy intake was computed from drift concentration (joules/volume), estimated from biomass of drifting invertebrates, and all invertebrates were treated as equally vulnerable. The second redd building behavior, dislodging fine sediment, could also increase the proportion of infaunal organisms. Larval elmids are often found in these finer sediments, and the increases in our lamprey samples might have been caused by lamprey disturbing these finer sediments they inhabit. These infaunal organisms are typically not susceptible to fish predators (Suttle et al. 2004); lamprey redd building appears to expose this typically inaccessible invertebrate guild. The change in composition of drift, favoring more vulnerable taxa, represents an intriguing benefit to this lamprey-salmonid interaction which could be characterized in future work by accounting for differences in prey quality.

Redd building behaviors and invertebrate size

The effect of lamprey redd building on the size of the drifting invertebrates is intriguing, though not significant in our study. Baetids and elmids dislodged by lamprey were

slightly but not significantly larger than in No-lamprey treatments (SM Fig. 1). Larger invertebrates are more calorie rich per individual, if redd building increases their concentration in drift, this could be another mechanism by which steelhead foraging is more profitable downstream of redd building lamprey. More sampling effort might detect a real difference, which would add to the positive effect of lamprey on drift foragers. We suggest this could be a fruitful topic for future study (SM Figure 1).

Figure 7. Two juvenile steelhead (*Oncorhynchus mykiss*) drift feed downstream of Pacific lamprey (*Entosphenus tridentatus)* building a redd but resting at this moment. Photo taken May 29, 2017 in the Angelo Coast Range Reserve, Mendocino County, California.

The Effect of Lamprey Redd Building on Steelhead Foraging Behavior

We observed juvenile steelhead ranging from 7-20 cm selectively foraging behind redd-building lamprey. Often, we observed size-mediated hierarchies of multiple individuals established downstream of these sites. As expected, steelhead foraging downstream of redd building lamprey had more foraging attempts per unit time (Figure 3C). This result suggests that steelhead capitalize on the increased invertebrate availability at these sites (Figure 3 A, B). It is important to note that foraging attempts may be a poor predictor of realized foraging success since many drift items are either inspected and not consumed or expelled after biting (Neuswanger et al. 2014); however, we did not observe appreciably more non-prey organic material in drift samples below lamprey redds. Thus, the increased invertebrate drift concentration *plus* the increased foraging rate suggests that if the ratio of attacks-to-ingested prey were equal in lamprey vs. no-lamprey sites, then it is likely that consumption of prey downstream of lamprey constructing redds was higher. Salmonids in other systems track the seasonal subsidies associated with Sockeye Salmon (*Oncorhynchus nerka)* spawning in Alaska, taking advantage of both eggs and disturbed invertebrates as trophic resources and in so doing, increase their potential growth (Scheuerell et al. 2007). These tracking events can occur at spatial scales that suggest

juvenile salmonids are capable of tracking these resources in our study system. Taken in this context, our observations of fish behavior support our hypothesis that steelhead in the South Fork Eel exploit the seasonal subsidy of dislodged invertebrates created by lamprey bioturbating river sediments.

The Effect of Lamprey Redd Building Juvenile Steelhead Growth Potential

Our bioenergetics models support our hypothesis that lamprey create an environment in which potential growth is enhanced for juvenile steelhead. The experimental design of this study allowed us to largely isolate the effect of lamprey redds on invertebrate drift as a mechanism for increased growth potential of beneficiary steelhead. Observations occurred in lateral positions in the same river cross section, at the same time. This resulted in similar physical habitats, stream hydraulics (depth and velocity) and water temperatures at 'Lamprey' vs. 'No-Lamprey' sites. Since these physical variables control the energetic costs in our models, most of the observed differences in net rate of energy intake, and subsequently potential growth, result from differences in invertebrate drift concentration (Figure 3 B). As a result of increased drift concentration, the NREI model suggests 25.1-27.5% greater potential growth when foraging behind lamprey compared to foraging in the 'No-Lamprey' treatment. However, this may be an underestimate as the model does not take into account (a) increased foraging rate or (b) the increased vulnerability of drifting prey behind lamprey redds.
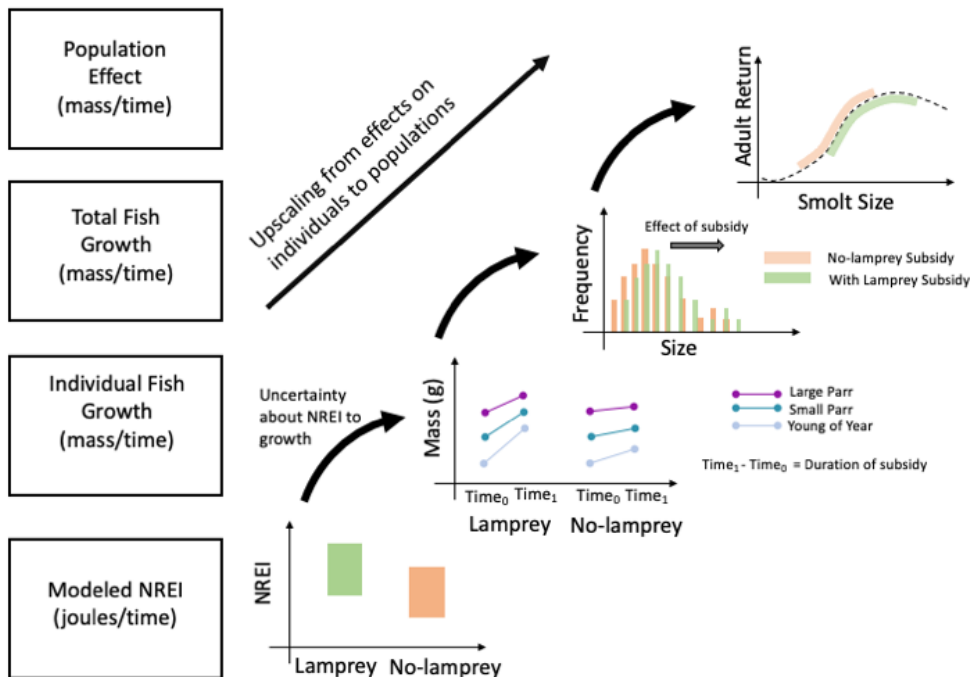

Figure 8. Conceptual diagram of the steps involved in upscaling from our bioenergetics model of individual foraging profitability at a site to population level consequences for Steelhead being subsidized by Pacific Lamprey.

Implications of bioenergetic differences

Spring and early summer, when lamprey construct redds, are important periods of growth for juvenile steelhead – both for out-migrating smolts/pre-smolts and for over-summering juvenile fish (Kelson and Carlson 2019; Hayes et al. 2008, Smith and Li 1983). During the spring-summer flow recession flows drop from winter highs and water temperature warms to levels that allow for higher growth (Rossi 2020). Thus, lamprey may be mobilizing attached benthic prey at a time when benthic invertebrate concentration is high *and* when salmonid foraging is most critical. A simple thought experiment can clarify how this interaction may affect both individual salmonids and population-level dynamics (Figure 8). The population effects of a lamprey-induced prey subsidy for juvenile steelhead would depend on: (*i*) the duration of the lamprey subsidy; (*ii*) it's effect on growth of individual trout; (*iii*) the number of salmonids that benefit; and (*iv*) the effect of this growth on downstream and ocean survival. Using our data, we can make informed hypotheses about points *i-iii*; and using an understanding of *O. mykiss* life history in coastal CA streams, as well as published information on size-specific survival, we can make inferences about how these dynamics affect population dynamics (point *iv*), for detailed description of each of these steps see supplemental material.

Our data suggest two alternate ways that increased growth from lamprey subsidies may affect *O. mykiss* populations (both under current and historic conditions). First, if downstream habitats are favorable and steelhead can grow to greater than 17cm after benefiting from the lamprey subsidy, subsidizing smaller fish might result in more returning adults since their relative benefit from the lamprey subsidy is greatest (Figure 5 A). Historically, smaller fish were likely the most numerous beneficiaries of mainstem lamprey spawning, as they were displaced from natal tributaries by intraspecific competition in late spring (Bailey et al. 2018). If, as likely under current conditions (Yoshiyama ad Moyle 2010, Power et al. 2015), downstream foraging opportunities are limited, however, the greatest boost to adult returns would occur from subsidizing larger fish, so they could attain the 15-17cm length threshold (Kabel and German 1967), to "push them over the edge" from modest to good ocean survival.

We unfortunately lack reliable estimates for downstream growth potential under current or historic conditions. Interannual and spatial variation in conditions in mainstem river, estuarine-ecotone and non-natal habitats could all affect growth and therefore ocean survival. In our study, estimated growth potential varied substantially among sites. For example, in our 'No-Lamprey' treatments, growth estimates for 10cm steelhead ranged from 0.3- 2.0g/day. Though potential growth was higher in all of our 'Lamprey' treatments, except site 5, where a single large beetle increased biomass in our 'No-Lamprey' treatment (Figure 2 B), this site-to-site variability makes picking a representative growth value challenging. Currently, we know little about steelhead use of mainstem habitats in the South Fork Eel River once they leave natal tributaries. More information on juvenile steelheads' foraging, survival and growth as they traverse mainstem habitats would greatly improve our predictions and management of this species. Finally, both lamprey and steelhead numbers fluctuate annually, and the ratio of steelhead:lamprey likely determines how many rearing juveniles receive the subsidy. In addition, in years with large lamprey numbers, redd sites are occupied longer (probably not by the same individuals), protracting the subsidy for juvenile steelhead.   If, as we and

others suspect (Yoshiyama and Moyle 2010, Katz et al. 2012, Power et al. 2015), environmental damage from deforestation, erosion or megafloods has degraded mainstem habitat in the Eel River for rearing and outmigrating steelhead, increased growth from subsidies delivered by lamprey redd building could be increasingly important in enhancing growth for juvenile steelhead (Figure 5 A & B), which in turn would increase ocean survival and adult returns of salmonids (Ward and Slaney 1988, Hotby et al. 1990).

Physical structure and hydraulic influence of redds as velocity and flow refugia

Flow velocity was lower in the bottom of the redd depression than outside the redd (Figure 6). A number of aquatic organisms appear to take advantage of this as a velocity refuge. During the late spring and summer in the South Fork Eel River, young-of-year steelhead are often seen holding position near the bottom of redds, where we measured very low velocities. In another California coastal river, Holmes et al. (2014), observed approximately five times the number of *O. mykiss* fry at 0.03 m/s (~1000 observations) compared to 0.1 m/s (~ 200 observations), suggesting the potential for the hydraulic influence of lamprey redds to support refugia for fry as well (see Figure 2, panel F in (Holmes et al. 2014)). Though we did not estimate the bioenergetic benefit that these velocity refuges provide, they are likely substantial. Because many redds are more than 30cm below the water surface, these velocity refuges also reduce risk from terrestrial and aerial predators, like Belted Kingfishers (*Megaceryle alcyon*), which are common at our site.

Lamprey redds are also used by foothill yellow-legged frogs (*Rana boylii)* as egg mass deposition sites. Water depth and velocity inside redds was suitable for egg masses (Kupferberg et al. 2009) and tadpoles (Kupferberg et al. 2011), whereas flows were too high (> 0.135 m/s) in adjacent areas surrounding the redds. Eggs masses deposited in lamprey redds at three lek sites were significantly deeper than those not in lamprey redds (Figure 6 B). The typical rate of stage recession in the spring in the South Fork Eel River is just over 1cm per day. The extra depth achieved by females that deposited egg masses in lamprey could keep egg masses wetted for around 10 additional days, compared to adjacent egg masses (Figure 6B). Frog egg masses require gentle water circulation and must remain submerged during the spring flow recession (Kupferberg 1996). Lamprey redds, then, might increase egg survival through at least three mechanisms: 1) by protecting eggs from higher velocities, reducing likelihood of scour; 2) creating deeper habitat that reduces chances of stranding during flow recession, and 3) providing refuge from some predators. The relative importance of each of these mechanisms likely varies with the type of water year and by lek site. In areas with smaller homogenous sediments and less turbulent flow, lamprey redds might be even more impactful. In these conditions, velocity refuges are more limiting, and we observed a higher proportion of redds with egg masses, indicating the frogs take advantage of these hydraulic refuges.

Conclusion

Lampreys have been important components of North American rivers for millions of years (Javier 2008). Their positive interactions within ecological communities have been

largely overlooked, but as we demonstrate, can be important. Our results further motivate the current momentum to restore lamprey to areas where they have been extirpated, return their numbers to historic levels, and learn more about their life history and ecological roles. Lamprey are intrinsically important to biodiversity and culturally important to Native communities. Like Pacific salmon, Pacific Lampreys' somatic nutrients and energy contribute to food-web productivity as their carcasses decompose after spawning and are consumed by a wide range of animals (Close et al. 2002, Weaver et al. 2018). In addition, our work demonstrates that their nesting behaviors and excavations that alter the streambed topography benefit other aquatic organisms. Both Foothill-yellow legged frogs and Steelhead in Northern California have experienced range reductions and population declines in recent decades, and populations of both are listed under California's Endangered Species Act. In addition to the habitat loss, flow management, invasive predators and competitors, we should also consider loss of beneficial ecological interactions as we seek to aid these threatened species. As Aldo Leopold implied in 1949, many interactions among members of ecological communities remain to be described, and the only way to preserve these interactions is to "keep every cog and wheel" if we tinker with their ecosystems. Historically migratory organisms were conceptually treated as envelopes of nutrients and energy, shipped from donor to recipient systems. Our work adds to growing recognition that migrants also take part in ecological interactions as they travel (Cohen and Satterfield 2020). Removing key players from food webs can result in loss of the interactions that can have negative indirect effects on species of conservation, commercial, or cultural interest (Janzen and Martin 1982, Power 1985, Power et al. 1996, Estes et al. 1998). If we can identify, restore, and conserve important species in interaction webs, our management and restoration efforts will be more efficacious than when targeted at single species.

Table 1. Summary of mean values across sites for bioenergetic model outputs (Net Rate of Energy Input and Growth) for juvenile steelhead from 10cm -20cm.

Fish size	Mean NREI (joules / hour)		Mean Potential Growth (grams / day)	
	No-Lamprey	Lamprey	No-Lamprey	Lamprey
10	2495	3121	0.907	1.135
10.5	24889	3114	0.860	1.076
11	2481	3107	0.816	1.022
11.5	2474	3100	0.777	0.973
12	2467	3092	0.741	0.929
12.5	2458	3084	0.707	0.888
13	2450	3076	0.677	0.850
13.5	2441	3067	0.648	0.815
14	2431	3058	0.621	0.782
14.5	2421	3048	0.597	0.752
15	2411	3037	0.574	0.723
15.5	2400	3026	0.552	0.696
16	2388	3015	0.532	0.671

16.5	2376	3003	0.513	0.648
17	2364	2991	0.495	0.626
17.5	2351	2978	0.477	0.605
18	2338	2964	0.461	0.585
18.5	2324	2950	0.446	0.566
19	2309	2936	0.431	0.548
19.5	2294	2921	0.417	0.531
20	2278	2905	0.403	0.514

Acknowledgements

Literature Cited

Bailey, C. J., D. C. Braun, D. McCubbing, J. D. Reynolds, B. Ward, T. D. Davies, and J. W. Moore. 2018. The roles of extrinsic and intrinsic factors in the freshwater life-history dynamics of a migratory salmonid. Ecosphere e02397. 10.1002/ecs2.2397

Baxter, C.V., Kennedy, T.A., Miller, S.W., Muehlbauer, J.D., Smock, L.A., 2017. Macroinvertebrate Drift, Adult Insect Emergence and Oviposition. In: Hauer, F.R., Lamberti, G.A. (Eds.), Methods in Stream Ecology: Volume 1: Ecosystem Structure. Elsevier, Academic Press, pp. 435–456. ISBN: 9780124165588

Benke, A. C., A. D. Huryn, L. A. Smock, and J. B. Wallace. 1999. Length-mass relationships for freshwater macroinvertebrates in North America with particular reference to the southeastern United States. Journal of North American Benthological Society 18:308–343.

Brower, L. P., O. R. Taylor, E. H. Williams, D. A. Slayback, R. R. Zubieta, and M. I. Ramirez. 2011. Decline of monarch butterflies overwintering in Mexico: is the migratory phenomenon at risk? Insect Conservation and Diversity 5:95–100.

Brown, L. R., P. B. Moyle, and R. M. Yoshiyama. 1994. Historical Decline and Current Status of Coho Salmon in California. North American Journal of Fisheries Management 14:237–261.

Brumo, A. F. 2006. Spawning, larval recruitment, and early life survival of Pacific lampreys in the South Fork Coquille River, Oregon. Master's thesis, Oregon State University

Bunte, K., and S. R. Abt. 2001. Sampling Frame for Improving Pebble Count Accuracy in Coarse Gravel-bed Streams. Journal of the American Water Resources Association 37:1001–1014.

Caldwell, T. J., G. J. Rossi, R. E. Henery, and S. Chandra. 2018. Decreased streamflow impacts fish movement and energetics through reductions to invertebrate drift body size and abundance. River Research and Applications 34:965–976.

Clemens, B. J., L. Weitkamp, K. Siwicke, J. Wade, J. Harris, J. Hess, L. Porter, K. Parker, T. Sutton, and A. M. Orlov. 2019. Marine biology of the Pacific Lamprey *Entosphenus tridentatus*. Reviews in Fish Biology and Fisheries 29:767–788.

Close, D. A., M. S. Fitzpatrick, and H. W. Li. 2002. The Ecological and Cultural Importance of a Species at Risk of Extinction, Pacific Lamprey. Fisheries 27:19–25.

Cohen, E. B., and D. A. Satterfield. 2020. "Chancing on a spectacle:" co-occurring animal migrations and interspecific interactions. Ecography 43:1657–1671.

Correa, S. B., K. O. Winemiller, H. Lopez-Fernandez, and M. Galetti. 2007. Evolutionary perspectives on seed consumption and dispersal by fishes. BioScience 57:748–756.

Estes, J. A., M. T. Tinker, T. M. Williams, and D. F. Doak. 1998. Killer whale predation on sea otters linking oceanic and nearshore ecosystems. Science 282:473–476.

Flecker, A. S. 1996. Ecosystem Engineering by a Dominant Detritivore in a Diverse Tropical Stream. Ecology 77:1845–1854.

Flecker, A. S., P. B. McIntyre, J. W. Moore, J. T. Anderson, B. W. Taylor, and R. O. Hall Jr. 2010. Migratory fishes as material and process subsidies in riverine ecosystems. American Fisheries Society Symposium 73:559–592.

Frick, K. E., S. C. Corbett, and M. L. Moser. 2017. Climbing success of adult Pacific lamprey on a vertical wetted wall. Fisheries Management and Ecology 24:230–239.

Gasith, A., and V. H. Resh. 1999. Streams in Mediterranean climate regions: abiotic influences and biotic responses to predictable seasonal events. Annual Reviews in Ecology and Systematics 30:51–81.

Gerlanc, N. M., and G. A. Kaufman. 2003. Use of Bison Wallows by Anurans on Konza Prairie. The American Midland Naturalist 150:158–168.

Goodman, D. H., and S. B. Reid. 2012. Pacific Lamprey (*Entosphenus tridentatus*) assessment and template for conservation measures in California. U.S. Fish and Wildlife Service, Arcata, California.

Goodman, D.H. and S.B. Reid. 2015. Regional Implementation Plan for Measures to Conserve Pacific Lamprey (*Entosphenus tridentatus*), California – North Central Coast Regional Management Unit. U.S. Fish and Wildlife Service, Arcata, California. Arcata Fisheries Technical Report TR 2015-27.

Goodman, D. H., S. B. Reid, N. Som, and W. Poytress. 2015. The punctuated seaward migration of Pacific lamprey (*Entosphenus tridentatus*): environmental cues and implications for streamflow management. Canadian Journal of Fisheries and Aquatic Sciences 72:1817–1828.

Goodman, D. H., and S. B. Reid. 2017. Climbing above the competition: Innovative approaches and recommendations for improving Pacific Lamprey passage at fishways. Ecological Engineering 107:224–232.

Harris, G., S. Thirgood, J. G. C. Hopcraft, J. P. G. M. Cromsight, and J. Berger. 2009. Global decline in aggregated migrations of large terrestrial mammals. Endangered Species Research 7:55–76.

Hayes, S. A., M. H. Bond, C. V. Hanson, E. V. Freund, J. J. Smith, E. C. Anderson, A. J. Ammann, and R. B. MacFarlane. 2008. Steelhead Growth in a Small Central California Watershed: Upstream and Estuarine Rearing Patterns. Transactions of the American Fisheries Society 137:114–128.

Helfield, J. M., and R. J. Naiman. 2001. Effects of salmon-derived nitrogen on riparian forest growth and implications for stream productivity. Journal of Animal Ecology 82:2403–2409.

Hogg, R. S., S. M. Coghlan Jr., J. Zydlewski, and K. S. Simon. 2014. Anadromous sea lampreys (*Petromyzon marinus*) are ecosystem engineers in a spawning tributary. Freshwater Biology 59:1294–1307.

Holthby, B.L., Anderson, B.C., Kadowaki, R.K. Importance of Smolt Size and Early Ocean Growth and Interannual Variability in Marine Survival of Coho Salmon. (*Oncorhynchus kisutch*). Canadian Journal of Fisheries and Aquatic Sciences . 47 (11)

Holmes, R. W., M. A. Allen, and S. Bros-Seeman. 2014. Seasonal microhabitat selectivity by juvenile steelhead in a central California coastal river. Pages 590–615 California Department of Fish and Wildlife.

Hughes, N. F., J. W. Hayes, K. A. Shearer, and R. G. Young. 2003. Testing a model of drift-feeding using three-dimensional videography of wild brown trout*, Salmo trutta*, in a New Zealand river. Canadian Journal of Fisheries and Aquatic Sciences 60:1462–1476.

Janvier, P. 2008. Living primitive fishes and fishes from deep time. In Primitive fishes. Edited by D.J. McKenzie, A.P. Farrell, and C.J. Brauner. Academic Press, Amsterdam, the Netherlands. pp. 1–53.

Janzen, D. H., and P. S. Martin. 1982. Neotropical Anachronisms - the Fruits the Gomphotheres Ate. Science 215:19–27.

Johnston, N. T., E. A. MacIsaac, P. J. Tschaplinski, and K. J. Hall. 2004. Effects of the abundance of spawning sockeye salmon (*Oncorhynchus nerka*) on nutrients and algal biomass in forested streams. Canadian Journal of Fisheries and Aquatic Sciences 61:384–403.

Kabel, C. S., and E. R. German. 1967. Some aspects of stocking hatchery-reared steelhead and silver salmon. California Department of Fish and Wildlife.

Katz, J., P. B. Moyle, R. M. Quiñones, J. Israel, and S. Purdy. 2012. Impending extinction of salmon, steelhead, and trout (Salmonidae) in California. Environmental Biology of Fishes 96:1169–1186.

Keefer, M. L., M. L. Moser, C. T. Boggs, W. R. Daigle, and C. A. Peery. 2009. Variability in migration timing of adult Pacific lamprey (*Lampetra tridentata*) in the Columbia River, U.S.A. Environmental Biology of Fishes 85:253–264.

Kelson, S. J., and S. M. Carlson. 2019. Do precipitation extremes drive growth and migration timing of a Pacific salmonid fish in Mediterranean-climate streams? Ecosphere 10:e02618–17.

Kupferberg, S. J. 1996. Hydrologic and geomorphic factors affecting conservation of a river-breeding frog (Rana boylii). Ecological Applications 6:1332–2344.

Kupferberg, S. J. (1997). Bullfrog (Rana catesbeiana) invasion of a California river: the role of larval competition. *Ecology*, *78*(6), 1736-1751.

Kupferberg, S. J., A. J. Lind, J. Mount, and S. Yarnell. 2009. Pulsed flow effects on the Foothill Yellow-legged Frog (*Rana boylii*): integration of empirical, experimental and hydrodynamic modeling approaches. California Energy Commission.

Kupferberg, S. J., A. J. Lind, V. Thill, and S. M. Yarnell. 2011. Water Velocity Tolerance in Tadpoles of the Foothill Yellow-legged Frog (Rana boylii): Swimming Performance, Growth, and Survival. Copeia 2011:141–152.

Mattocks, S., C. J. Hall, and A. Jordaan. 2017. Damming, Lost Connectivity, and the Historical Role of Anadromous Fish in Freshwater Ecosystem Dynamics. BioScience 67:713–728.

Mayield, M. P., Schultz, L.D., Wyss L. A., Clemens, B. J., and C. Schreck. 2014. Spawning Patterns of Pacific Lamprey in Tributaries to the Willamette River, Oregon, Transactions of the American Fisheries Society, 143:6, 1544

McDonald, M. 1894. Notes on the fisheries of the Pacific coast, sturgeon and the sturgeon fishery. Bulletin of the United States fish commission 14.

Montgomery, D. R., J. M. Buffington, N. P. Peterson, D. Schuett-Hames, and T. P. Quinn. 1996. Stream-bed scour, egg burial depths, and the influence of salmonid spawning on bed surface mobility and embryo survival. Canadian Journal of Fisheries and Aquatic Sciences 53:1061–1070.

Moore, J. W., and D. E. Schindler. 2008. Biotic disturbance and benthic community dynamics in salmon-bearing streams. Journal of Animal Ecology 77:275–284.

Moore, J. W., D. E. Schindler, and M. D. Scheuerell. 2004. Disturbance of freshwater habitats by anadromous salmon in Alaska. Oecologia 139:298–308.

Moyle, P. B. 2002. Inland fishes of California: revised and expanded. University of California Press, Berkeley.

Nakano, S., K. D. Fausch, and S. Kitano. 1999. Flexible Niche Partitioning via a Foraging Mode Shift: A Proposed Mechanism for Coexistence in Stream-Dwelling Charrs. Journal of Animal Ecology 68:1079–1092.

Naman, S. M., J. S. Rosenfeld, J. R. Neuswanger, E. C. Enders, and B. C. Eaton. 2019. Comparing correlative and bioenergetics-based habitat suitability models for drift-feeding fishes. Freshwater Biology 64:1613–1626.

Nawa, R. K., J. E. Vaile, P. Lind, T. M. K Nadananda, T. McKay, C. Elkins, B. Bakke, J. Miller, W. Wood, K. Beardslee, and D. Wales. 2003. A petition for rules to list: Pacific lamprey (*Lampetra tridentata*); river lamprey (*Lampetra ayresi*); western brook lamprey (*Lampetra richardsoni*); and Kern brook lamprey (*Lampetra hubbsi*) as threatened or endangered under the Endangered Species Act. January 23, 2003.

Neuswanger, J., M. S. Wipfli, A. E. Rosenberger, and N. F. Hughes. 2014. Mechanisms of drift-feeding behavior in juvenile Chinook salmon and the role of inedible debris in a clear-water Alaskan stream. Environmental Biology of Fishes 97:489–503.

Peterson, D. P., and C. J. Foote. 2000. Disturbance of small-stream habitat by spawning sockeye salmon in Alaska. Transactions of the American Fisheries Society 129:924–934.

Piccolo, J. J., B. M. Frank, and J. W. Hayes. 2014. Food and space revisited: The role of drift-feeding theory in predicting the distribution, growth, and abundance of stream salmonids. Environmental Biology of Fishes 97:475–488.

Polis, G. A., W. B. Anderson, and R. D. Holt. 1997. Toward an integration of landscape and food web ecology: the dynamics of spatially subsidized food webs. Annual Reviews in Ecology and Systematics 28:289–316.

Post, J. R., and E. A. Parkinson. 2001. Energy allocation strategy in young fish: allometry and survival. Ecology 82:1040–1051.

Power, M. E., W. J. Matthews, and A. J. Stewart. 1985. Grazing minnows, piscivorous bass, and stream algae: dynamics of a strong interaction. Ecology 66:1448–1456.

Power, M. E., Tilman, D., Estes, J. A., Menge, B. A., Bond, W. J., Mills, L. Scott, Daily, G., Castilla, J. C., Lubchenco, J., and Paine, R. T. 1996.Challenges in the Quest for Keystones Wildlife Biology Faculty Publications. Paper 1. http://scholarworks.umt.edu/wildbio_pubs/1

Power, M. E., J. R. Holomuzki, and R. L. Lowe. 2013. Food webs in Mediterranean rivers. Hydrobiologia 719:119–136.

Power, M. E., K. Bouma-Gregson, P. Higgins, and S. M. Carlson. 2015. The Thirsty Eel: Summer and Winter Flow Thresholds that Tilt the Eel River of Northwestern California from Salmon-Supporting to Cyanobacterially Degraded States. Copeia 103:200–211.

Quinn, T. P., S. M. Carlson, S. M. Gende, and H. B. Rich Jr. 2009. Transportation of Pacific salmon carcasses from streams to riparian forests by bears. Canadian Journal of Zoology-Revue Canadienne De Zoologie 87:195–203.

Reid, S. B., and D. H. Goodman. 2015. Detectability of Pacific Lamprey Occupancy in Western Drainages: Implications for Distribution Surveys. Transactions of the American Fisheries Society 144:315–322.

Rosenberg, K. V., A. M. Dokter, P. J. Blancher, J. R. Sauer, A. C. Smith, P. A. Smith, J. C. Stanton, A. Panjabi, L. Helft, M. Parr, and P. P. Marra. 2019. Decline of the North American avifauna. Science 366:120–124.

Rosenfeld, J. S., and J. Taylor. 2009. Prey abundance, channel structure and the allometry of growth rate potential for juvenile trout. Fisheries Management and Ecology 16:202–218.

Rossi, G. J. 2020. Food, Phenology, and Flow—How Prey Phenology and Streamflow Dynamics Affect the Behavior, Ecology, and Recovery of Pacific Salmon. PhD Dissertation, University of California, Berkeley

Sabo, J. L., J. L. Bastow, M. E. Power. 2002. Length–mass relationships for adult aquatic and terrestrial invertebrates in a California watershed. Journal of North American Benthological Society 21:336–343.

Scheuerell, M. D., J. W. Moore, D. E. Schindler, and C. J. HARVEY. 2007. Varying effects of anadromous sockeye salmon on the trophic ecology of two species of resident salmonids in southwest Alaska. Freshwater Biology 52:1944–1956.

Smith, J.J. and Li, H.W., 1983. Energetic factors influencing foraging tactics of juvenile steelhead trout, *Salmo gairdneri*. Predators and prey in fishes. pp. 173-180. Springer, Dordrecht.

Stillwater Sciences. 2010. Pacific lamprey in the Eel River basin: a summary of current information and identification of research needs. Prepared by Stillwater Sciences, Arcata, California for Wiyot Tribe, Loleta, California.

Stone, J. 2006. Observations on Nest Characteristics, Spawning Habitat, and Spawning Behavior of Pacific and Western Brook Lamprey in a Washington Stream. Northwestern Naturalist 87:225–232.

Suttle, K. B., M. E. Power, and J. M. Levine. 2004. How fine sediment in riverbeds impairs growth and survival of juvenile salmonids. Ecology 14:969–974.

Tucker, S., and J. B. Rasmussen. 2000. Using radiocesium[137] Cs to measure and compare the bioenergetic budgets of juvenile Atlantic salmon(*Salmo salar*) and brook trout (*Salvelinus fontinalis*). Canadian Journal of Fisheries and Aquatic Sciences 56:875–887.

Uno, H., and M. E. Power. 2015. Mainstem-tributary linkages by mayfly migration help sustain salmonids in a warming river network. Ecology Letters 18:1012–1020.

[USFWS] U.S. Fish and Wildlife Service. 2004. 90-Day finding on a petition to list three species of lamprey as threatened or endangered. Federal Register: December 27, 2004 (Volume 69, Number 2) Proposed Rules pages 77158-77167.

[USFWS] U.S. Fish and Wildlife Service. 2012. Pacific Lamprey Conservation Agreement. Portland, OR: U.S. Fish and Wildlife Service; 57 pp; [accessed 2020 October 10]. http://www.fws.gov/pacific/ Fisheries/sphabcon/Lamprey/lampreyCI.html.

Walters, A. W., R. T. Barnes, and D. M. Post. 2009. Anadromous alewives (*Alosa pseudoharengus*) contribute marine-derived nutrients to coastal stream food webs. Canadian Journal of Fisheries and Aquatic Sciences 66:439–448.

Wang, C. J., H. A. Schaller, K. C. Coates, M. C. Hayes, and R. K. Rose. 2020. Climate change vulnerability assessment for Pacific Lamprey in rivers of the Western United States. Journal of Freshwater Ecology 35:29–55.

Ward, B. R., & Slaney, P. A. 1988. Life history and smolt-to-adult survival of Keogh River steelhead trout (*Salmo gairdneri*) and the relationship to smolt size. Canadian Journal of Fisheries and Aquatic Sciences. *45*(7), 1110-1122.

Weaver, D. M., S. M. Coghlan Jr., and J. Zydlewski. 2018. Effects of sea lamprey substrate modification and carcass nutrients on macroinvertebrate assemblages in a small Atlantic coastal stream. Journal of Freshwater Ecology 33:19–30.

Wilcove, D. S., and M. Wikelski. 2008. Going, Going, Gone: Is Animal Migration Disappearing. PLoS biology 6:e188–4.

Yoshiyama RM, Moyle PB. 2010. Historical review of Eel River anadromous salmonids, with emphasis on Chinook salmon, Coho salmon and steelhead. Report for California Trout. Center for Watershed Sciences, University of California, Davis http://watershed.ucdavis.edu/ library.html.

Supplemental Material

Details of the thought experiment translating Pacific Lamprey subsidy on Juvenile steelhead to population level effects

i. Duration of Subsidy

We observed spawning sites occupied for 1–4 weeks. This suggests turnover of individuals on redd sites is likely over this time period, but the duration of subsidy is probably longer than any individual lamprey is on a redd. There is also likely variation in

arrival time, though lamprey do migrate upstream in pulses (Goodman et al. 2015). If juvenile steelhead are subsidized for 15 days during the spawning season, we can estimate growth for steelhead of different sizes in both out 'Lamprey' and 'No-Lamprey' treatments.

ii. Effect of Subsidy on Individual Growth

Using our mean estimates for potential growth, a 10 cm steelhead could add up to 12.7g foraging in our 'No-Lamprey' treatment, and 15.9g foraging behind redd building lamprey for 15 days, a difference of 3.2g of growth attributed to the lamprey subsidy. Using length-weight ratios from the SF Eel River, this increase in mass translates to nearly 5 mm of growth, that is attributable to the lamprey subsidy. For a 15cm steelhead, potential growth averaged 10.1g when foraging behind lamprey, 2.1g greater than no lamprey, and for a 20 cm fish mean growth potential was 7.2g behind lamprey, 1.6g greater than in the 'No-Lamprey' treatment (table 2) – which translates to growth to 2.3 mm of growth attributable to the lamprey subsidy. These growth potentials illustrate the smallest fish size classes had the highest potential growth overall (Figure 5 A), and benefit proportionally more (Figure 5 B), potentially doubling their mass over a two-week subsidy. Our largest size class (20 cm) added 6.7% to their mass when foraging behind lamprey for 2 weeks. We note that NREI models may be poor predictors of realized growth (see Hughes et al. 2003, Piccolo et al. 2014), however, this effect is probably consistent across 'Lamprey' and 'No-Lamprey' sites, and the effect of lamprey invertebrate subsidy may be conservative as mentioned above.

iii. Number of fish benefitted

In late May 2016, we counted a total of 524 adult lamprey and 1537 10-20 cm steelhead in our 10km study reach. This is a ratio of roughly three steelhead for each lamprey. However, lamprey often build more than one redd per individual (Brumo 2006), and we observed this behavior during our observations. We also observed multiple steelhead feeding downstream of active redds. For these reasons, it seems likely that at least one third of steelhead in this reach received a substantial subsidy from redd building lamprey in 2016 and potentially all the 10-20cm steelhead might have benefited.

iv. The effect of growth from lamprey subsidy on downstream and ocean survival

This last, and critical, step in inferring population-level effects from a lamprey-steelhead interaction remains speculative, because we don't know the downstream life history pathways and growth of steelhead after they leave the lamprey subsidy area (in our study, in the upper South Fork Eel). We know, however, that increased growth from a lamprey subsidy would likely benefit steelhead. Kabel and German (1967) estimated from smolt-to-adult return (SAR) rates from a hatchery in the SF Eel watershed that the survival increased most when steelhead grew from 15 cm (0.04% SAR) to 17cm (1.4% SAR) (Kabel and German 1967).
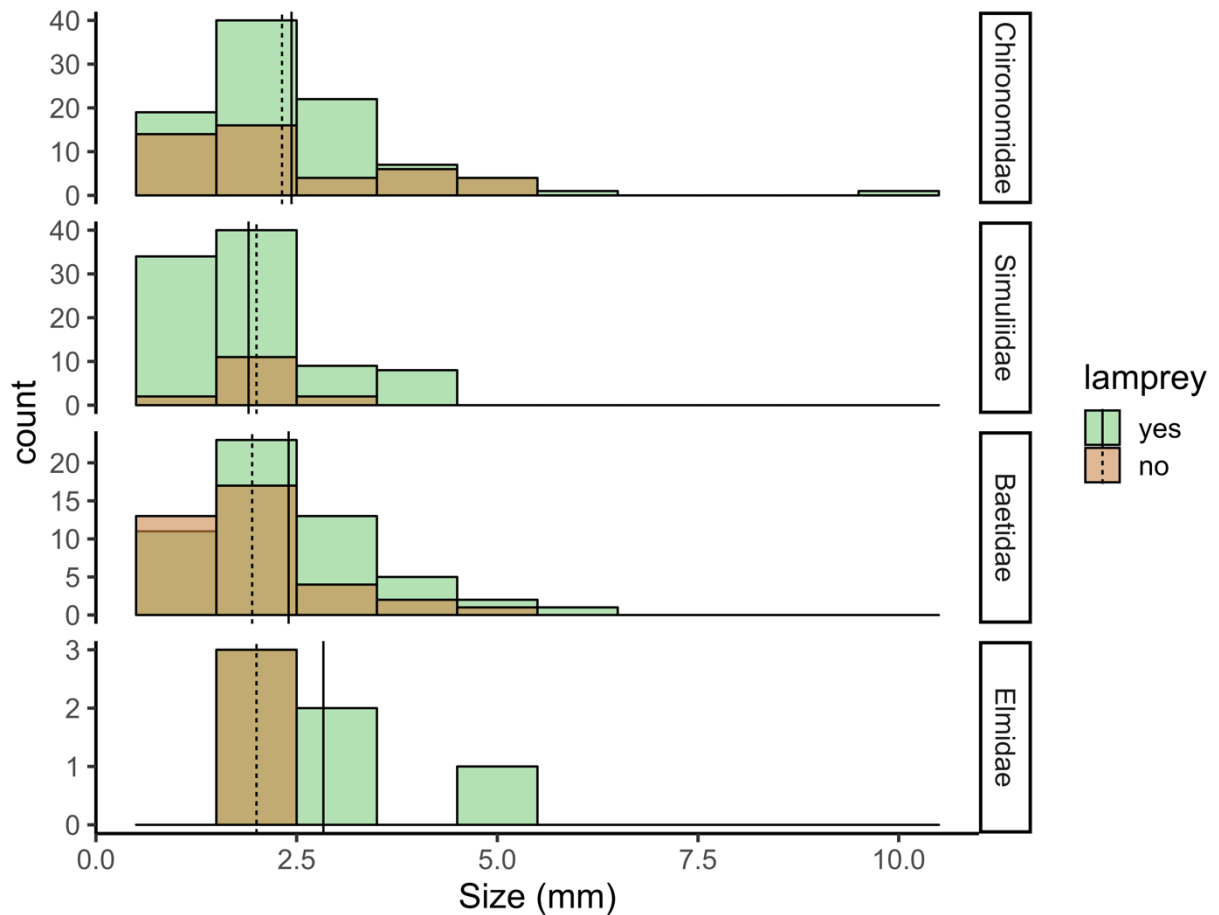
Supplemental Figure 1. Size frequency histograms of the 4 most common taxa. Green bars are sample from Lamprey treatment and tan bars are No-lamprey treatment. Vertical lines are treatment means, dashed for No-Lamprey, solid for Lamprey.

Table S1. Summary of lamprey counts and corresponding density estimates. * denotes estimated numbers from a subset of units with measured density. † denotes counts estimated from a subset of units and previously documented lower densities in downstream reaches

Year	Species	Size class	Total count	Density (individuals/km)
2016	Pacific Lamprey (*Entosphenus tridentatus*)	adult	524	49.2
2016	Steelhead (*Oncorhynchus mykiss*)	10-15cm	1011	95.2
2016	Steelhead (*Oncorhynchus mykiss*)	15-20cm	426	40.0
2016	Foothill Yellow-legged Frog (*Rana boylii*)	Egg masses	1031†	100.7
2017	Pacific Lamprey (*Entosphenus tridentatus*)	adult	126	24.2
2017	Steelhead (*Oncorhynchus mykiss*)	10-15cm	1440	137.6
2017	Steelhead (*Oncorhynchus mykiss*)	15-20cm	280	26.8
2017	Foothill Yellow-legged Frog	Egg masses	1140†	111.5

	(*Rana boylii*)			
2018	Pacific Lamprey (*Entosphenus tridentatus*)	adult	253	11.2
2018	Steelhead (*Oncorhynchus mykiss*)	10-15cm	1287	114.2
2018	Steelhead (*Oncorhynchus mykiss*)	15-20cm	346	30.7
2018	Foothill Yellow-legged Frog (*Rana boylii*)	Egg masses	1240†	121.1
2019	Pacific Lamprey (*Entosphenus tridentatus*)	adult	39*	3.4
2019	Steelhead (*Oncorhynchus mykiss*)	10-15cm	351*	63.6
2019	Steelhead (*Oncorhynchus mykiss*)	15-20cm	114*	20.6
2019	Foothill Yellow-legged Frog (*Rana boylii*)	Egg masses	1170†	114.4

Table S2. Opportunity for, and extent of, Foothill Yellow-legged Frog and Pacific Lamprey interactions in the South Fork Eel River. Spatial overlap in a 5.2 km study reach at Angelo Reserve is assessed as the proportion of 45 frog lek sites with lamprey redds present. Number of clutches observed inside redds at the South Fork Eel River at Angelo Coast Range Reserve and 3 km reaches sampled at Humboldt Redwoods State Park and Benbow State Recreation Area.

Year	Spatial Coincidence of spawning		Clutches in Redds		Index of frog population density (clutches/km)	
	% leks with redds	redds / lek site	Angelo Reserve	Humboldt County	Angelo Reserve	State Parks
2015	n/a		0	13 (2 leks)	69.8	34.666667
2016	22		0	0	106.2	269
2017	24	8.4 ± 2.8	0	19 (3 leks)	117.5	188.82883
2018	18		32 (3 leks)	7 (3 leks)	127.7	195
2019	4		0	4 (2 leks)	120.6	182.8
2020	18		6 (2 leks)	0	106.2	109.7

Conclusion

Below I present some of the key findings from my dissertation work and their implications.

In Chapter 1, I found almost all species varied longitudinally, and their longitudinal densities changed over time (either between seasons or years). Invasive animals were more abundant in downstream reaches and in slower water habitats. Populations of native species tended to be denser upstream, especially in late summer, when invasive numbers were high downstream. By describing these distributions we can identify conditions that favor native species, and could help guide restoration efforts to shift assemblages towards desirable states.

In Chapter 2, I describe how pikeminnow migrate upstream in spring and early summer and this migration occurred earlier in years when river water was warmer. Pikeminnow were more likely to occur in pools where their primary prey, North Coast Range Roach (*Hesperoleucus venustus)* were more abundant and dense, suggesting that feeding motivates seasonal pikeminnow migration. In years with low flow and high air temperature, we predict pikeminnow will move upstream earlier and overlap there with native fishes for a longer period of time. Pikeminnow consume or compete with all the native fishes of the South Fork Eel River, including culturally and economically important salmonids. Understanding the conditions which limit overlap between pikeminnow and threatened salmonids in important refuge habitat can direct habitat restoration efforts and aid the recovery of these native fishes. Additionally, insight into the phenology of life history events, like migration, exposes invasive pikeminnow to potential control. We suggest that capturing individuals as they move upstream or downstream or decreasing water withdrawals to keep river temperatures cool to limit co-occurrence of pikeminnow and rearing salmonids could minimize the negative impact of pikeminnow on native fishes. Invasive pikeminnow will likely have larger impacts in the South Fork Eel River with global warming and increasing drought severity. As with other invasive organisms, understanding pikeminnow life history and phenology can focus control efforts to take advantage of vulnerable life stages and seasonal time windows to benefit native species.

In Chapter 3, I found more invertebrates were collected in drift samples downstream of lamprey that were actively building redds and biomass of drifting invertebrates more concentrated, relative to drift in adjacent lateral positions not influenced by lamprey redd construction. Additionally, different taxa were more abundant in drift samples downstream of lamprey: Simuliids, Chironomids, and Elmids were more numerous. Juvenile Steelhead foraged more frequently while drift feeding downstream of redd building lamprey, and results of our bioenergetics models suggest that these locations were more profitable for growth than adjacent areas. Foothill yellow-legged frogs (*Rana boylii)* deposited their egg masses in completed lamprey redds, capitalizing on the flow refuge that both decreased scour risk and added depth that kept clutches submerged as spring flow receded. Salmonid fry also held positions in the low-velocity areas within redds. Our findings emphasize the importance of semelparous migratory organisms as ecological interactors that can benefit other native species in addition to subsidizing

spawning areas with nutrients and energy from their carcasses. The historical abundance of lamprey in coastal California rivers suggests these interactions could influence population dynamics of salmonids and foothill yellow-legged frogs. Our insights support the need to continue efforts to restore Pacific Lamprey to their historic ranges and abundance.

Collectively, these findings demonstrate how the aquatic assemblage of organisms has shifted from historic states. My work highlights how additional climate warming might have unexpected consequences by increasing overlap between native species and invasives. The strength of these interactions, in many cases, will also shift as conditions change in the future (Chapter 2). Not only are native species negatively impacted through competition and predation, but also from a reduction in positive interactions. Lamprey declines could contribute declines in salmonids for this reason. Here, I make the case that species conservation cannot happen through a single species lens. Context is important, and organisms occur in communities. Effective management, conservation, and restoration often require considering ecological communities and the interactions that occur within them.